1972

Feasibility study of using a steam power system in a small garden tractor

Niranjan Kumar Doshi

FEASIBILITY STUDY OF USING A STEAM POWER SYSTEM IN A SMALL GARDEN TRACTOR

BY

NIRANJAN KUMAR DOSHI, 1947-

A

THESIS

Submitted to the Faculty of the Graduate School of the

UNIVERSITY OF MISSOURI-ROLLA

in partial fulfillment of the requirements for the Degree

of

MASTER OF SCIENCE IN MECHANICAL ENGINEERING

Rolla, Missouri

1972

Approved by

(Advisor)

ABSTRACT

This thesis is a feasibility study of using a steam power system in a small garden tractor. The relative advantages of steam power are discussed and compared with the characteristics of internal combustion engines. A monotube boiler is designed where steam is generated in stacked tube spirals. The boiler generates 225 lbs/hr of dry saturated steam at 500 psia, which corresponds to an engine output of 20 IHP. A rotary positive displacement engine is employed to expand the steam to 16 psia. A rotor instead of a piston eliminates the conventional connecting rod and crank shaft. The engine developes 15 IHP at 1000 r.p.m. and can produce 20 IHP continuously at maximum boiler capacity. An air cooled condenser is designed to condense all the steam produced at maximum boiler generating capacity. An inexpensive V-belt and pulley power system (which eliminates the need for a conventional sliding gear or hydraulic transmission) is described. An arrangement of components is specified such that the dimensions of the tractor are similar to those of a typical 12 HP garden tractor. Construction of a prototype tractor is recommended on the basis of this study.

ACKNOWLEDGEMENT

The author wishes to thank Professor W. S. Gatley, for suggesting this research and for his assistance and advice throughout the course of this study. The author is also indebted to John Deere for providing valuable literature, a model and drawings of the John Deere 112 Tractor. The author also wishes to thank Mrs. Nancy Amador for her careful and expert typing.

TABLE OF CONTENTS

Page

LIST OF FIGURES

LIST OF TABLES

I. INTRODUCTION

A relatively small and efficient steam engine has been attracting the attention of the automotive industry as a possible low pollution prime mover. Other potential advantages of the steam engine are low noise levels and a more favorable torque-speed characteristic [1,2,3]*.

This thesis is a feasibility study of using a steam engine in a small garden tractor. A rotary positive displacement steam expander is employed as the prime mover. This expander eliminates the connecting rod and the conventional crank shaft. It is designed to operate at speeds up to 1000 rpm. A monotube boiler is used for the generation of steam at an operating pressure of 500.0 psia. The tube configuration consists of several 0.5 inch od tube sections, each wound in a plane spiral. The spirals are stacked one above another and in the central core a high temperature flame is blown from a burner located at the base of the stack. An air cooled condenser is used to condense the exhaust steam and is sized to condense all of the steam required for 20 continuous indicated horsepower. The entire design is described under the following categories:

---

*Numbers in parentheses designate references at end of the thesis.

(1) Power Requirements

(2) Thermodynamic Considerations

(3) Boiler Design

(4) Prime Mover Design

(5) Condenser Design

(6) Arrangement of the Components and Power Take-Off

(7) Summary and Conclusion

II. POWER REQUIREMENT

The tractor must be able to negotiate steep terrain under normal working conditions and on that basis the normal power requirement will be calculated.

While climbing a slope of angle β, the forces acting will be as shown in Figure 1.

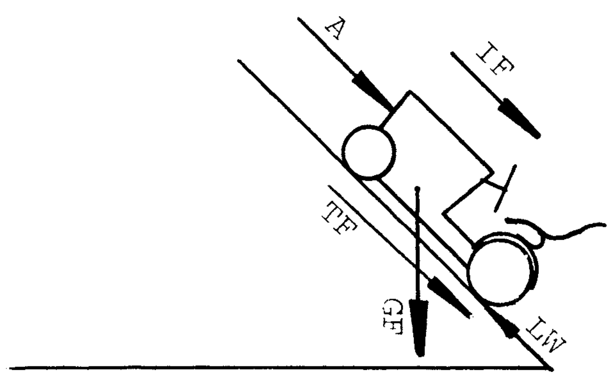

Figure 1. FBD of Forces Acting on the Tractor.

A = Aerodynamic force

TF = Tire friction force

GF = Gravity force

LW = Locomotive force at wheels

IF = Inertia force

The effective components of the resistive forces in the direction of motion are:

$$A = 1/2\rho v^2 C_D S \qquad (1.1\ A)$$

$$TF = C_f W_t \mathrm{Cos}\beta \qquad (1.1\ B)$$

$$GF = W_t \mathrm{Sin}\beta \qquad (1.1\ C)$$

$$IF = W_t \times a/g \qquad (1.1\ D)$$

where

ρ = Density of air at NTP,

v = Velocity of tractor,

C_D = Coefficient of drag,

S = Frontal area of the tractor,

C_f = Coefficient of friction,

W_t = Weight of tractor,

β = Angle of slope,

a = Acceleration of tractor,

g = Gravity constant.

The power required at the rear wheels to overcome each of the forces described by equation 1.1 A can be obtained in terms of h.p. by multiplying each term by v/550.

When the tractor begins to move from rest the engine will not be operating at its rated 1000 rpm speed. However it is reasonable to assume that the engine reaches a speed of 250 rpm within ten seconds after starting from rest up an incline of 45°. Hence through the differential after 5:1 speed reduction the rear wheels rotate at 50 rpm. Assuming a rear wheel diameter of 22.0 inches, gives a forward vehicle speed

$$v = r \times \frac{2\pi N}{60},$$

where

v = Speed in ft/second,

r = Wheel radius in ft,

N = Wheel rpm.

Substituting appropriate values in equation the forward speed is found to be

$$v = 4 \cdot 8 \text{ fps or } 3 \cdot 3 \text{ mph},$$

after 10.0 seconds, hence the vehicle acceleration will be

$$a = 0.48 \text{ ft/seconds}^2.$$

The power required at wheels to overcome aerodynamic drag will be

$$P_{wa} = 1/2 \rho v^3 C_D S/550.0,$$

and for

$$\rho = 0.0803 \text{ lbs/cubic ft},$$

$$v = 4.8 \text{ fps},$$

$$C_D = 0.5^*,$$

$$S = 6.0 \text{ square ft},$$

$$P_{wa} = 0.0133 \text{ h.p.}$$

The power required to overcome tire friction force will be

$$P_{wt} = C_f W_t \text{Cos}\beta \; v/550,$$

and for

---

*Suggested by reference [4]

C_f = 0.2* for rolling friction over tilled loam,

W_t = 1000** lbs,

v = 4·8 fps,

β = 45°,

the value of P_{wt} will be

$$P_{wt} = 1.25 \text{ h.p.}$$

The power required to overcome gravity force will be

$$P_{wg} = W_t \sin\beta \; v/550$$
$$= 6.15 \text{ h.p.}$$

The power required to overcome the inertia force will be

$$P_{wi} = W_t/g \times a \; v/550.$$

For

a = 0.48 ft/seconds^2,

v = 4·8 fps,

the power will be

$$P_{wi} = 0.13 \text{ h.p.}$$

Hence the power required at the wheels to overcome all these resistive forces will be

$$P_w = 7.5 \text{ h.p.}$$

---

*Suggested by reference [4]

**Estimated weight of tractor with operator

The maximum power required for power plant acessories can be estimated as follows:

Boiler feed pump	= 0.5 h.p.	[page 71]
Condenser fan	= 2.5 h.p.	[page 203]
Burner blower	= 0.5 h.p.	[page 75]
Total	3.5 h.p.	

Friction losses in the engine and drive train are estimated to be 3 h.p.

Therefore an engine of 15 indicated horse power should suffice for normal continuous operation. The power required for mower blades and other accessories will be approximately 5 h.p. which is readily available both on level terrain at normal vehicle speeds, and on hilly terrain at reduced speed.

As is shown in Chapter V, Section F, the engine can develop 20 continuous horse power by increasing the steam supply and can develop even more power for short periods. Hence a 15 i.h.p. engine should be adequate for continuous operation.

III. THERMODYNAMIC CONSIDERATIONS

A. Introduction

Before going into a detailed discussion of the thermodynamic principles involved in a vapor power system, the advantages and disadvantages of the external combustion cycle will be compared with those of the internal combustion cycle [2,5].

Regardless of the type of fluid used the advantages of an external combustion vapor cycle are as follows:

(1) The generation of mechanical power by high pressure vapor occurs in two steps:

(a) In a boiler through release of energy by combustion of fuel and its transfer as heat to a working fluid; and

(b) In an expander where the energy thus stored in the working fluid is converted to mechanical work.

This simplifies the thermochemical processes involved, compared to an internal combustion cycle, where the energy released by the fuel during combustion is directly converted to work in an expander [5].

(2) Physical separation of compression and expansion functions: In an external combustion cycle the pressure of the working fluid is increased in the vapor generator (compression function) and is then decreased

in an expander (expansion function). Thus these functions are separate and so can more easily be controlled, giving efficient control over the entire system [5].

(3) Low noise level: Since there is no series of explosions (as occurs in an internal combustion engine), a vapor cycle engine is inherently less noisy.

(4) Low pollution: As the combustion process is separate and leisurely performed, it is possible to achieve complete combustion, thus minimizing levels of pollutants. Figure 2 shows a comparison for the three chief pollutants, in grams per mile for a typical American car and a steam powered automobile [3].

(5) Low fuel cost: A cheaper quality of fuel can be burned in a suitably designed burner. This helps to reduce operating costs.

B. Advantages and Disadvantages of Employing External Combustion in Automotive Vehicles.

All of the previously mentioned advantages are applicable to any type of power plant employing the external combustion cycle. The following are special advantages resulting from the application of the

L.E.M.V. = Low Emission Motor Vehicle

S.C. = Steam Car

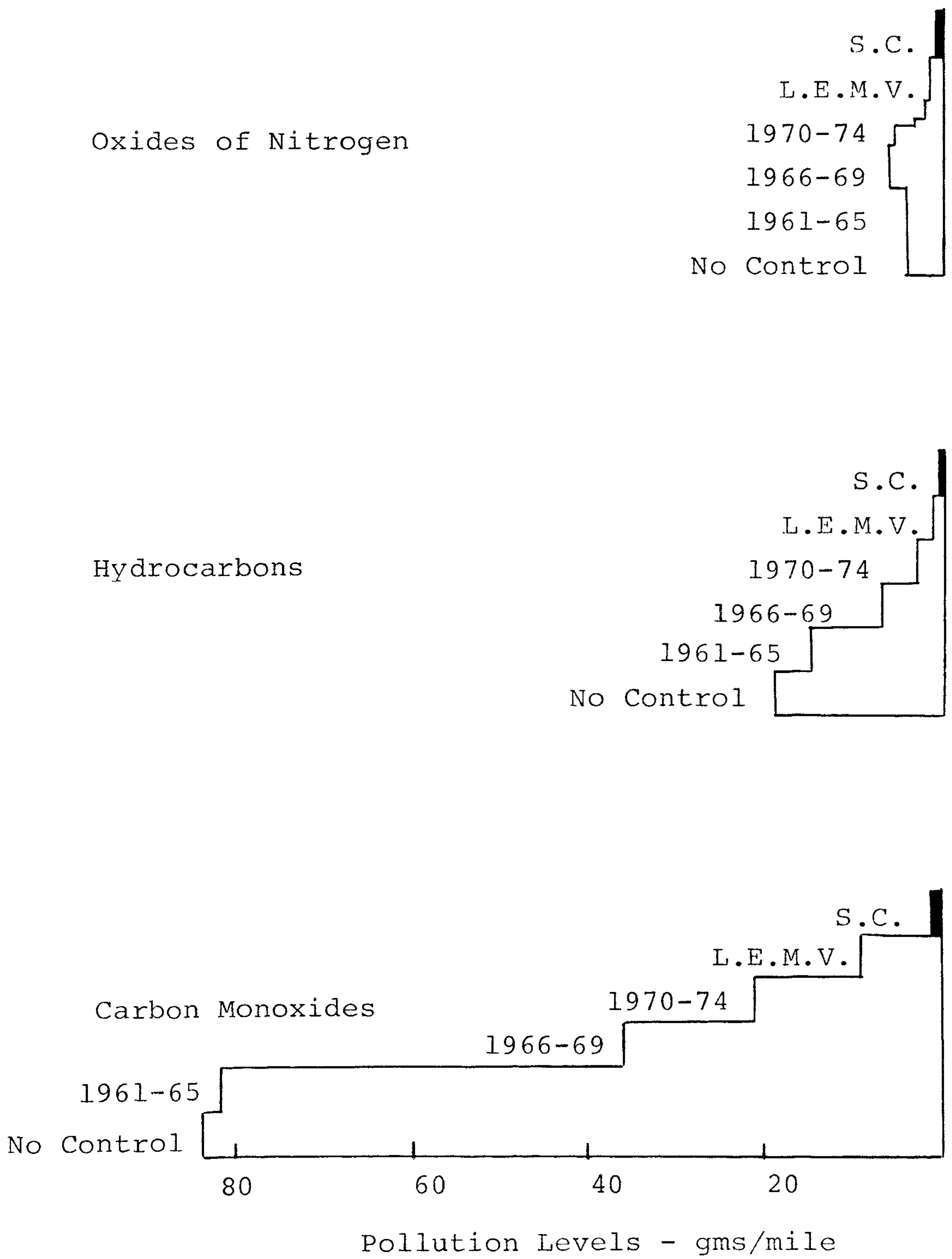

Figure 2. Pollution Levels of a Typical American Car.

external combustion principle to automotive vehicles [5].

(1) Torque-crank angle characteristics: If a double acting vapor expanding positive displacement engine is employed, driving torque is available throughout the entire cycle (no negative torque). Thus the characteristic torque is more uniform over a cycle compared to single cylinder two or four cycle internal combustion engines as shown in Figure 3 [6,7,8].

Besides such a vapor engine produces higher starting and stalling torque. Also maximum torque is available at zero speed [Figure 4]. Furthermore the uniformity of the torque characteristic reduces the inertia of the flywheel required to obtain a given coefficient of speed fluctuation.

A steam engine has fairly constant speed torque characteristic over low speed ranges. The torque drops off at higher speed because of improper valve operation, while the speed-torque characteristic of an internal combustion engine drops off at both higher and lower speeds as shown in Figure 4.

(2) Wide range of mean effective pressures and expansion ratios: The expansion ratio of a

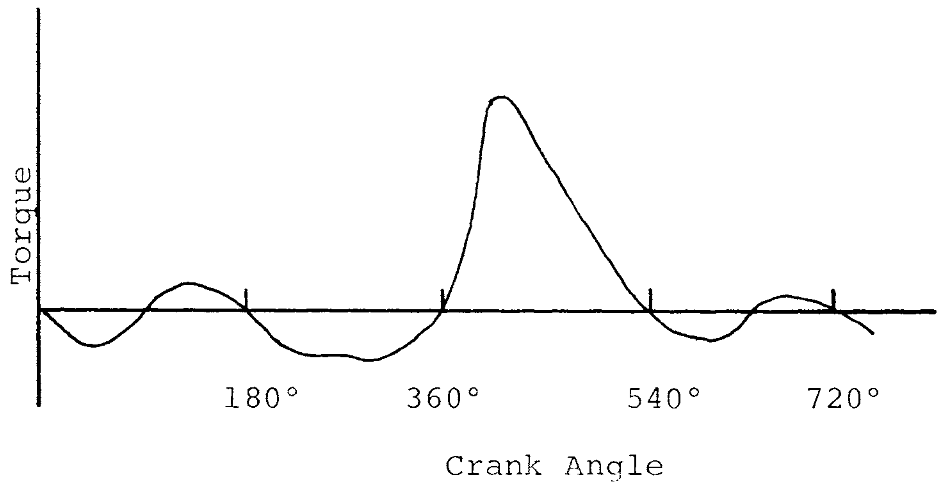

4 Stroke, 1 Cylinder, I. C. Engine.

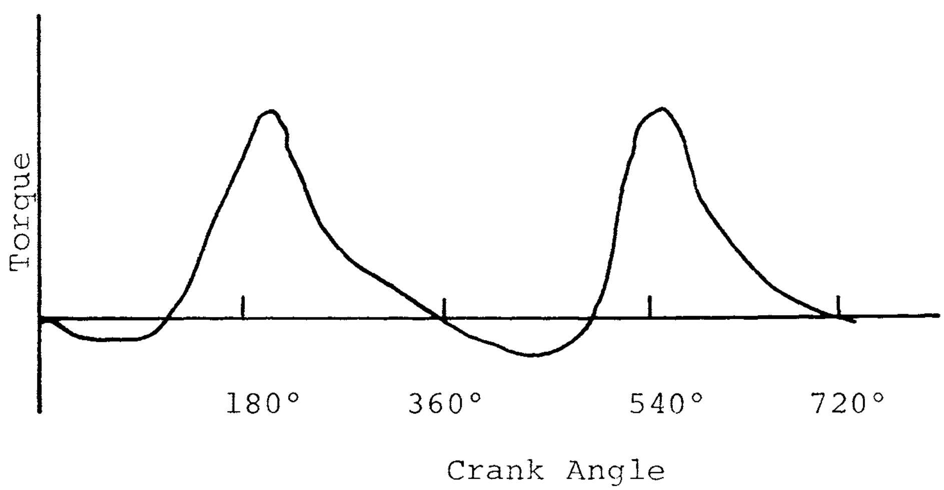

2 Stroke, 1 Cylinder, I. C. Engine.

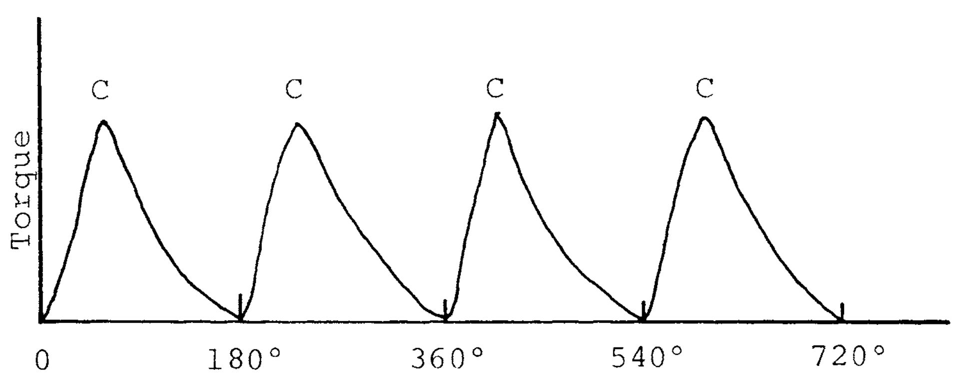

Double Acting, 1 Cylinder, Steam Engine.

Figure 3. Torque-Angle Comparison of 4 Stroke and 2 Stroke Cycle I. C. Engine with Double Acting Steam Engine.

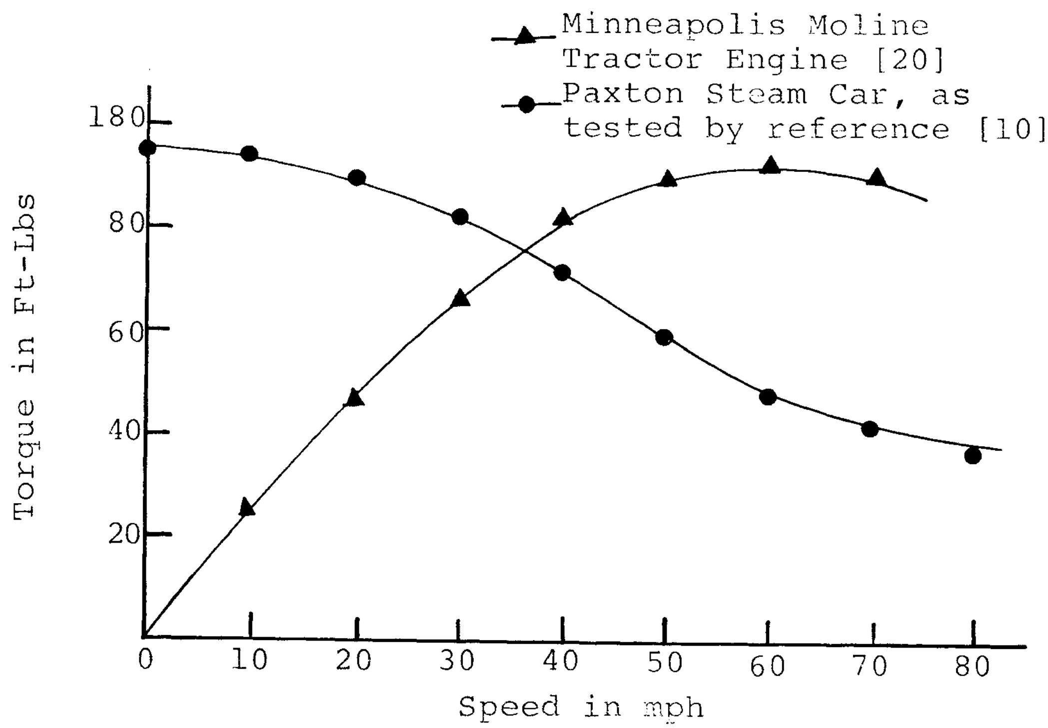

Figure 4. Torque Speed Characteristics Comparison.

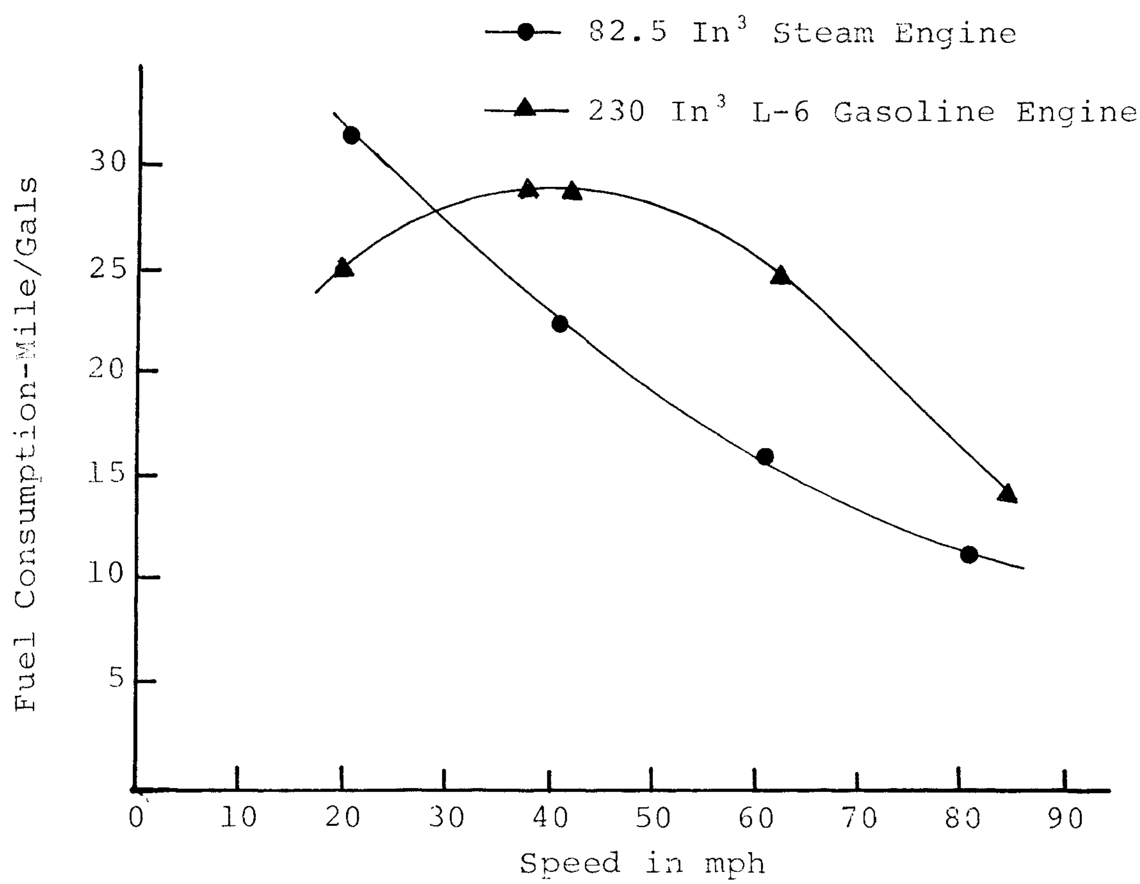

Figure 5. Comparative Fuel Consumption of Petrol and Steam Engined Chevelle Cars at Steady Speeds [3].

steam engine is defined as ratio of the steam volume in the expander at the beginning of exhaust to the volume of steam at the end of steam admission. It is possible to attain a wide variation in expansion ratios and mean effective pressures giving favorable torque-speed characteristics and improving efficiency under some operating conditions.

(3) Fuel consumption: It has been observed that the economy of a steam plant is superior to the gasoline engine at speeds below 20 or 30 miles/hr, while from 40 to 80 miles/hr it is some 6-8 miles/gallon worse. This suggests that for slow vehicles a steam engine will be more economical. Figure 5 indicates this comparison [3].

(4) Relatively simple design of the engine: Because of the good low-speed torque characteristic of a steam engine, a transmission with multiple forward speeds is not needed. The fuel ignition system will be simple and cold starts will be easy. There will be reduced vibrations because of the smoother torque characteristic and virtual silence. Also the overall acceleration would be smooth, for the same reason.

The disadvantages associated with the use of an external combustion system cannot be overlooked [3,5].

(1) The change of state of the working fluid introduces heat losses and in turn a loss in efficiency.

(2) The engine and auxiliary components are relatively heavier and the system is even more bulky and complicated, when the cycle is a condensing one.

(3) Even when the cycle is condensing, some make up of the working fluid may be needed, especially during heavy loading conditions, when all the vapor may not be condensed.

(4) A longer start-up period is required.

(5) The working fluid may freeze during the winter months.

(6) Different operating techniques will be required.

In addition to these factors, one should not overlook the specific reasons, why steam cars were not developed. This can be summarized as follows [5].

(1) A lack of research work and forward planning.

(2) Strong promotion of gasoline powered cars by trade associations.

(3) Lack of familiarity with steam car control.

(4) An initial high cost because of low production and a lack of design improvements.

(5) The lack of knowledge about efficient steam generation.

C. Choice of Working Fluid

Before selecting the working cycle, it is important to select a suitable working fluid. Water is just one of the many fluids that might be employed in a vapor cycle engine. However, water has many advantages as a working fluid for the most suitable working cycle; viz., the Rankine cycle [2,3].

(1) Ready availability and low cost.

(2) High enthalpy as a vapor.

(3) Stability at high temperature.

(4) Good heat transfer properties.

(5) Nontoxicity.

However, water also possesses several disadvantages as a working fluid:

(1) As it is discussed later, the higher the temperature of the working fluid, the greater is the cycle efficiency. Since water has a high vapor pressure, it requires high operating pressures at the temperatures necessary for acceptable efficiency as shown in Figure 6 [3].

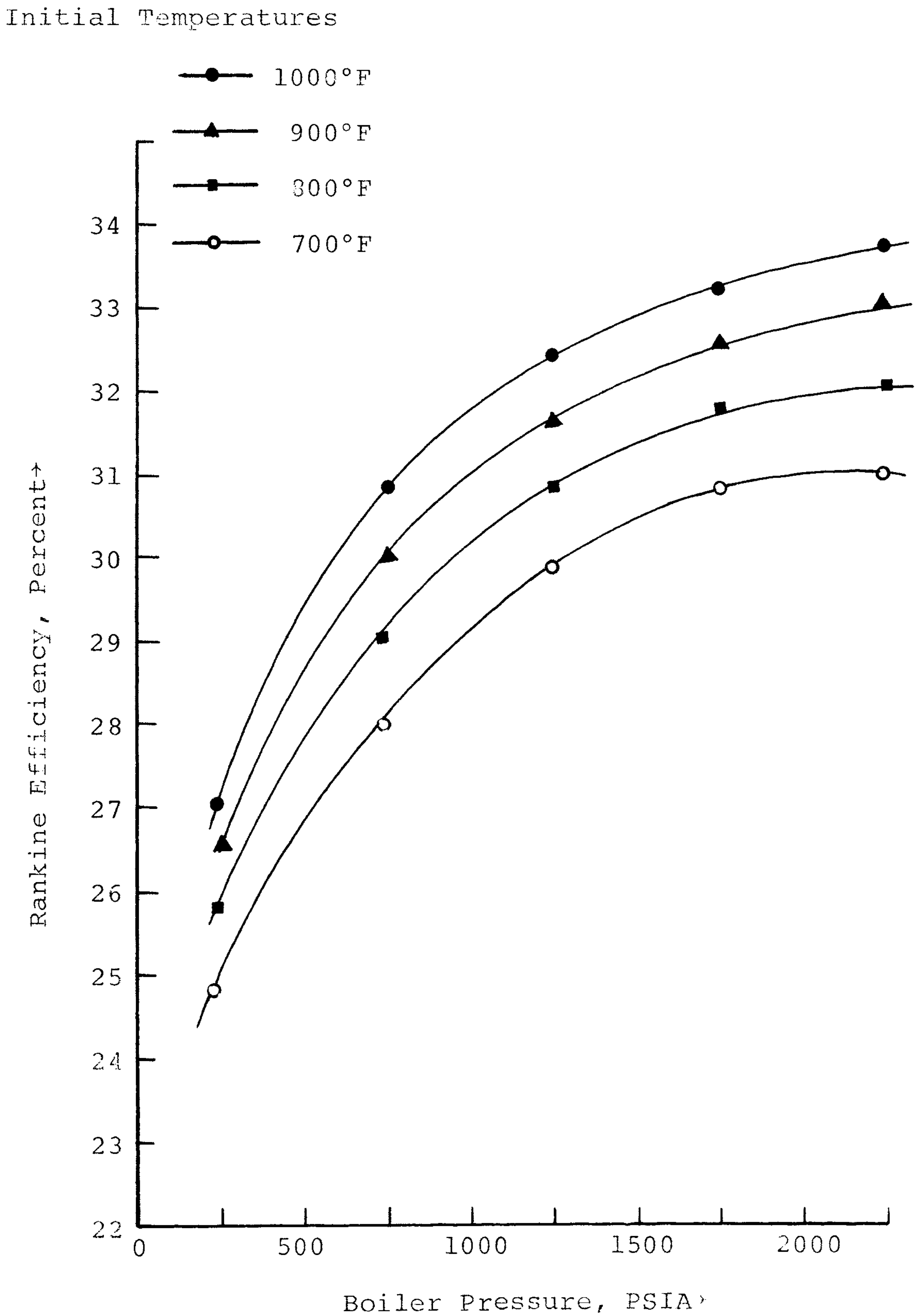

Figure 6. Ideal Efficiency of Simple Rankine Steam Cycle.

(2) Water freezes with expansion in a normal winter climate.

In spite of these drawbacks, water will be the choice because of its low cost, availability and has attractive and well known thermodynamic properties. Next to water the flourocarbon family has the greatest potential for a working fluid; however it is poisonous and its behavior at high temperature is not well known [2].

D. Selection and Analysis of Working Cycle

A heat engine is based on some kind of cycle to convert heat energy into mechanical energy. The Carnot cycle has the maximum theoretical efficiency and is the basis for all vapor cycle engines.

The Carnot cycle is bounded by two isothermal and two adiabatic lines, as shown on the temperature-entropy (T-S) diagram and pressure volume (P-V) diagram of Figure 7 [6,9].

The ideal Carnot cycle can be described as follows; with reference to Figure 7.

The working fluid at point d (temperature T_1 and entropy S_1) is heated in the boiler. This is liquid heating and the temperature rises to T_2, but entropy remains S_1. After the saturation temperature T_2 is reached, evaporation of the working fluid takes place at constant temperature. Heat supplied increases the entropy to S_2. At "b" the dry saturated vapor is supplied to the engine and is expanded adiabatically to "c". The expansion process terminates at temperature T_1 and the vapor is exhausted to the condenser, where it is condensed at constant temperature T_1 and its entropy drops from S_2 to S_1. From this point the cycle is repeated.

Now the cycle efficiency can be calculated.

Heat supplied (H_s) is the area hbS_2S_1 on the T-S diagram

$$H_s = T_2(S_2-S_1),$$

and the work done (W) is given by the area bounded by the cycle, i.e., hbcd

$$W = (T_2-T_1)(S_2-S_1).$$

Cycle efficiency =

$$\frac{\text{Work done}}{\text{Heat Supplied}} = \frac{T_2-T_1}{T_2}\ .$$

Thus, the efficiency of the ideal Carnot cycle depends only on the temperature range of the working fluid. The cycle has greater efficiency if the upper limit of the temperature is higher and lower limit still lower. However in a steam engine, the lower limit of temperature results in higher exhaust steam volume and this leads to a large condenser volume. Hence, the lower temperature limit is restricted, so far as

Figure 7. Ideal Carnot Cycle

(a) Temperature - Entropy and

(b) Pressure - Volume Diagram

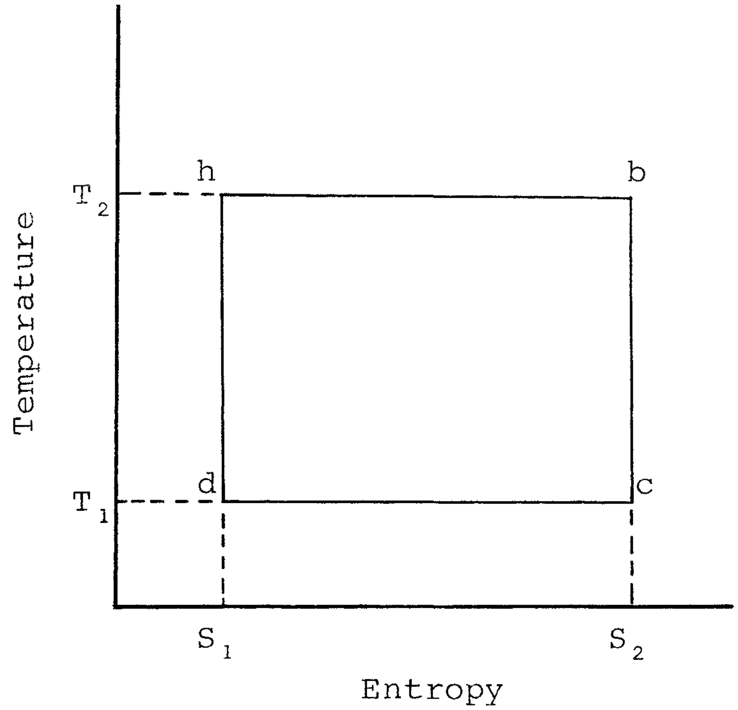

(a) T-S Diagram for Carnot Cycle

dh = Liquid Heating

hb = Evaporation

bc = Expansion

cd = Condensation

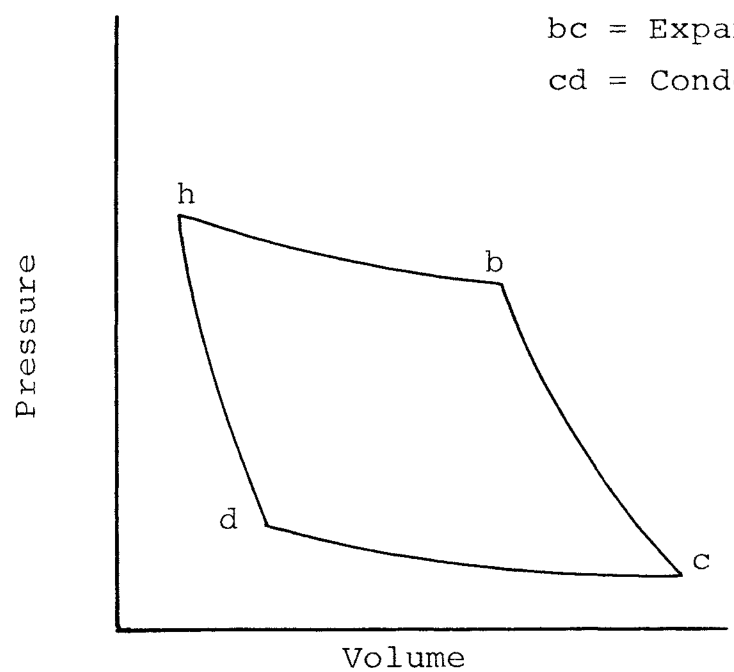

(b) P-V Diagram for Carnot Cycle

applications to automotive power plants are concerned.

As shown previously in Figure 6 the higher working temperature leads to higher working pressure and hence the maximum cycle temperature is limited by the practical limit for the working pressure.

In actual practice, the ideal Carnot cycle cannot be achieved when water is used as working fluid. This limitation can be demonstrated by considering T-S and P-V diagrams of the Rankine cycle as shown in Figure 8 [5,9].

As water is heated from point d (Figure 8), it follows the water vapor boundary (de). This is liquid heating and is not an adeabatic process. During this process entropy and temperature both increase. When the steam is expanded in the engine its volume increases and requires a large engine volume for complete expansion. However, after a certain expansion of steam, further expansion is uneconomical, because the gain of work is less than the friction required to overcome the expansion [page 107]. Hence, along the expansion line "bc", steam is delivered to the condenser at "g" instead of "c", thus deviating by area "gqc" from the ideal Carnot cycle. Therefore, the most practical cycle (debgqd) has almost three boundaries out of four in common with the ideal Carnot cycle "dhbcd". This practical cycle is known as the Rankine cycle.

Figure 8. Ideal Rankine Cycle

(a) Temperature-Entropy (T-S) and

(b) Pressure - Volume (P-V) Diagram

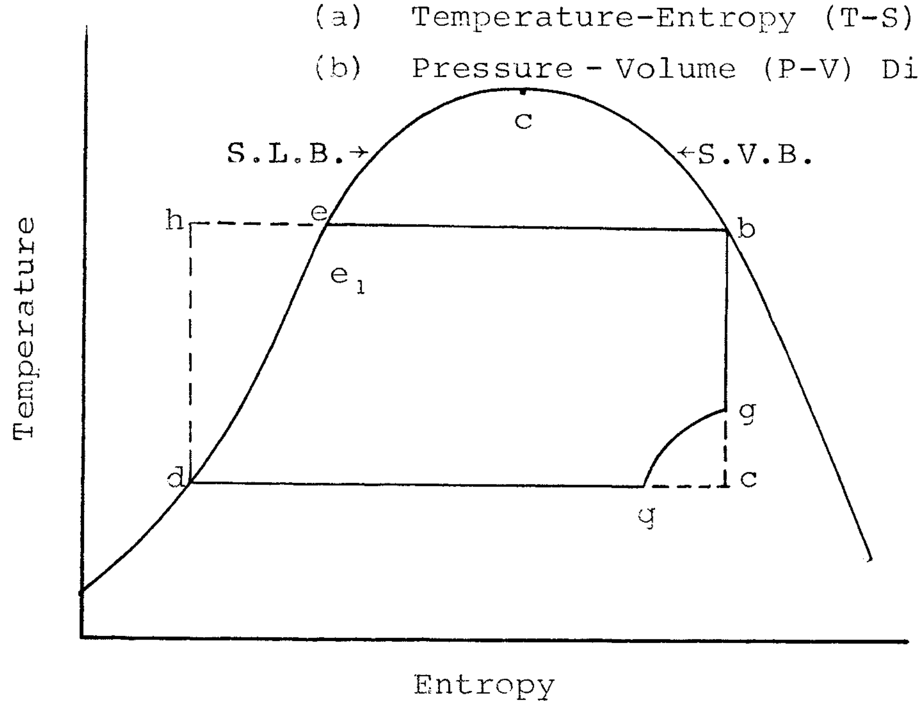

c = Critical Point

S.L.B. = Saturated Liquid Boundary

S.V.B. = Saturated Vapor Boundary

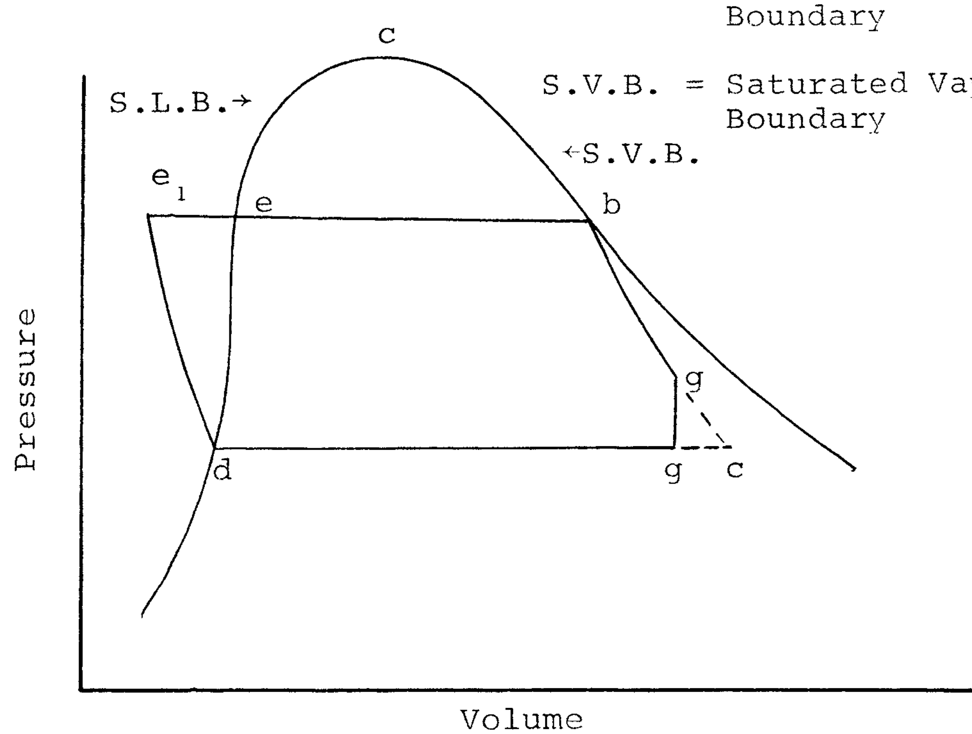

The Rankine cycle can be brought closer to the Carnot cycle if [5]:

(1) Expansion of steam in the engine is as complete as possible.

(2) Superheated steam is used.

(3) During condensation just enough heat is extracted to condense the steam completely. This reduces heat to be supplied in the boiler.

E. Selection of the Type of Cycle

The first decision concerns whether the cycle should be condensing or non-condensing. Condensation is essential in large steam power plants because it saves boiler feed water and improves efficiency by reducing the lower temperature limit. For automotive applications, condensation is essential in order to recycle boiler feed water, because make-up water is unavailable as a practical matter. In earlier steam powered automobiles the system was non-condensing, with auxiliary pumps to take water from roadside horse watering troughs. However modern requirements for high reliability, low maintainance and convenience make a condensing system mandatory.

IV. DESIGN OF THE STEAM GENERATOR

A. Introduction

The steam generator is the bulkiest component of the whole steam power system and plays a very important role in achieving maximum efficiency and in determining the maximum horse power that can be obtained. Steam generators or boilers can be classified in many ways depending upon the positions of the steam generating or water tubes, the path of flowing gases, etc. Early steam cars dating back to 1900 used vertical fire tube boilers, where the unit was vertical and hot gases passed through vertical tubes surrounded by water. The boiler was usually large in size and capacity because the system was non-condensing [10]. Thus the boiler had a large thermal storage capacity, which was desirable for minimizing boiler control problems. However, the system required a relatively long time to reach operating temperature. Later steam cars, which were produced in the 1920's (namely the White and Doble), used monotube boilers, in which steam was generated in a number of single long tubes of relatively small diameter [10].

B. Design Objectives

Before a particular type of boiler is selected, it is essential to check the requirements to be met for modern automotive units. These can be summarized as follows [4,11]:

(1) The steam generating unit, being a bulky component, should be optimized with respect to weight and volume.

(2) The unit should be able to reach operating temperature in a reasonable time.

(3) The water capacity should be minimal to prevent leaks at high pressure and to achieve quick start-ups from cold.

(4) The unit should be able to withstand temporary overload conditions, i.e. have good reserve capacity.

(5) The unit should respond rapidly to any change in demand.

(6) Should have small pressure drop in both air and water sides.

(7) The unit should be safe at all operating condititions.

C. Selection

Several variations of water tube boilers have been used in the past. Recent development in burner design have contributed to quick start-up and economical operation of monotube boiler because of high gas temperature and heat transfer rate. For this reason the monotube boiler has been the most popular configuration for modern steam powered vehicles. In this case a continuous tube is formed in either spiral or helical coils and products of combustion flow over the outside. This tends to reduce both the surface area requirements and the water inventory. Since the tubes are the only pressurized elements, the likelihood of a catastrophic explosion is virtually eliminated [2,4].

However in a monotube boiler, reserve capacity is reduced and therefore it should be designed with excess capacity so it can respond rapidly to change in power requirements. This is very important for automotive vehicles like tractors which are liable to encounter a wide range of load conditions [4].

Since the diameter of the tubes is of the order 0.5 to 0.7 inch, there is usually a substantial pressure drop on the water side. For this reason forced circulation should be adopted.

In summary the monotube boiler appears best suited for automotive applications and has, in fact, been selected by General Motors, McCulloch Corporation and Ricardo and Company, England.

D. Selection of Steam Pressure

To operate the system at the highest possible pressure is desirable because it reduces the specific steam consumption, as shown in Table 4.1 [10]. In

TABLE 4.1

COMPARISON OF VARIOUS STEAM SYSTEMS

SYSTEM	STANLEY STEAM CAR	WHITE STEAM CAR	DOBLE STEAM CAR	McCULLOCH STEAM CAR
Type of Boiler	Fire Tube	Mono-Tube	Mono-Tube	Mono-Tube
Operating Pressure P.S.I.	600	600	1500	2000
Temperature °F	800	800	800	1200
Specific Steam Consumption in Lbs./HP/Hr.	over 20	17	12	6.5

early steam cars high specific steam consumption, resulting from low operating pressure, was a problem because it increased the size of the boiler, condenser and condenser fan. With present technology higher pressures are feasible and the engine size has been correspondingly reduced.

Although the Doble steam car operated at 1500 p.s.i. and 800°F to reduce the steam consumption, lubrication was unsatisfactory. However in 1930, Doble claimed to have achieved satisfactory lubrication with steam at 850 p.s.i. and 850°F. As a result of subsequent advances, McCulloch Corporation suggests 2000 p.s.i. steam inlet pressure. In this study, 500.0 p.s.i. inlet pressure is selected in order to avoid lubrication problems and to minimize leakage problems which may arise in the rotory expander [10].

E. Boiler Design

(1) Description of the unit [4]: The design selected employs a number of spirally-wound tubes of small diameter, stacked on each other as shown in Figures 9 and 10. The ends of the tube spirals are connected to common vertical headers. Figure 10 shows how tubes can be placed. The burner is mounted at the bottom while the blower is mounted outside to simplify power transmission. A

high temperature flame passes through the open central core and thus direct impingement of the flame on the tube is avoided. At the top of the tube stack, a cone of ceramic material reflects the hot gases downward and they are exhausted from the bottom after passing through the tube stack as shown in Figure 10.

(2) Determination of independent parameters: As a first step in design the following independent parameters will be determined:

(a) Maximum heat transfer rate required: The steam consumption can be estimated to be 10.0 lbs/hr-i.h.p. [page 120]; under a 50% overload condition, the system develops 22.5 i.h.p., resulting in a steam consumption rate of 225.0 lbs/hr. As discussed previously, this steam capacity would permit temporary overloads (say 40 i.h.p.) by a delayed steam cut-off, for 10 to 15 minutes.

Since the steam is to be supplied at 500 psia and dry saturated, the heat transfer rate required in the boiler will be 225,000 BTU/hr, assuming that the boiler feed water is at 200°F.

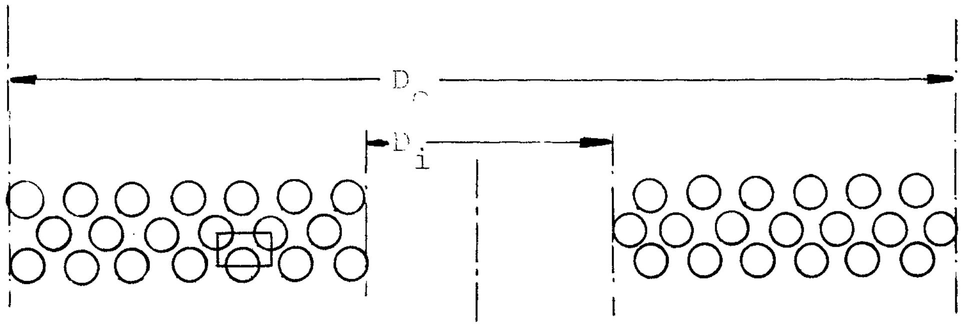

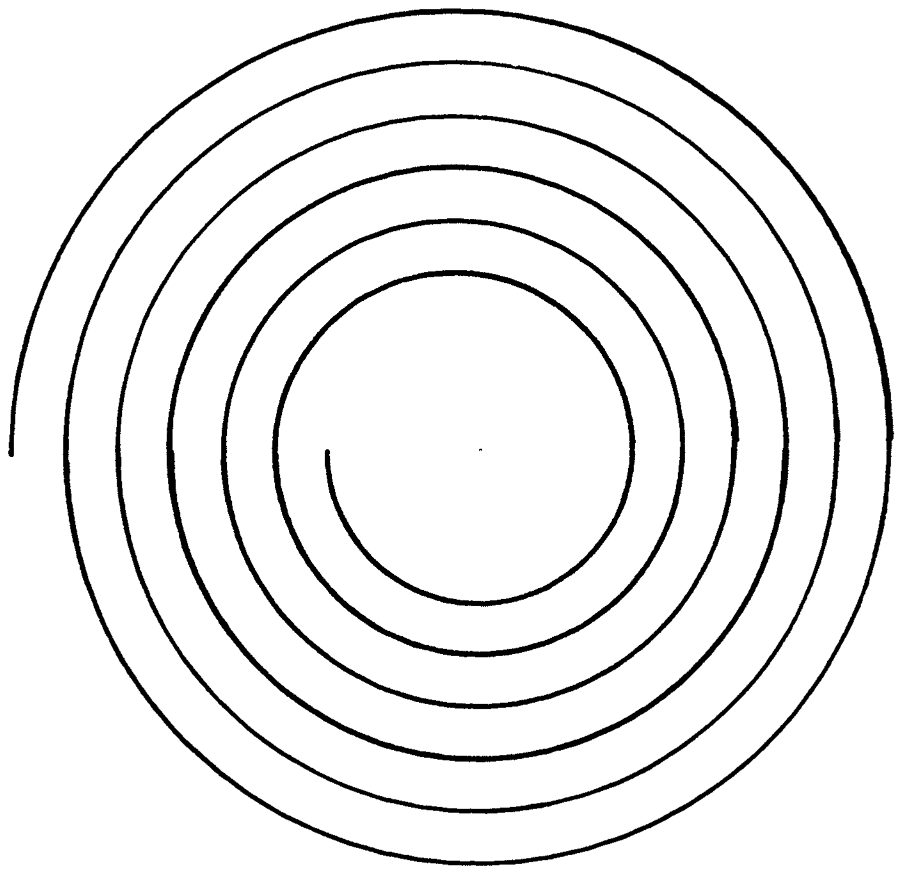

Figure 9. A Single Tube Wound in a Spiral.

D_o = 14.0 inches, N = Number of turns = 6.

$D_i = \frac{1}{3} D_o$,

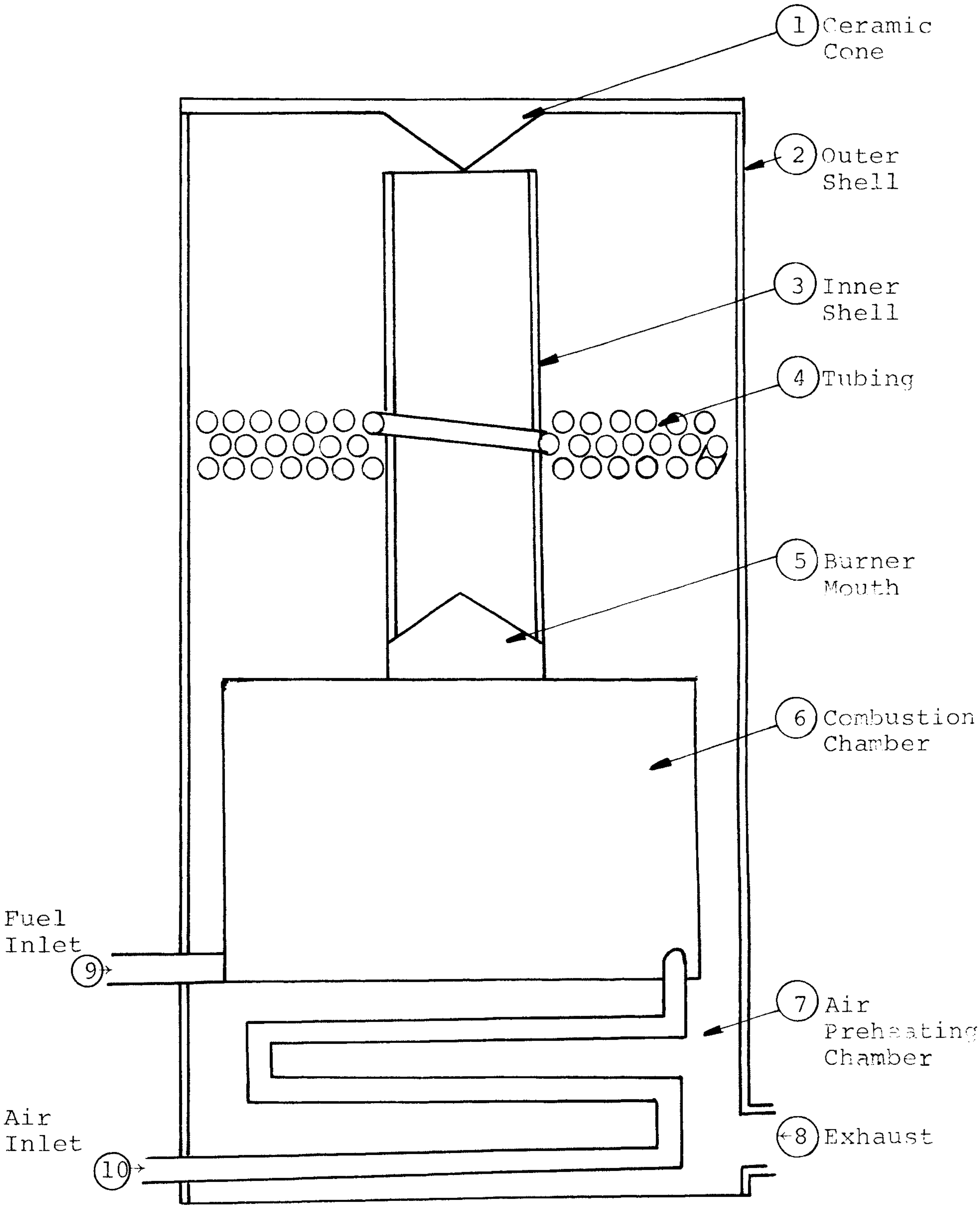

Figure 10. Boiler.

(b) Boiler tube material and diameter: Modified 9M steel is selected for the tube material because of its low cost, considerable resistance to corrosion and high strength at high temperature. Figure 11 indicates the strength temperature relation for this material.

Most of the recent work in design of monotube boilers is done with small diameter tubes of 0.5 inch to 0.7 inch. For this application 0.5 inch od tubes are selected [2,4].

(c) Tube spacing transverse and parallel to gas flow: The arrangement is as shown in Figure 12 and is recommended by reference [4].

(d) Water temperature at condenser outlet and steam temperature at boiler outlet: The water temperature at the condenser outlet can be predicted to be 200°F, corresponding to the saturation temperature at 16 to 17 psi pressure. However this is difficult to specify exactly, because it depends on other factors, such as ambient air temperature and average condenser pressure.

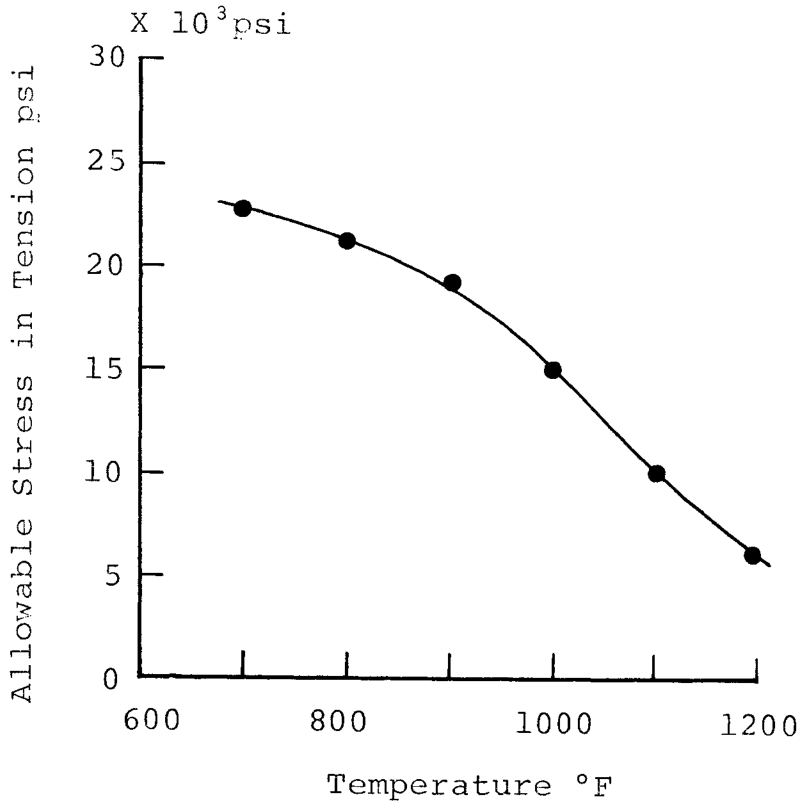

Figure 11. Strength of Modified 9M Steel [12].

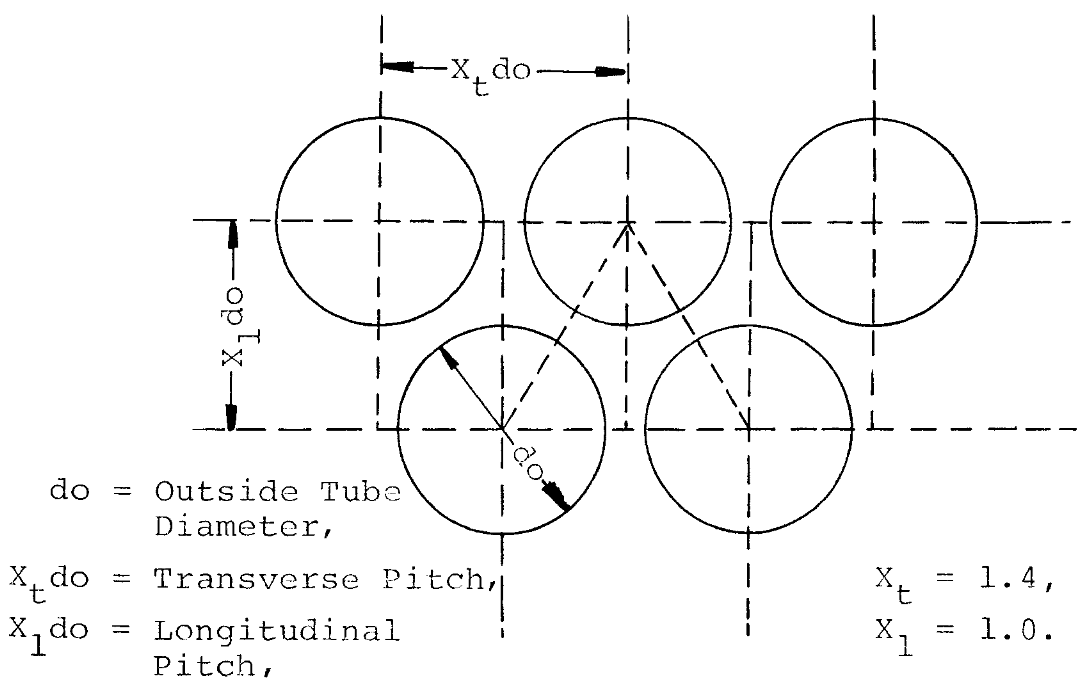

Figure 12. Boiler Tube Spacing.

The temperature of steam at the boiler outlet will correspond to the the saturation temperature of steam at 500.0 psia i.e. 460°F.

(e) Combustion gas temperature at the boiler inlet and exhaust: The inlet temperature is controlled by the air fuel ratio, and a ratio of about 25:1 (with kerosene as fuel) will yield about 2300°F in a suitably designed burner [2]. During part-load conditions the air fuel ratio is increased to give lower inlet temperature as shown in the Figure 15 [2].

The exhaust gas temperature is estimated at about 300°F, which is verified in Section E3.C of this chapter.

(f) Steam supply pressure: This is selected as 500 psia for the reasons specified earlier.

(g) Boiler diameter: With the view of available space, a boiler shell of outside diameter of 14.0 inches is selected.

(h) Boiler efficiency: Boiler efficiency is calculated in Section E3 of this chapter.

(3) Details of Analysis

(a) Geometry: Figure 12 indicates the geometrical configuration of the boiler.

Important geometrical parameters are defined and calculated as follows:

(i) The gas side net frontal area is defined as

$$A_{fr,g} = \frac{\pi}{4} (D_o{}^2 - D_i{}^2)$$

where

$A_{fr,g}$ = Net frontal area on gas side,

D_o = Outside diameter of spiral,

D_i = Inside diameter of spiral,

and substituting for D_o and D_i, gives

$$A_{fr,g} = 0.844 \text{ sq ft.}$$

(ii) From Figure 9, the unrestricted or free flow area for flow of gases across one spiral of tubes for unit depth will be

$$A_{c,g} = (X_t d_o - d_o) \times (2n-1),$$

n = Number of turns,

where

$$X_t d_o = \text{Transverse pitch},$$

and the net frontal area will be

$$A_{fr,g} = X_t d_o (2n-1).$$

So the ratio of gas side free flow area to the gas side net frontal area will be

$$\sigma_g = \frac{A_{c,g}}{A_{fr,g}} = \frac{X_{t-1}}{X_t} ,$$

and for $X_t = 1.4$,

$$\sigma_g = 0.286.$$

(iii) Total gas side heat transfer area will be

$$A_g = \pi d_o L,$$

where

d_o = od of tubes,

L = Total length of the tubes.

The heat exchanger core volume for unit length of the tube will be (Figure 12)

$$V_u = (X_t d_o)(X_l d_o),$$

and for length of tube L, it will be

$$V_{b,c} = X_t X_l d_o^2 \; L.$$

So the ratio of total gas side heat transfer area to the heat exchanger core volume will be

$$\alpha_g = \frac{A_g}{V_{bc}} = \frac{\pi}{X_t X_l d_o} ,$$

and for

$X_t = 1.4,$

$X_l = 1.0,$

$d_o = 0.5$ inch,

$\alpha_g = 54.0 \quad ft^2/ft^3.$

Next, the gas side flow passage hydraulic radius is determined; this is defined as the area of the passage filled with the fluid, divided by the wetted perimeter. It can be arrived at by taking the ratio of previously determined two quantities σ_g and α_g.

So the hydraulic radius for the gas side flow passage is

$$r_{h,g} = (\frac{\sigma}{\alpha})_g = 0.0053 \text{ ft.}$$

(b) Flow rates: The water flow rate is determined to be 225 lbs/hr. The gas flow rate can be estimated from basic heat transfer relations, as follows:

$$\overset{\circ}{M}_g (T_i - T_o) \times C_p = \overset{\circ}{M}_w \times \Delta H_w \quad (4.1),$$

where

$\overset{\circ}{M}_g$ = Mass flow rate of gas,

T_i = Gas temperature inlet to the boiler,

T_o = Exhaust gas temperature from the boiler,

C_p = Average specific heat of the gases,

$\overset{\circ}{M}_w$ = Mass flow rate of water,

ΔH_w = Enthalpy required to form dry saturated steam at 500.0 psia, from the feed water at 200°F.

Substituting the following values in equation 4.1:

T_i = 2300°F,

T_o = 300°F,

C_p = 0.27 BTU/lb °F,

$\overset{\circ}{M}_w$ = 225.0 lbs/hr,

ΔH_w = 1080 BTU/lb.

The value of mass flow rate of gas is found to be $\overset{\circ}{M}_g$ = 426.6 lbs/hr.

(c) Gas temperatures: Gas temperatures throughout the boiler can be estimated by using the basic heat transfer relation; expressed by equation (4.1).

The boiler is divided into two sections.

1. Evaporator and,
2. Liquid heater.

In the evaporator section the saturated water is evaporated and dry saturated steam is generated. The heat transfer taking place can be expressed as

$$\overset{\circ}{M}_g (T_i - T_{ob}) \times C_p = \overset{\circ}{M}_w \times \Delta H_s \, . \qquad (4.2)$$

where

$\overset{\circ}{M}_g$ = Mass flow rate of hot gases,

T_i = Gas temperature at inlet to boiler,

T_{ob} = Gas temperature at outlet to boiling region,

C_p = Average specific heat of hot gases,

$\overset{\circ}{M}_w$ = Mass flow rate of water,

ΔH_s = Enthalpy of evaporation to dry saturated steam at 500 psi from saturated water at 500 psi.

The values of the above quantities are

$\overset{\circ}{M}_g$ = 426.6 lbs/hr, as calculated,

T_i = 2300°F,

C_p = 0.27 [13],

$\overset{\circ}{M}_w$ = 225.0 lbs/hr,

ΔH_s = 755.0 BTU/lbs.

Thus, T_{ob} is found to be 825°F.

In the same fashion, the exhaust temperature of the gases can be estimated using T_{ob} as temperature of gases at the inlet to the liquid heating region, and employing the same heat transfer relation (equation 4.1).

$$\overset{\circ}{M}_g(T_{ob}-T_o) \times C_p = \overset{\circ}{M}_w \times \Delta H_w. \qquad (4.3)$$

T_o = Exhaust gas temperature,

C_p = Average specific heat,

H_w = Enthalpy required to heat the water from 15 psi and 200°F to 500 psi and saturation temperature.

The values for these quantities are:

$\overset{o}{M}_g$ = 426.6 lbs/hr,

T_{ob} = 825.0°F,

C_p = 0.27,

$\overset{o}{M}_w$ = 225.0 lbs/hr,

H_w = 265.0 BTU/lbs.

Substituting these into equation 4.3, the value of T_o is found to be 304°F, which is in close agreement to the assumed value of 300°F.

In summary, the temperatures in various parts of the boiler are;

Boiling Region:

Inlet gas temperature = 2300°F,

Outlet gas temperature = 825°F.

Liquid Heating Region:

Inlet gas temperature = 825°F,

Outlet gas temperature = 300°F.

(d) Air side heat transfer coefficient and flow friction factor: The heat transfer coefficient is a function of temperature-dependent qualities such as viscosity, specific heat and density. Since the temperatures are known at the inlets and outlets of both the liquid heating and vapor heating sections the gas properties can be found using standard tables [13]. Heat transfer coefficients at all the local points can then be evaluated using the definition of Nusselt Number. Appropriate average value should be taken for each region.

The Nusselt number is a function of Prandtl and Reynold's numbers and the relationship can be expressed as

$$N_{nu} = \frac{h_{gc}}{C_p G_g} = f(N_{pr}, N_r) , \qquad (4.4)$$

where

N_{nu} = Nusselt number,

h_{gc} = Heat transfer coefficient due to convection,

C_p = Specific heat,

G_g = Mass flow rate of gas per unit area,

N_{pr} = Prandtl number,

N_r = Reynold number.

The Reynold's number N_r is given by

$$N_r = \frac{4r_h G_g}{\mu} ,$$

where

r_h = Hydraulic radius,

G_g = Mass flow rate of gas per unit area,

μ = Viscosity of gas in lbs/hr-ft.

The value of G_g can be found using the relation

$$G_g = \frac{\mathring{M}_g}{\sigma_g (A_{frg})} ,$$

where

$\mathring{M}_g$ = Gas flow rate,

σ_g = ratio of gas side free flow, area to the gas side net frontal area,

$A_{fr,g}$ = Gas side net frontal area.

Using the value of μ at different temperatures given by reference [14], the values of the Reynold's numbers are evaluated, and values of the Prandtl numbers and C_p are found from the references [13,14].

From equation 4.4 the heat transfer coefficient can be expressed as

$$h_{gc} = C_p G_g f(N_{pr}, N_r).$$

This relationship is expressed as

$$h_{gc} = C_p G_g C_h (N_{pr})^{-0.67} (N_r)^{-0.4} \qquad (4.5)\,[14]$$

where C_h is the correlation factor dependent on the tube arrangement. Using the equation 4.5 the values of h_{gc} are calculated and tabulated as shown in Table 4.2.

The value of friction factor f is given by

$$f = C_f N_r^{-0.18}, \qquad (4.6)\,[14]$$

where C_f is the correlation factor dependent on tube arrangement.

For $G_g = \dfrac{\mathring{M}_g}{\sigma_g(a_{fr,g})}$,

where

$$\mathring{M}_g = 426.6 \text{ lbs/hr},$$

$$\sigma_g = 0.286,$$

$$A_{fr,g} = 0.865 \text{ sq ft}.$$

The value of G_g is found to be

$$G_g = 1720.0 \text{ lbs/hr-sq ft}.$$

Values of C_h and C_f are

$C_h = 0.28$ Figure 13 [14],

$C_f = 0.22$ Figure 13 [14].

TABLE 4.2

CALCULATED VALUES OF h_{gc} AND FRICTION FACTORS

Temperature °F	Specific Heat BTU/LB	μ Viscosity LBS/ HR FT	N_r	N_{pr}	h_{gc} BTU/ HR FT °F	f
2300	0.296	0.14	260.0	0.65	20.56	0.084
820	0.257	0.08	455.0	0.66	14.12	0.078
300	0.244	0.06	607.0	0.68	11.7	0.069

These heat transfer coefficients are supplemented by the heat transfer due to radiation, which can be estimated as follows:

$$h_r = \frac{q_r}{T_g - T_w} \qquad (4.7)\ [17]$$

where

h_r = Heat transfer coefficient

q_r = Total radiative heat

T_g = Gas temperature

T_w = Wall temperature

Since the exhaust gases are largely of carbon dioxides and water vapor, the total radiative heat can be expressed as summation of radiation due to carbon dioxides and water vapor:

$$q_r = (q_r)_{CO_2} + (q_r)_{H_2O} .$$

$$(q_r)_{CO_2} = \sigma X \varepsilon_w [\varepsilon_{CO_2} T_g{}^4 - \varepsilon^1_{CO_2} T_w{}^4] \qquad (4.8)$$

$$(q_r)_{H_2O} = \sigma X \varepsilon_w [\varepsilon_{H_2O} T_g{}^4 - \varepsilon^1_{H_2O} T_w{}^4] \qquad (4.9)$$

where

σ = Stefan-Boltzman constant 0.173 X 10^{-8} BTU/hr-sq ft$°R^4$,

ε_w = Tube wall emissivity.

ε_{CO_2} and $\varepsilon^1_{CO_2}$ = Carbon dioxide emissivities at gas temperature T_g and wall temperature T_w respectively,

ε_{H_2O} and $\varepsilon^1_{H_2O}$ = Water vapor emissivities at gas temperature T_g and wall temperature T_w respectively,

T_g = Gas temperature in °R,

T_w = Wall temperature in °R.

The carbon dioxide and water vapor emissivities are given in graphical form in references [15,16], as a function of the product of equivalent gas layer length and partial pressures of carbon dioxide and water vapor. The equivalent gas layer length for the proposed tube configuration (Figure 12) is

$$L_{eq} = 3.0[X_t d_o - d_o] \qquad [17]$$

where

L_{eq} = Equivalent gas layer length,

X_t = Longitudinal pitch,

d_o = od of tube.

Substituting the values of X_t and d_o,

$$L_{eq} = 0.05'.$$

The partial pressures of carbon dioxide and water vapor are given by [4]

$$P_{CO_2} = \frac{8}{52.75 + 58.5\ X} ,$$

$$P_{H_2O} = \frac{8.5}{52.75 + 58.5\ X} .$$

The units are in atmospheres and the value of X is obtained from

$$X = \frac{(\frac{a}{f}) - (\frac{a}{f})_{st}}{(\frac{a}{f})_{st}} .$$

$(\frac{a}{f})$ = Air fuel ratio,

$(\frac{a}{f})_{st}$ = Stoichometric air fuel ratio.

For $(\frac{a}{f})$ = 25.0, and

$(\frac{a}{f})_{st}$ = 14.9 (for Kerosene) [4].

The value of X = 0.67.

The partial pressures are:

P_{CO_2} = 0.0865 atm,

P_{H_2O} = 0.0919 atm,

and

$P_{CO_2}L_{eq}$ = 0.0043 atm-ft,

$P_{H_2O}L_{eq}$ = 0.0046 atm-ft.

The tube wall temperature is assumed to be 100°F above the steam or water temperature inside. This assumption is verified in Section E of this chapter.

The respective emissivity and heat transfer coefficients are calculated using equations 4.8 and 4.9 and are tabulated in Table 4.3.

(e) Water side heat transfer coefficient: the heat transfer taking place from the tube surface to the flowing water occurs due to convection. This depends primarily on type of flow i.e. turbulent or laminar. When the Reynold's number exceeds 3000, the flow is termed as turbulent and the heat transfer coefficient is larger than for laminar flow [16].

The Reynold's number is defined as

$$N_R = \frac{d_i G}{\mu}$$

where

N_R = Reynold's number,

d_i = Inside diameter of the tube,

G = Mass rate of flow for unit area,

μ = Dynamic viscosity.

At this stage it is necessary to assume a tube wall thickness, which will be checked later on for strength. Since the outside diameter of the tube is 0.5 in an assumed thickness of 0.05 in, will give

TABLE 4.3

CALCULATED VALUE OF HEAT TRANSFER COEFFICIENT

T_g °R	ε_{CO_2}	ε_{H_2O}	T_w °R	$\varepsilon^1_{CO_2}$	$\varepsilon^1_{H_2O}$	$(q_r)_{CO_2}$ BTU/HR-FT^2	$(q_r)_{H_2O}$ BTU/HR-FT^2	h_r	h_{gc}	h_g
2760	0.0095	0.00	1020	0.019	0.014	754.16	0	0.38	20.56	20.94
1285	0.019	0.008	1020	0.019	0.014	62.92	23.72	0.17	14.12	14.29
760	0.019	0.014	760	0.019	0.014	0.0	0	0	11.70	11.70

Average $h_{g\ \text{boiling}}$ = 17.61

Average $h_{g\ \text{liquid}}$ = 13.0

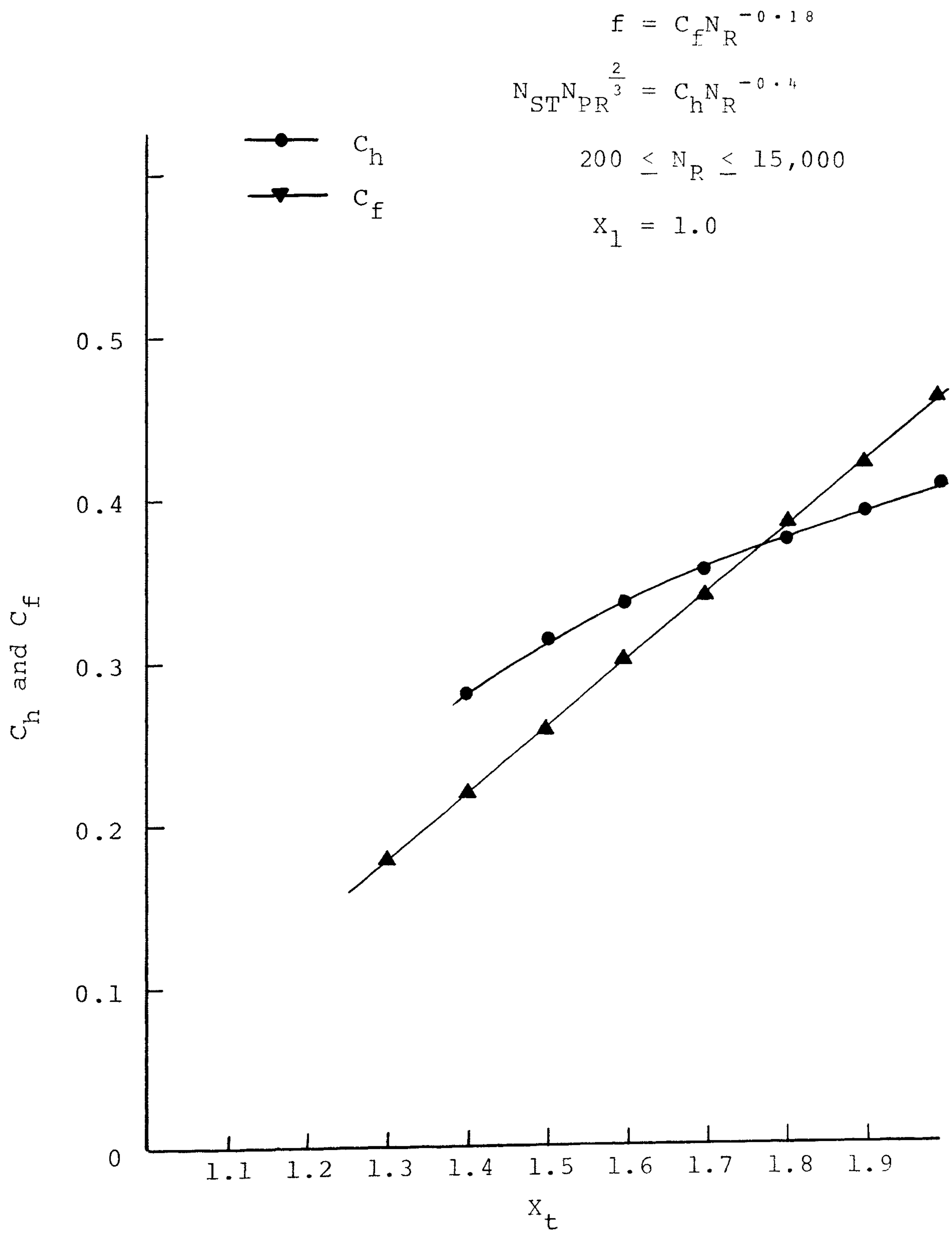

Figure 13. Approximate Heat Transfer Correlation and Friction Factor for Flow Normal to the bank of Staggered Tubes [14].

inside diameter of 0.4 ins.

The mass flow rate per unit area will be

$$G_w = \frac{\overset{\circ}{M}_w}{\frac{\pi}{4}(d_i)^2},$$

where

G_w = Mass flow rate of water per unit area,

$\overset{\circ}{M}_w$ = Mass flow rate of water,

d_i = Inside diameter.

Substituting $\overset{\circ}{M}_w$ = 225.0 lbs/hr,

and d_i = 0.4 in, gives

$G_w = 257.96 \times 10^3$ lbs/hr-sq ft.

Substituting this value of G_w, and the value of dynamic viscosity for water at 200°F, i.e. μ = 0.0654 lbs/hr-ft [14] into the equation defining Reynold's number gives

$N_R = 13747.$

This indicates that the flow is highly turbulent and is ideal for desired heat transfer [15].

The heat transfer coefficient for

for this type of forced convection obtained from

$$h_w = 0.023\left(\frac{K}{d_i}\right)(N_{PR})^{0.4}(N_R)^{0.8}\left[N_R\left(\frac{d_i}{D_M}\right)^2\right]^{0.05} \qquad (4.10)\ [4]$$

where

h_w = Heat transfer coefficient,

K = Thermal conductivity of water,

N_{PR} = Prandtl Number,

N_R = Reynold Number,

d_i = Inside diameter of tube,

D_m = Mean diameter of spiral.

The mean diameter can be found by using

$$D_m = D_o\left[0.5\left(1+\left(\frac{D_i}{D_o}\right)^2\right)\right]^{0.5} \qquad (4.11)\ [4]$$

where

D_o = Outside diameter of the spiral,

D_i = Inside diameter of the spiral.

Substituting:

D_o = 1.1 ft,

D_i = 0.366 ft in equation (4.11).

D_m is found to be = 0.82 ft. Finally substituting the following values found from standard tables [14], into equation (4.10), the value of h_w can be obtained, at the entrance of liquid heating region:

$K = 0.395$ BTU/lb-ft °F at 200°F,

$N_{PR} = 1.163$,

$N_R = 13147.9$ as calculated previously,

$d_i = 0.4$ inch,

$D_m = 0.82$ ft.

The heat transfer coefficient at 200°F is found to be

$$(h_w)_{200} = 768.0 \text{ BTU/hr-ft}^2 \text{°F}.$$

In the same way, at the end of liquid heating section where temperature is 460°F, the heat transfer coefficient is found to be

$$(h_w)_{460} = 1209.9 \text{ BTU/hr-ft}^2 \text{°F}.$$

The average of $(h_w)_{200}$ and $(h_w)_{460}$ is taken as the heat transfer coefficient for the entire liquid heating region:

$$(h_w)_l = 988.9 \text{ BTU/hr-ft}^2 \text{°F}.$$

The heat transfer coefficient in the boiling region is given by:

$$(h_w)_b = 3.6 \text{ X } (h_w)_l, \quad [15]$$

$(h_w)_b$ = Heat transfer coefficient in boiling region,

$(h_w)_l$ = Heat transfer coefficient in liquid heating region,

$(h_w)_b$ = 3580.18 BTU/hr-ft^2°F.

(f) Overall heat transfer coefficient: The overall heat transfer coefficients for both liquid heating and boiling can now be expressed as follows [4].

$$\frac{1}{U_l} = \frac{1}{(h_g)_l} + \frac{1}{(\frac{d_i}{d_o})(h_w)_l} + \frac{2d_o t_t}{K_t(d_i+d_o)} \quad (4.12)$$

$$\frac{1}{U_b} = \frac{1}{(h_g)_b} + \frac{1}{(\frac{d_i}{d_o})(h_w)_b} + \frac{2d_o t_t}{K_t(d_i+d_o)} \quad (4.13)$$

where

U_l = Overall heat transfer coefficient of liquid heating,

U_b = Overall heat transfer coefficient for boiling region,

$(h_g)_l$ = Gas side heat transfer coefficient in liquid heating,

$(h_g)_b$ = Gas side heat transfer coefficient in boiling region,

$(h_w)_l$ = Water side heat transfer coefficient in liquid heating,

$(h_w)_b$ = Water side heat transfer coefficient in boiling,

d_i = Inside diameter of tube,

d_o = Outside diameter of tube,

t_t = Tube thickness,

K_t = Conductivity of tube.

Substituting appropriate values and

K_t = 215.0 BTU/hr °F ft, in equations (4.12, 4.13).

The overall heat transfer coefficients are found to be

U_l = 12.78 BTU/hr °F sq ft,

U_b = 17.50 BTU/hr °F sq ft.

(g) Calculation of tube length: The length of tube required can be calculated from the necessary area based on simple heat-transfer.

Heat gained by water = Heat lost by gases.

$$A_l U_l (\Delta T)_{lm} = \mathring{M}_g X C_p X (T_{in} - T_{out}) \quad (4.14)$$

where

A_l = Area required in liquid heating,

U_1 = Overall heat transfer coefficient,

$(\Delta T)_{lml}$ = Log mean temperature difference for liquid heating,

$\overset{\circ}{M}_g$ = Mass flow rate of gases,

C_p = Specific heat of gases,

$T_{in}-T_{out}$ = Temperature drop in the gases.

The log mean temperature* is given as

$$(\Delta T)_{lml} = \frac{(T_{bo}-T_s)-(T_o-T_{wi})}{\ln\left(\frac{T_{bo}-T_s}{T_o-T_{wi}}\right)}$$

After substituting the values of all temperatures, the log mean temperature is found to be

$$(\Delta T)_{lml} = 187.0\ {}^\circ F.$$

Substituting the following values in equation (4.14)

U_1 = 12.78 BTU/hr °F sq ft,

$\overset{\circ}{M}_g$ = 426.6 lb/hr,

C_p = 0.27 BTU/lb, gives

---

*A schematic diagram of boiler and a temperature profile are shown in Figure 14.

$T_{in}-T_{out} = 525°F.$

The necessary area for liquid heating is found to be

$A_l = 25.30$ sq ft.

The length of tube in the spiral is

$l = \pi D_m n$

where

l = Total length,

D_m = Mean diameter,

n = Number of turns.

Thus for

$D_m = 0.82$ ft,

and

$n = 6.0$ turns.

The length of tube in one spiral will be

$l = 15.3$ ft,

The surface area of one spiral will be

$a_s = \pi d_o l,$

where

a_s = Surface area,

d_o = Outside diameter,

l = Length of tube.

For

$d_o = 0.5$ in,

$l = 15.3$ ft,

$a_s = 2.0$ sq ft.

The number of spirally wound tubes required is obtained from A_L/a_s. For liquid heating, the number of tubes is 12.65, say 13.

Similarly for the boiling region, equation (4.14) takes the form of

$$A_b U_b (\Delta T)_{lmb} = \mathring{M}_g C_p (T_{in} - T_{out}) \qquad (4.16)$$

where

A_b = Area required for boiling,

U_b = Overall heat transfer coefficient for boiling,

$(\Delta T)_{lmb}$ = Log mean temperature difference for boiling,

$\mathring{M}_g$ = Mass flow rate of gases,

$T_{in}-T_{out}$ = Temperature drop in the gases.

The log mean temperature* difference is given by,

$$(\Delta T)_{lmb} = \frac{(T_i - T_s) - (T_{bo} - T_s)}{\ln\{\frac{T_i - T_s}{T_{bo} - T_s}\}} \qquad (4.17)$$

---

*A schematic diagram of boiler and temperature profiles are shown in Figure 14A.

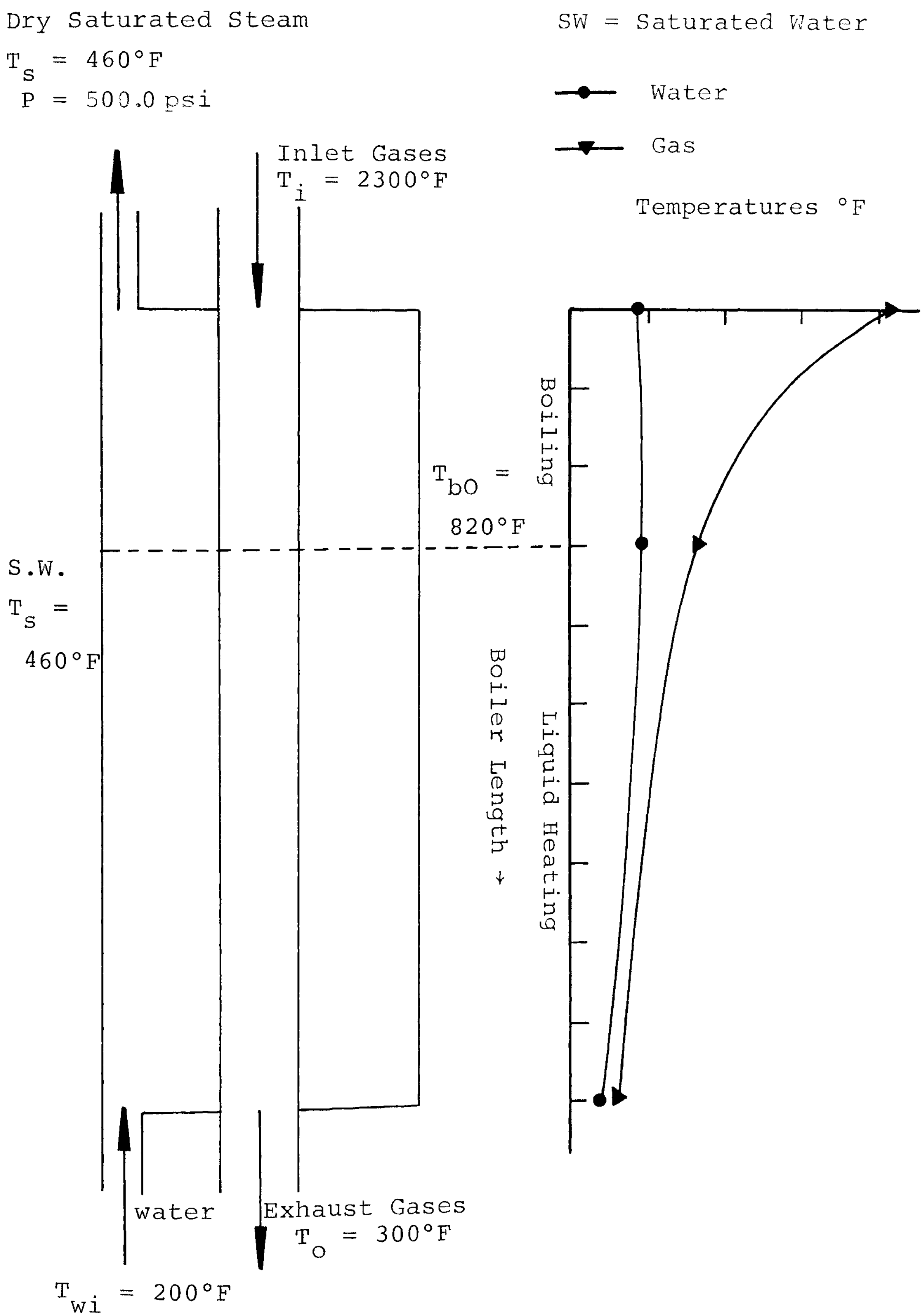

Figure 14A. Boiler and Temperature Profiles Schematic.

Substituting the values of temperature in equation (4.16)

$$(\Delta T)_{lmb} = 911.8°F.$$

The necessary area for the boiling region is calculated by substituting the following values in equation (4.16).

$$U_b = 6.75 \text{ BTU/hr-°F-ft},$$
$$(\Delta T)_{lmb} = 911.8°F,$$
$$\overset{\circ}{M}_g = 426.0 \text{ lbs/hr},$$
$$C_p = 0.287 \text{ BTU/lb/°F},$$
$$T_{in}-T_{out} = 1475°F.$$

The area is found to be

$$A_b = 11.31 \text{ sq ft},$$

and the number of tubes required will be 5.65, say 6.

(h) Tube wall temperatures: At this point it is necessary to check the tube wall thickness estimate made earlier. This requires knowledge of the maximum tube wall temperature in each region, because the strength of tubes depend on temperature, as shown in Figure 11.

Figure 14B, indicates the temperature profile in the tube. The tube wall temperatures may be determined from the

the heat balance equation. Since for steady state conditions the heat rate through the two fluid films equals the heat rate through the tube wall [4]:

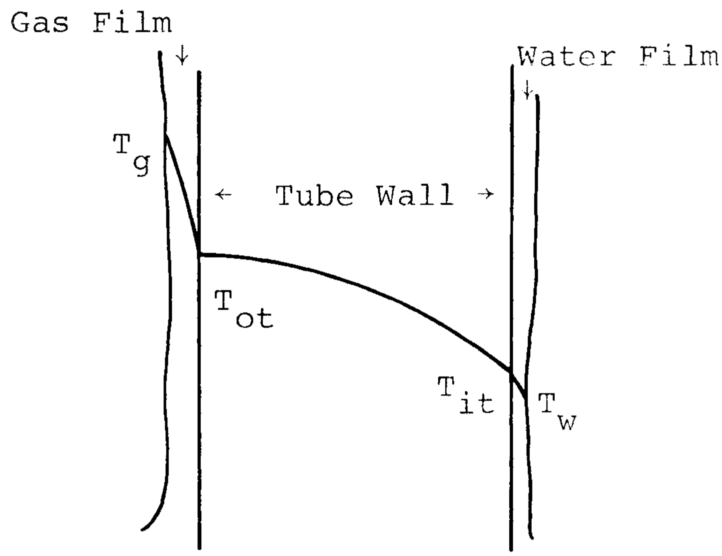

Figure 14B. Temperature Profile Across the Tube Wall.

$$q = A_g h_g (T_g - T_{ot}) = A_w h_w (T_{it} - T_w) =$$

$$\frac{A_m K}{t_t} (T_{ot} - T_{it}), \tag{4.18}$$

where

q = Steady state heat transfer rate,

A_g = Tube area on gas side,

A_w = Tube area on water side,

A_m = Mean area,

h_g = Heat transfer coefficient on gas side,

h_w = Heat transfer coefficient on water side,

K = Thermal conductivity of the tube,

t_t = Thickness of the tube,

T_g = Gas film temperature,

T_{ot} = Tube wall outside temperature,

T_{it} = Tube wall inside temperature,

T_w = Water film temperature.

A_g, A_w and A_m can be expressed as follows:

$$A_g = \pi d_o l,$$

$$A_w = \pi d_i l,$$

$$A_m = (A_g + A_w)/2,$$

where

d_o = Outside diameter of tube,

d_i = Inside diameter of tube,

l = Tube length.

Rearranging equation (4.18), yields

$$T_{it} = T_{ot} - \frac{h_g(T_g - T_{ot})\left(\frac{t}{K}\right)_t}{\left(1-\frac{t}{d_o}\right)}, \qquad (4.19)$$

$$T_{it} = T_w + \frac{h_g}{h_w}\frac{(T_g - T_{ot})}{\left(1-\frac{2t}{d_o}\right)}. \qquad (4.20)$$

Equation 4.19 and 4.20 can be solved simultaneously for T_{it} and T_{ot} at various sections of the boiler; the results are tabulated in Table 4.4.

(i) Pressure drops in tube: Since the tube diameter is small, there is considerable pressure drop for the water flow, particularly inside the boiling region where two-phase flow occurs.

The friction factor for the flow is given by

$$f = 0.046(N_R)^{-0.2}\left[N_R\left(\frac{d_i}{D_m}\right)^2\right]^{0.05} \qquad [4]$$

where

f = Friction factor,

N_R = Reynold's number,

d_i = Inside diameter of tube ,

TABLE 4.4

CALCULATED VALUES OF TUBE WALL TEMPERATURES

Section	T_g °F	T_w °F	h_g BTU/ Hr Ft^2 °F	h_w BTU/ Hr Ft^2 °F	T_{ot} °F	T_{it} °F
Inlet to Liquid Heating	300	200	11.70	768.0	293.6	293.5
Inlet to Boiling Region	825	460	14.29	1209.9	466.5	465.2
Outlet to Boiling Region	2300	460	20.94	3580.18	482.3	473.0

D_m = Mean diameter of coil

For the liquid heating region:

N_R = 13147. [page 53]

d_i = 0.4 in

D_m = 0.82 ft (4.11).

Thus the friction factor for the liquid heating region is

$f_l = 0.00769$;

and for boiling region,

$f_b = 0.00708$.

The pressure drop for liquid heating is given by

$$\Delta P_{wl} = \frac{f_l G^2}{d_i g} L_t \{V_l + V_{sat}\} \qquad (4.21)[18]$$

where

ΔP_{wl} = Pressure drop in liquid heating region

f_l = Friction factor for liquid heating

G = Mass flow rate of water per unit area

g = Gravitational constant

L = Length of the tube

V_l = Specific volume of water

V_{sat} = Specific volume of saturated water.

Substituting the following, previously calculated values in equation (4.21):

$f_l = 0.00769$,

$G = 257.96 \times 10^3$ lbs/hr--ft °F,

$L = 15.3 \times 13$ ft,

$V_l \simeq V_{sat} = 64.45$ in^3/lbs [16],

$g = 32.2$ ft/sec^2.

The pressure drop is found to be

$\Delta P_{wl} = 4.79$ psia.

The pressure drop for the boiling region is given by [18].

$$\Delta P_{wb} = \frac{V_l G^2}{g} r_2 + \frac{2 f_b G^2 V_l l}{g d_i} r_3 \qquad (4.22)$$

where

ΔP_{wb} = Pressure drop for boiling region,

V_l = Specific volume of steam,

G = Mass flow rate of water per unit,

g = Gravitational constant,

r_2 = Acceleration pressure drop multiplier for boiling flow of steam and water,

r_3 = Friction pressure drop multiplier for boiling flow of water and steam,

f_b = Friction factor in the boiling region.

Substituting the following values in equation (4.22), the pressure drop is calculated:

$V_l = 0.9278\ ft^3/lb$ [16],

$G = 257.96 \times 10^3\ lbs/hr\text{-}ft^2\,°F$,

$g = 32.2\ ft/sec^2$,

$r_2 = 45.0$ [18],

$f_b = 0.00708$,

$r_3 = 24.0$ [18].

The pressure drop is found to be

$P_{wb} = 145.2$ psia.

Therefore the total pressure drop is

$\Delta P_t = \Delta P_{wl} + \Delta P_{wb}$,

$\Delta P_t \simeq 150.0$ psia.

As a result, the boiler feed pump should develop a pressure of 650 psia.

Next, the required minimum tube thickness will be calculated according to

$$t_t = \frac{P_w d_o}{2S} \qquad (4.23)\,[4]$$

where

t_t = Minimum tube thickness,

P_w = Pressure inside the tube,

d_o = Outside diameter of tube,

S = Allowable stress.

Substituting the following value in equation (4.22),

P_w = 650.0 psi,

d_o = 0.5 in,

$S = 25 \times 10^3$ psi (Figure 11).

The minimum thickness is found to be

$t = 0.006$ in.

Hence the selected thickness of 0.05 in is adequate.

(j) Boiler feed pump: A boiler feed pump delivers the condensate from the condenser to the boiler. Here the pump has to deliver 225.0 lbs/hr (i.e. 0.475 gmp) of water at 650.0 psia.

The hydraulic h.p. will be

$$\text{h.p.} = \frac{H X gpm}{1714} \qquad [16]$$

where

H = Head in psia,

gpm = Fluid flow in gallons per minute,

Substituting

$$H = 650.0 \text{ psia}$$

$$\text{gpm} = 0.47$$

the hydraulic h.p. is found to be 0.17 and with 50% mechanical efficiency it will be 0.34 h.p. This is relatively small; the maximum power consumption of the pump will therefore be less than 0.5 h.p., the value assumed in Chapter II. A motor driven positive displacement pump is usually adopted because the pressure to be developed is relatively high. It is necessary to select electric motor drive so the pump can be started to generate steam during starting while the engine is at rest. Besides, it will be possible to run the pump in only one direction, even when engine is reversed.

(k) Gas side pressure drop and blower power.

The gas side pressure drop is given by

$$\left(\frac{\Delta P}{P_1}\right) = \frac{G^2}{2g}\left\{\frac{V_1}{P_1}\right\}\left\{(1+\sigma^2)\left(\frac{P_1T_2}{P_2T_1}-1\right) + f\frac{L}{V_1}\left(\frac{P_1T_2}{P_2T_1}+1\right)\right\} \qquad (4.24)\ [14]$$

where

$(\frac{\Delta P}{P_1})$ = Relative pressure differential across tube stack,

P_1 = Exhaust pressure from burner,

G = Gas mass flow rate per unit area,

g = Gravitational constant,

R = Universal gas constant,

T_1 = Inlet gas temperature,

σ = Ratio of free flow area to total area,

P_2 = Exhaust pressure at boiler stack,

T_2 = Exhaust temperature,

f = Fanning factor [Table 3.2],

L = Length of flow,

V_h = Flow passage hydraulic radius.

Substituting the following values in equation 4.23:

G = 1720.0 lbs/hr-ft sq,

g = 32.2 ft/sec^2,

R = 53.3 lb-ft °R,

T_1 = 2760°R,

σ = 0.286 [page],

T_2 = 760°R,

$f = 0.068$ (average),

$l = 12.5$ in,

$V_h = 0.064$ ft,

the pressure drop evaluated in terms of inlet and outlet pressure will be

$$\left(\frac{\Delta P}{P_1}\right) = \frac{3173.68}{P_1^2} + \frac{1184.6}{P_2} .$$

But since

$$P_2 = P_1 - \left(\frac{\Delta P}{P_1}\right) P_1 ,$$

the equation 4.23 reduces to the form of

$$P_2 + \frac{1184.6}{P_2} = P_1 - \frac{3173.63}{P_1} .$$

For $P_2 = 16.0$ psia exhaust pressure the value of P_1 is found to be slightly higher than 16.0 psia. This indicates that the pressure drop across the tubing stack is negligible relative to the pressure drop across the burner.

However a substantial pressure drop may occur across the burner. For a 10.0 in diameter burner a pressure drop of 51.0 in of water i.e. about 1.83 psia occurs for a typical GM burner design

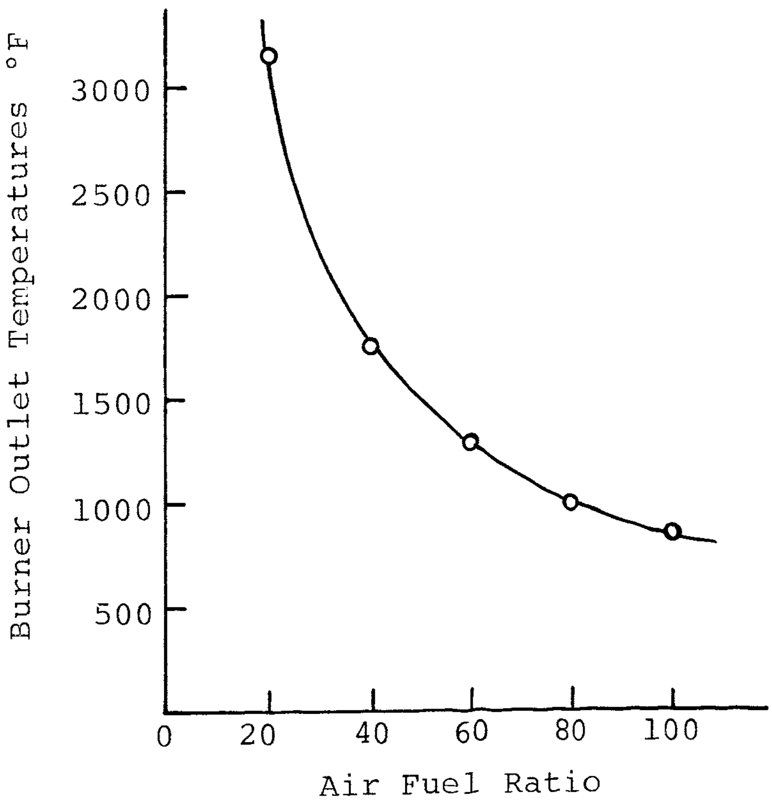

Figure 15. Burner Outlet Temperature Versus Overall Air Fuel Ratio [2].

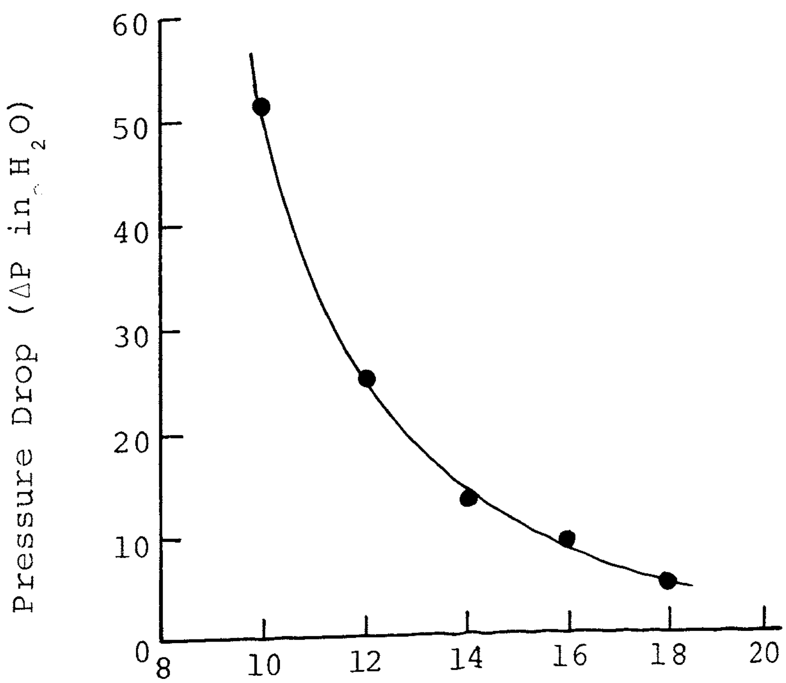

Figure 16. Effect of Burner Diameter on Burner Pressure Drop [2].

(Figure 16). So if the boiler exhaust pressure is 16.0 psia i.e. a blower should be designed for about 11% pressure drop.

The blower power can be estimated by

$$P_{bl} = \overset{\circ}{M}_a C_p T_1 [(1+\frac{\Delta P}{P})^{\frac{\nu-1}{\nu}} - 1] \quad (4.25)\ [4]$$

where

P_{bl} = Ideal blower power,

$\overset{\circ}{M}_a$ = Amount of air handled per hour,

C_p = Specific heat of air,

T_1 = Air inlet temperature,

$\frac{\Delta P}{P}$ = Percentage pressure drop.

Substituting the following values in equation 4.24:

$\overset{\circ}{M}_a$ = 460.0 lbs/hr,

C_p = 0.24 at temperature 80°F,

T_1 = 80°F,

$\frac{\Delta P}{P}$ = 0.11,

ν = 1.4 adiabatic index of air.

The blower power P_{bl} is found to be P_{bl} = 1790.0 BTU/hr or 0.7 h.p., and with 80% mechanical efficiency the power required will be 0.875 h.p., which is slightly higher than assumed value of 0.5 hp in Chapter II.

(1) Combustion system: The combustion system consists of fuel tank, fuel pump, atomizer, igniter and blower. Conventional types of fuel tank, fuel pump and atomizer can be employed. The design of burner is very important to control pollution and improve system efficiency. Unfortunately there is very little literature available about modern burners and very little published research data exist.

Engineers at General Motors have designed a burner which gives the burner gas outlet temperature and air fuel ratio characteristic as shown in Figure 15. The fuel used was kerosene.

A typical arrangement is to mount the burner on top of the boiler; in this study, however, the burner is located beneath the boiler and an air preheating chamber is employed as shown in Figure 10. Again, as mentioned previously the drive for the pump and blower should be electric and independent of engine speed. This is necessary because when the engine load increases, engine speed decreases and simultaneously the steam requirement increases as late cut-off* is applied to meet the load. If the blower speed is proportional to the engine speed, it will slow down and consequently amount of heat supplied to the boiler will be reduced, which will reduce the amount of steam generated. The burner diameter is limited to 10.0 ins because of the space limitation. Futher reduction in diameter will lead to excessive pressure drop as indicated in Figure 16.

(m) Boiler control: The two variables to be controlled in a boiler are steam pressure and temperature. The pressure can be regulated by controlling the fuel rate and hence changing the air fuel ratio for a constant blower speed. To accomplish this a pressure sensor in the boiler can control a metering valve in the fuel line, which can increase or decrease the flow rate as needed [2].

*Cut-off is defined as ratio of volume of steam admitted inside to the volume of steam at the end of expansion.

The temperature can be controlled by controlling the rate at which feed water is supplied to the boiler. General Motors has developed a bimetalic element temperature sensor [2]. A thin walled tube of high expansion stainless steel enclosing a ceramic rod is placed into the direct steam flow to sense temperature and control feedwater flow. When the temperature reaches the operating limit, this sensor operates a solenoid valve to meter more water into the boiler [2].

(n) Fuel analysis and boiler efficiency: As discussed previously, the air fuel ratio of 28:1 for kerosene (C_8H_{18}) gives 2300°F inlet temperature to the boiler flue gases. The total amount of flue gases is 462.0 lbs/hr for maximum continuous rating. These can be expressed as follows:

$$\frac{a}{f} = 28.0$$

$$a+f = 462.0$$

where

a = Weight of air

f = Weight of fuel.

Solving the above two equations simultaneously the weight of fuel per hour is found to be f = 15.9 lbs/hr and weight of air 446.1 lbs/hr.

The amount of air required for complete combustion can be calculated from the combustion equation as follows:

$$2C_8H_{18} + 25O_2 = 16CO_2 + 18H_2O \quad [6],$$

and substituting molecular weights it is found that 1.0 lbs of C_8H_{18} fuel will require 1.9 lbs of oxygen or 8.3 lbs of air for complete combustion. So for the fuel rate of 15.9 lbs/hr, the minimum amount of air required for complete combustion will be 132.0 lbs/hr. Hence the amount of excess air supplied is 314.1 lbs/hr which should eliminate unburned hydrocarbons and carbon moxonides from the exhaust gases.

The thermal efficiency of the boiler is defined as heat gained by generated steam to the heat available from fuel [6].

The heat gained by generated steam is 225,000 BTU/hr for a continuous load of 20 h.p. The calorific value of the fuel is about 18,000 BTU/lb and so the amount of heat generated per hour will be

18,000 BTU/lb X 15.9 lbs/hr

= 290,000 BTU/hr.

Hence the boiler thermal efficiency at maximum continuous load is about 75.%.

This concludes the boiler design and it can be tabulated as follows in Table 4.5.

TABLE 4.5

BOILER DESIGN

Parameters	Values
Overall Dimensions:	
Outside diameter D_o	14.0 inches
Length (including burner assembly)	28.0 inches
Weight	190 lbs.
Tube Geometry	
Number of tube rows	19
Number of coils per row	6
Longitudinal pitch X_l	1.0
Transverse pitch X_t	1.4
Total heat transfer area	38 sq. ft.
Outside tube diameter	0.5 inch
Tube wall thickness	0.05 inch
Tube length total	290 ft.
Boiling region	92 ft.
Liquid region	198 ft.
Gas Side Characteristics:	
Gas flow	426.0 lbs./hr.
Total pressure drop on gas side	51.0 in. of H_2O

TABLE 4.5 (Continued)

Parameter	Values
Blower power	0.5 h.p.
Gas inlet temperature	2300°F
Gas outlet temperature	300°F
Average Heat Transfer Coefficient on Gas Side:	
Boiling region	17.61 BTU/hr.-ft. °F
Liquid heating region	13.0 BTU/hr.-ft. °F
Water Side Characteristics:	
Water flow	225.0 lbs./hr.
Outlet pressure (steam)	500.0 psia
Inlet pressure	650.0 psia
Outlet temperature	460°F
Inlet temperature	200°F
Feed pump power	0.5 h.p.
Heat transfer rate	225,000.0 BTU/hr.
Ratio of water flow to shaft power	10.5 lbs./h.p.-hr.
Boiler efficiency	75%

V. STEAM EXPANDER

A. Introduction

There are two types of steam expander to convert the heat energy of steam into mechanical energy. They can be classified as follows:

(1) Continuous flow machine,

(2) Positve displacement machine.

The first class includes the steam turbine, in which high pressure steam is continuously flowing and expanded. In the second class some quantity of steam is admitted and that quantity is expanded within the machine to develop mechanical work. The conventional crank and piston type of reciprocating engine is included in this class.

B. Choice of the Machine

The choice between these two types is very important. The turbine is very attractive, because of its compactness, smooth torque production and freedom from annoying vibration. In addition, because the bearing surfaces are well removed from the working fluid, the turbine is free from major lubrication problems. Nearly universal use of steam turbines in central power stations testifies to their reliability. But when the power plant output is scaled down by four or five orders of magnitude to the automotive power range, the steam turbine does not remain attractive for the following reasons [2].

(1) In power plant turbine practice, steam is expanded from 2500 psi to 5 psi. Thus the ratio of expansion is around 500, and in automotive applications, the present practice is to expand steam from about 1000 psi to 15.0 psi giving a ratio of expansion around 70.0. For such a low expansion ratio a turbine is not suitable.

(2) If a typical steam turbine is to expand 1000 psi, 960°F steam, it will require five axial stages to expand the steam efficiently to atmospheric pressure. In the automotive power range of 15 to 200 hp such a turbine would have a diameter of 2.5 inches and would require a rotational speed of about 100,000 rpm. A 50:1 reduction would then be needed to attain automotive drive line speeds.

(3) A turbine requires clean, superheated steam. This requirement will increase system maintenance and boiler cost.

In general, at low volumetric flow rates a positive displacement device is more efficient and convenient than a steam turbine. For these reasons, a positive displacement machine is selected rather than a turbine [2,3].

Instead of a conventional piston and crank type reciprocating machine, an inversion of the slider crank mechanism is employed. This engine consists of a cylindrical housing, cover plates, an oblong rotor, and an output shaft having cylindrical ends and a square central section.*

The geometry of these parts is illustrated in figures.

C. Description of the Components

(1) Housing: (Figure 17) The housing is a cylinder of an internal radius R and width B, provided with suitable inlet and exhaust steam ports and flanges for cover plates, (Figure 17). The shaft axis passes through the point O_2 and rotates in bearings located on the cover plates. The eccentricity O_1O_2 is one fifth of the housing radius R. Two steam ports for exhaust and inlet are located as shown.

(2) Rotor: The rotor is of oblong shape, formed by two arcs of a circle with radius equal to the housing radius. The zero degree position of the rotor housing assembly is shown in Figure 18.

---

*Author has worked on similar kind of pump in India during his undergraduate work. This pump was originally designed by Dr. C. S. Shah, Professor in Mechanical Engineering at B.V.M. Engineering college, S.P. University, Gujrut.

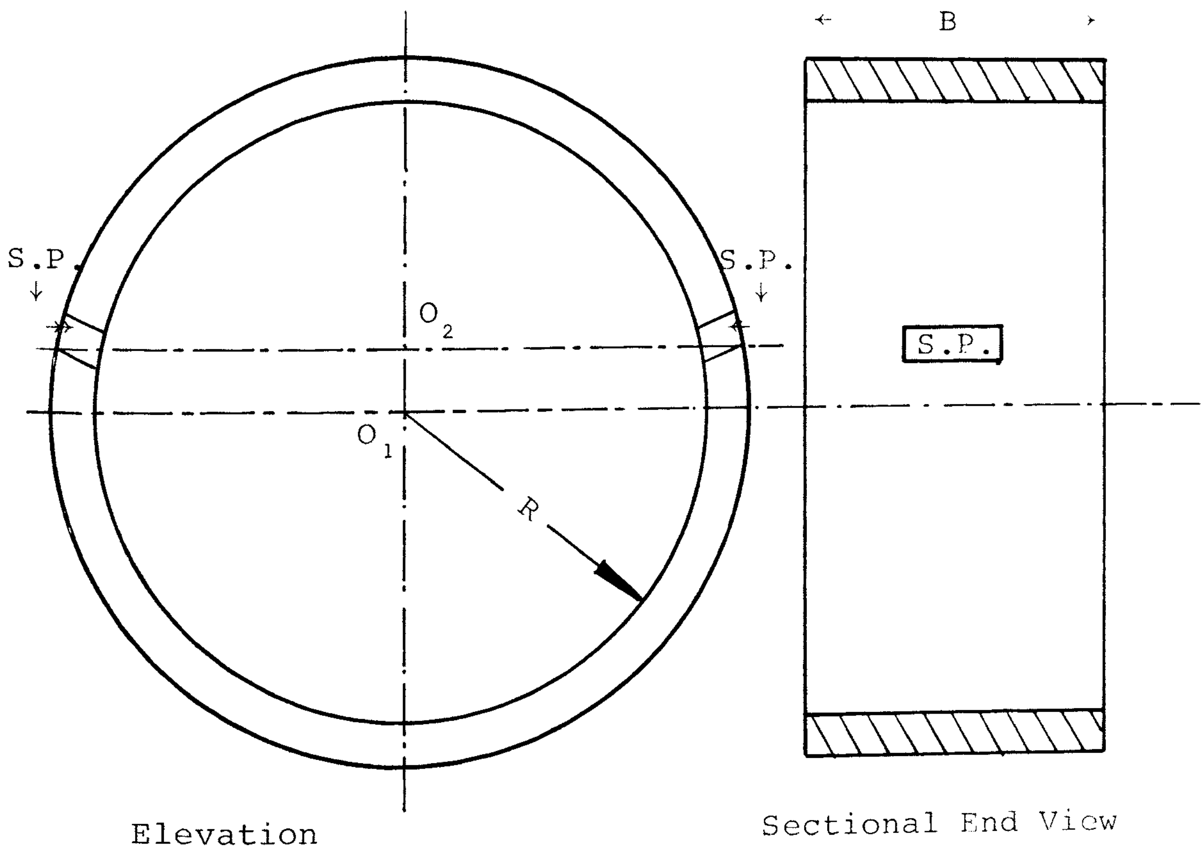

Figure 17. Housing.

O_1 = Geometric Center

O_2 = Shaft Center

R = Radius

B = Width

O_1O_2 = R/5

SP = Steam Ports

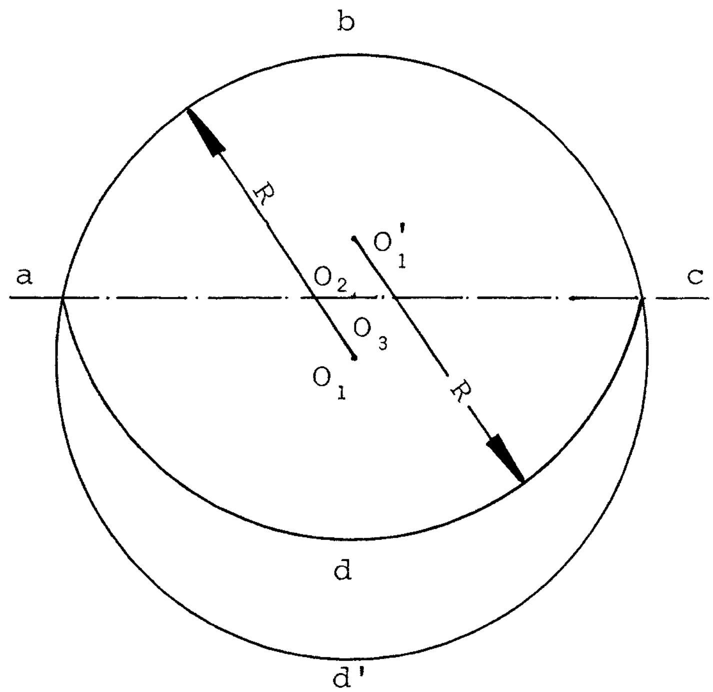

Figure 18. 0° Rotor Position

abcda = Rotor

abcd'a = Housing

O_1 = Housing Center and Center for Rotor Arch abc

O_2 = Shaft Center

O_3 = Rotor Center Coinciding With O_2 for Zero Degree Position

O_1' = Center for Rotor Arch adc

ac = Major Axis of the Rotor

bd = Minor Axis of the Rotor

R = Housing Radius

O_1O_2 = R/5

The values of rotor major and minor axes in terms of housing radius can be evaluated by referring to Figure 18.

$$\frac{1}{2}\, ac = aO_2 = [(aO_1)^2 - (O_1O_2)^2]^{0.5}$$

$$\frac{1}{2}\, bd = bO_2 = [(bO_1) - (O_1O_2)]$$

Substituting $aO_1 = bO_1 = R$,

$O_1O_2 = R/5$,

the values of ac and bd are found to be

$$ac = \frac{2}{5}\sqrt{24}\ R$$

$$bd = 2 \cdot \frac{4}{5}\ R.$$

The rotor is provided with a rectangular slot as shown in Figure 19. The square section of the output shaft fits into this hole. The rotor reciprocates relative to the shaft; hence the hole length should be adequate to prevent contact between the shaft and the ends of the slot. At the rotor ends "a" and "c" spring loaded seals (Figure 19) are provided to stop leakage.

(3) Output Shaft: The output shaft is as shown in Figure 20. The square section fits in the

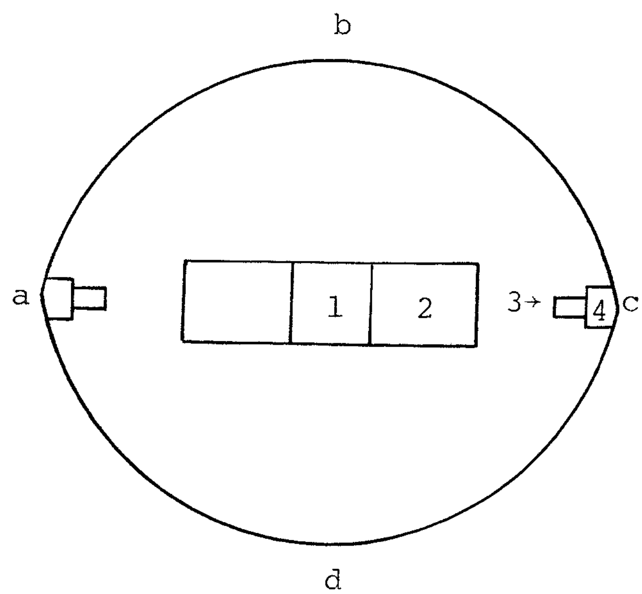

Figure 19. Rotor and Output Shaft

abcd = Rotor

1 = Output Shaft

2 = Rectangular Slot in the Rotor

3 = Springs

4 = Sliding Seals

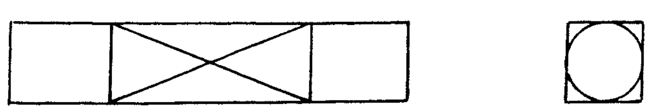

Elevation   End View

Figure 20. Output Shaft

rectangular slot of the rotor. Thus the rotor can slide on the shaft along its major axis but cannot rotate relative to the shaft. The shaft has cylindrical ends to fit in suitable bearings in the cover plates.

D. Construction and Operation

A view of rotor-housing and shaft assembly is shown in Figure 21.

The following geometric constraint result from the rotor and housing configuration.

(1) The major axis of the rotor always passes through the shaft center.

(2) The minor axis of rotor passes through the shaft center only at zero degree position, but very nearly passes through the point O_4. O_4 lies along the line of vertical symmetry for the housing and is coincident with the rotor center at its 90-degree position. If the path of rotor center were circular, the minor axis would pass through O_4 for all the rotor position. In the actual case the path of the rotor center is nearly circular* and

*Maximum deviation from circular path of radius r is 0.04r, (Figure 31).

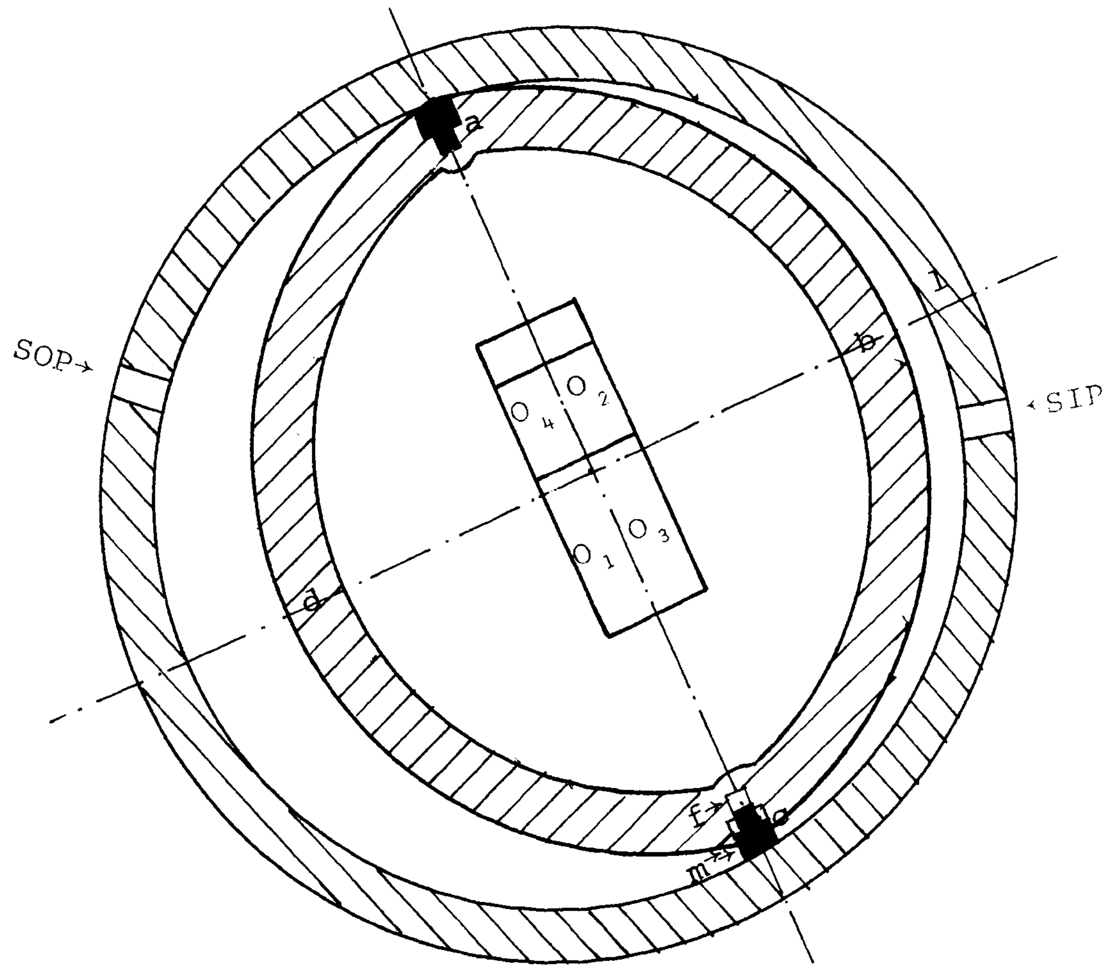

Figure 21. Rotor-Housing Assembly.

abcd = Rotor

O_1 = Housing Geometric Center

O_2 = Shaft Center

O_3 = Rotor Center

a and c = Leakage Prevention Seals

SIP = Steam Inlet Port

SOP = Steam Outlet Port

the minor axis very nearly passes through O_4. (The distance O_1O_4 is 0.02R as shown in Figure 24).

(3) Now at certain rotor position as shown in Figure 21, pressurized steam is admitted from steam inlet port SIP into the space between the housing and rotor denoted by abcmla. This space is almost symmetrical about the minor axis bd and hence the steam load will act along the line bd. This will cause turning movement on the shaft and the rotor end "a" will be pressed against the housing. This contact pressure between the housing and rotor will have a component acting along the major axis of the rotor and will cause it to slide on the shaft. This in turn will allow the rotor and shaft to rotate. The path of rotor center is shown in Figure 31 and is approximately a circle.

Four different rotor positions are shown in Figure 22. Figure A shows the zero degree position of the rotor. The steam inlet port is denoted by SIP and steam outlet port by SOP. At the zero degree position, the rotor side abc is in complete contact with the housing. Both the minor and major axes pass through the shaft center.

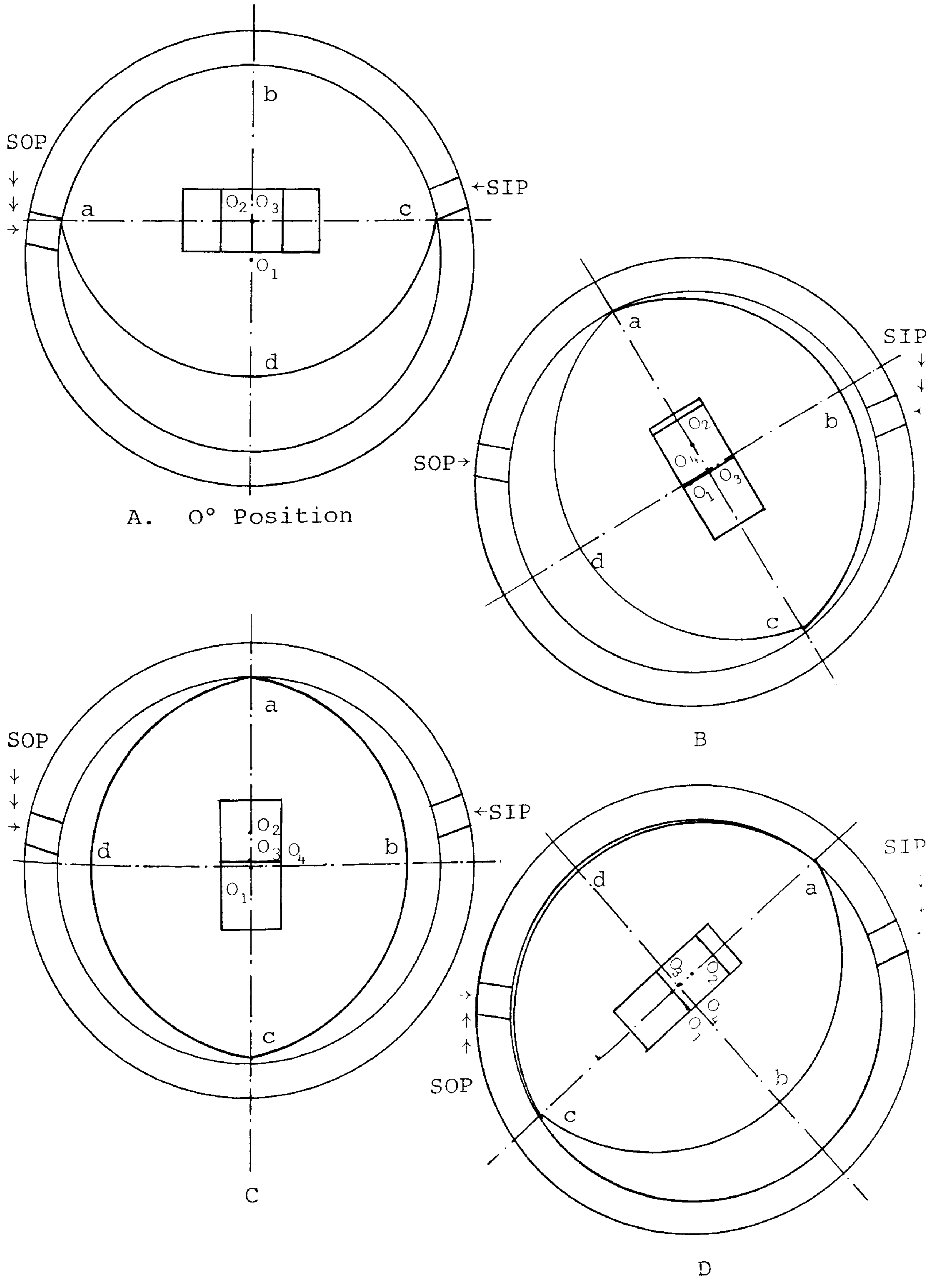

Figure 22. Working of the Engine.

As the rotor rotates clockwise (Figure B), it also slides along the shaft as discussed previously, creating some space between the housing and the rotor surface abc.

The minor axis no longer passes through the shaft center. Pressurized steam from the steamchest (Figure 43) occupies the space created and produces an effective force on the rotor acting along the minor axis. Since the minor axis does not pass through the shaft center, this steam load produces a torque on the shaft equal to the product of the off-center distance of the minor axis and the effective force. This causes the output shaft and rotor to rotate creating more space between the side abc and the housing. Either more steam is supplied or the high pressure steam expands further, doing further work on shaft. Figure C indicates the 90° shaft position, where the rotor is vertical. Figure D shows the rotor position just before exhaust of the steam on side abc begins. At the same time, side adc of the rotor is nearly in contact with the housing. Exhaust of steam from side abc begins when point c, crosses the exhaust port SOP, and pressurized steam admission occurs on side adc. Thus when steam exhaust takes place from side abc, expansion of high pressure steam occurs on side adc.
It should be noted that during expansion the output shaft rotates through 180°, but the rotor center has traveled through 360°. Thus the device is equivalent to a

conventional double-acting reciprocating steam engine. However, the use of a rotor rather than a piston eliminates the need for an exhaust valve.

E. Engine Design

(1) Fundamental relationship of volume displacement to shaft rotation: It is essential to establish relation between shaft position and correspon- ding volume displaced in the housing. This can be done by using principles of geometry.

Assuming a unit depth the relationship reduces to one between area displaced and shaft position. First it is necessary to calculate the rotor area.

Figure 23 indicates a zero degree rotor position. O_1 and O_1' are the centers of arcs abc and adc respectively and 2θ is the included arc angle.

The semi-rotor area can be calculated considering the area of segment O_1abcO_1 and then substracting the area of the triangle O_1ac.

$$\text{Area of segment } O_1abc\, O_1 = \frac{1}{2} R^2(2\theta).$$

$$\text{Area of triangle } O_1ac = \frac{1}{2} R^2 \text{Sin}(2\theta).$$

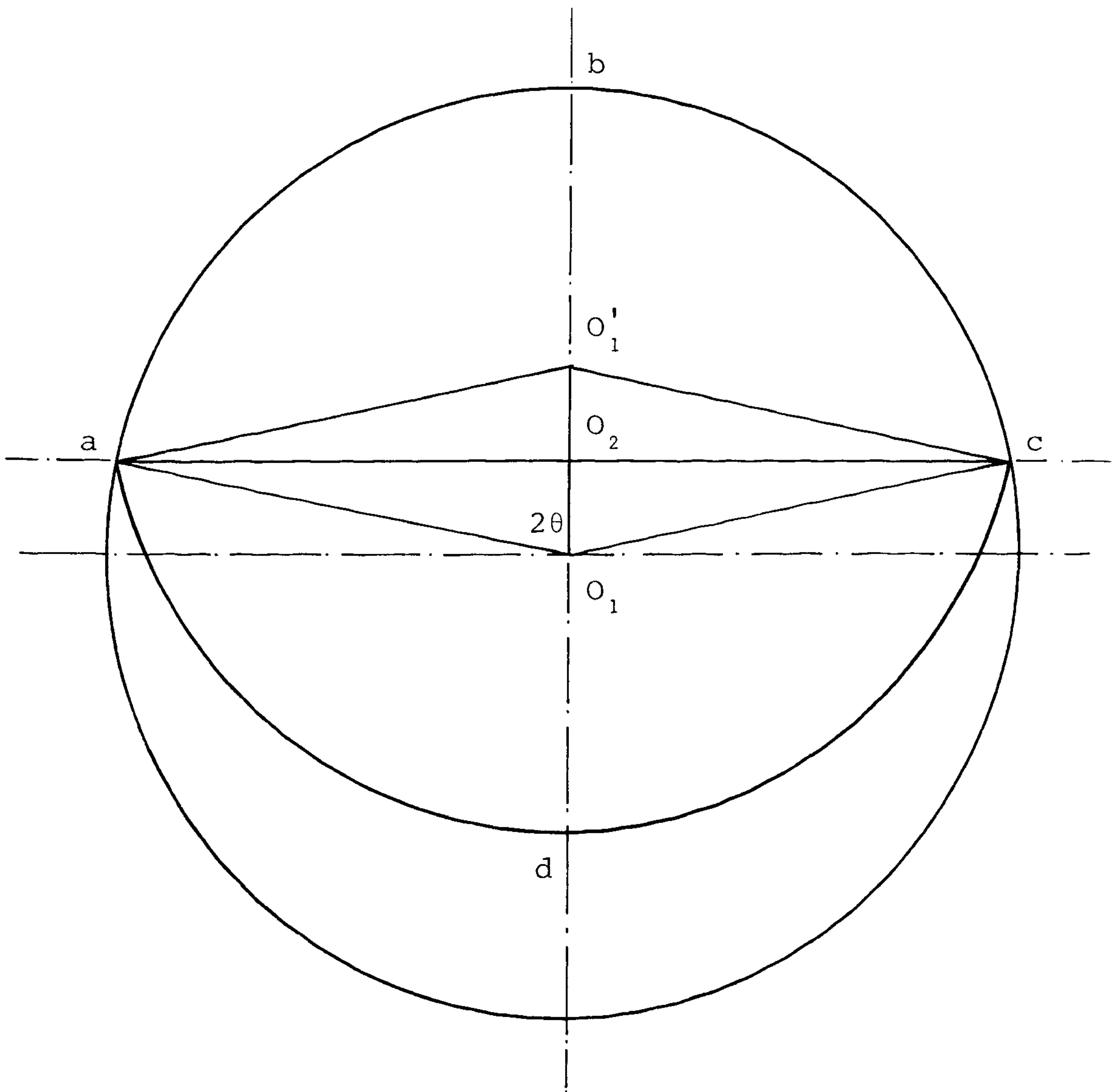

Figure 23. Zero Degree Rotor Position

abcd = Rotor

O_1 = Housing Center

O_2 = Rotor Center

O_1' = Center of Arc adc

$O_1a = O_1b = O_1c = R$ (Housing Radius)

$O_1O_2 = R/5$

Angle $aO_1c = 2\theta$

So the rotor area can be expressed as

$$a_r = 2 \text{ area abca} = 2[\frac{1}{2} R^2(2\theta) - \frac{1}{2} R^2(\text{Sin}2\theta)]$$

$$= R^2[2\theta - \text{Sin}2\theta]. \qquad (5.1)$$

Once the rotor area is known the displacement area within the housing can be calculated using the same principles of geometry.

A general position of the rotor at shaft rotation of $\beta°$ is shown in Figure 24. Point a remains in contact with the housing. Point c does not remain in contact with the housing but a sliding seal bridges the gap cm. The path of the rotor center O_3 is very nearly a circle with diameter O_2O_4 and center O_5 (Figure 31).

The area aklmcba is the displacement because of shaft rotation $\beta°$. This area can be calculated by subtracting area O_1abcmO_1 from area O_1aklmO_1. The area O_1abcmO_1 can be divided into two parts as follows:

area O_1abcmO_1 = semi rotor area abca + area of triangle aO_1m.

The area of triangle aO_1m is given by

$$\text{Triangle } aO_1m = \frac{1}{2} \text{Sin}(aO_1m).$$

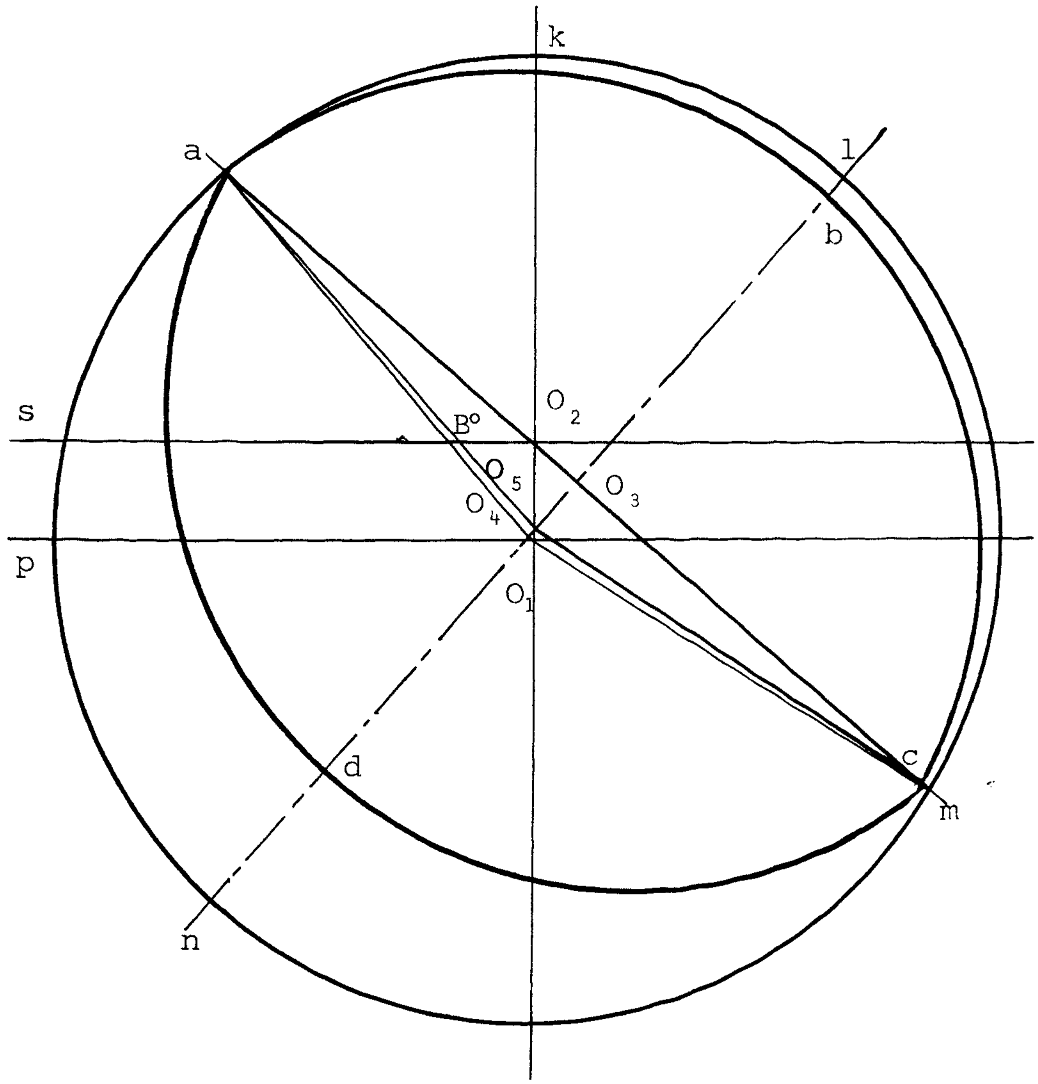

Figure 24. A General Rotor Position After $\beta°$ of Shaft Rotation.

abcd = Rotor

aklmnps = Housing

O_1 = Housing Center

O_2 = Shaft Center

O_3 = Rotor Center

O_4 = Point through which minor axis always passes

O_2O_4 = Diameter of the circle over which rotor center travels

Angle aO_2s = $\beta°$ shaft rotation

Angle O_2aO_1 = α

In triangle aO_1m, since the sides aO_1 and O_1m are equal, the angle O_2aO_1 = angle O_2mO_1. Thus angle O_2aO_1 = angle $O_1mO_2 = \alpha$, and angle $aO_1m = \pi - 2\alpha$. The area of triangle aO_1m is expressed as

$$\text{Triangle } aO_1m = \frac{1}{2} R^2 \text{Sin}(\pi - 2\alpha),$$

and the values of angle α in terms of shaft rotation can be expressed by applying the law of Sines to the triangle O_2aO_1.

$$\frac{\text{Sin}(O_2aO_1)}{O_1O_2} = \frac{\text{Sin}(aO_2O_1)}{aO_1}.$$

Substituting

$$\begin{aligned} \text{Angle } \quad O_2aO_1 &= \alpha, \\ aO_2O_1 &= \frac{\pi}{2} + \beta, \\ O_1O_2 &= \frac{R}{5}, \\ aO_1 &= R, \\ \text{Sin}\alpha &= \frac{1}{5} \text{Cos}(\frac{\pi}{2} + \beta), \end{aligned}$$

and so $\alpha = \text{Arc Sin}(0.2\text{Cos}\beta)$,

$$\text{area } O_1abcmO_1 = \frac{1}{2} R^2 [2\theta - \text{Sin}2\theta] + \frac{1}{2} R^2 \text{Sin}(\pi - 2\alpha),$$

and the area displaced will be given by:

$$a = \frac{1}{2} R^2 [\pi - 2\alpha] - \frac{1}{2} R^2 \mathrm{Sin}(\pi - 2\alpha)$$

$$- \frac{1}{2} R^2 [2\theta - \mathrm{Sin}2\theta]$$

$$= \frac{1}{2} R^2 [\pi - 2\alpha - \mathrm{Sin}(\pi - 2\alpha) - (2\theta - \mathrm{Sin}2\theta)]$$

where

$$\alpha = \mathrm{Arc\ Sin}(0.2\mathrm{Cos}\beta)$$

and the volume displaced for any engine with width B and shaft rotation β will be

$$V(\beta) = \frac{1}{2} R^2 B[\pi - 2\alpha - \mathrm{Sin}(\pi - 2\alpha)$$

$$- (2\theta - \mathrm{Sin}2\theta)]$$

where

$$\alpha = \mathrm{Arc\ Sin}(0.2\mathrm{Cos}\beta). \qquad (5.2)$$

At the zero degree rotor position, on one side of the rotor occurs minimum i.e. zero volume and on the other side occurs the maximum volume. This can also be obtained by subtracting rotor volume from the housing volume.

$$V_{max} = R^2 B - R^2 [2\theta - \mathrm{Sin}2\theta] B,$$

where

R = Housing radius,

B = Housing width,

θ = Rotor arc included angle.

Substituting the value for θ(Arc Cos0.2) in the above equation,

$$V_{max} = 0.794584063\ R^2B,$$

when equation 5.2 is used (for β = 180) the result is

$$V(180°) = 0.7945424420\ R^2B,$$

so the maximum value of volume

$$V_{max} = 0.795\ R^2B. \tag{5.3}$$

(2) Comparison of rate of change of displaced volume for the rotory expander and a conventional reciprocating engine: For typical values of R and B (R = B = 4.0) equation 5.2 for the volume displaced was computed at various shaft positions. Corresponding values for a reciprocating engine with the same maximum displacement were also computed. The results are tabulated in Table 5.1. A graph of volume displaced as a function of shaft angle for both engines is plotted in Figure 25. Since the volumetric variations of the rotory and reciprocating engines are almost identical, the ratio of expansion, maximum necessary volume, and theoretical engine

TABLE 5.1

COMPARISON OF VOLUME DISPLACED BY ROTORY AND RECIPROCATING ENGINE WITH SAME MAXIMUM VOLUME

DEGREES	CUBIC INCHES	RECIPROCATING CUBIC INCHES
0	0.0	0.0
10	0.422	0.254
20	1.556	1.500
30	3.413	3.300
40	5.940	5.850
50	9.066	9.150
60	12.700	12.720
70	16.732	16.800
80	21.038	21.001
90	25.485	25.445
100	29.931	29.800
110	34.236	34.000
120	38.266	38.210
130	41.897	41.750
140	45.019	45.001
150	47.541	47.613
160	49.392	49.500
170	50.521	50.611
180	50.890	50.891

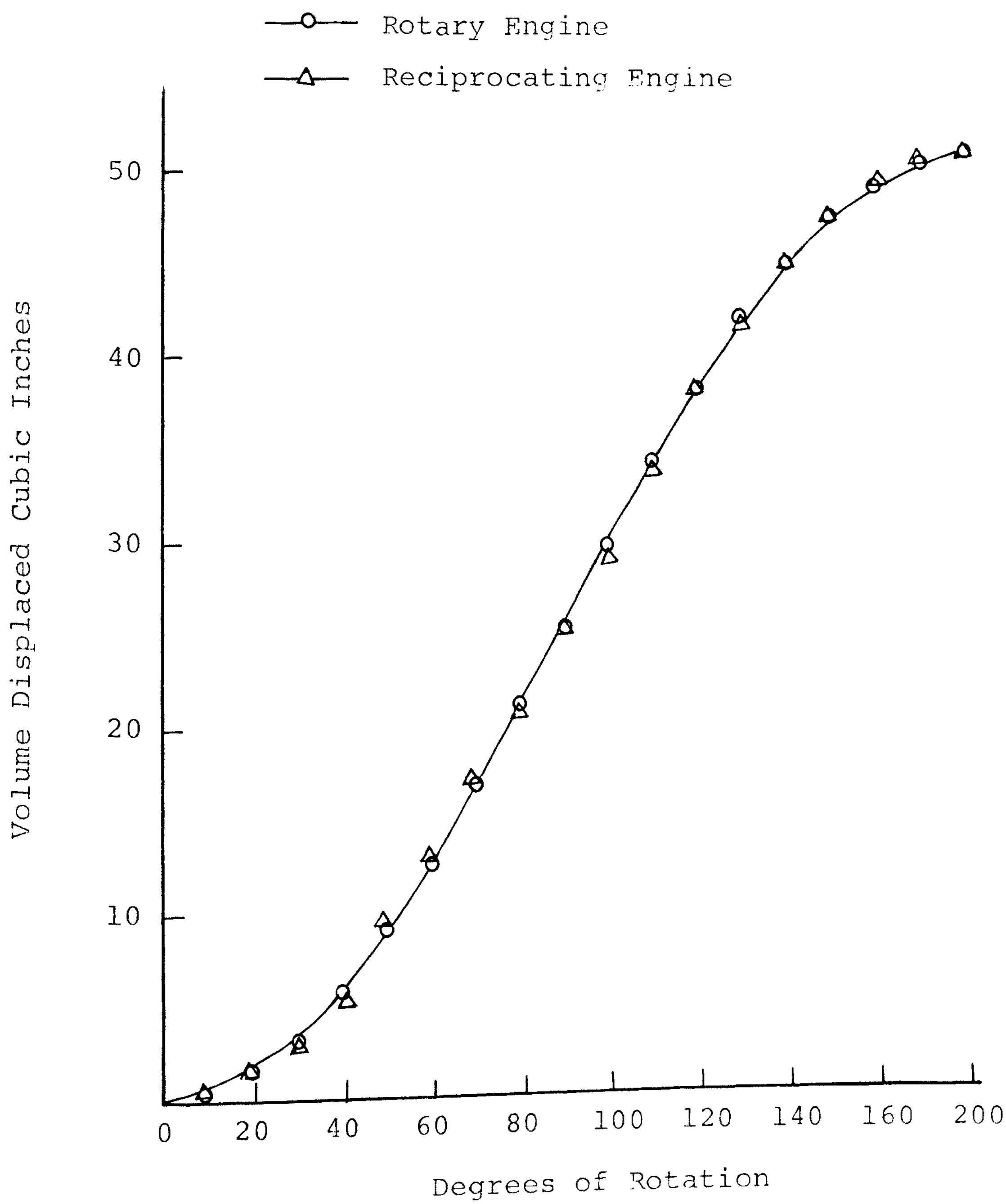

Figure 25. Comparison of Volume Displaced by Rotary and Reciprocating Engine With Same Maximum Volumes.

performance can be determined for the rotory engine, on the same basis as for the reciprocating engine.

(3) Determination of the ratio of expansion: The volume of steam in the housing when the admission valve closes, divided by the volume of steam when the exhaust port or valve opens, is called the "cut-off". The reciprocal of this fraction is called the ratio of expansion [19].

It is very difficult to determine the exact value of the ratio of expansion which will be most economical over the entire engine life. The principal factors affecting this choice are wear of the rotor seals and the amount of energy lost in the form of heat transfer from the engine walls.

Rankine [19] gave the following guideline for determination of optimum cut-off:

> "The greatest useful work is obtained by making the expansion cease when the forward pressure is just equal to the back pressure, added to a pressure equivalent to the friction of the engine."

This statement can be explained by using the ideal pressure volume diagram for a reciprocating engine shown in Figure 26. P_i is the inlet steam pressure and the admission valve

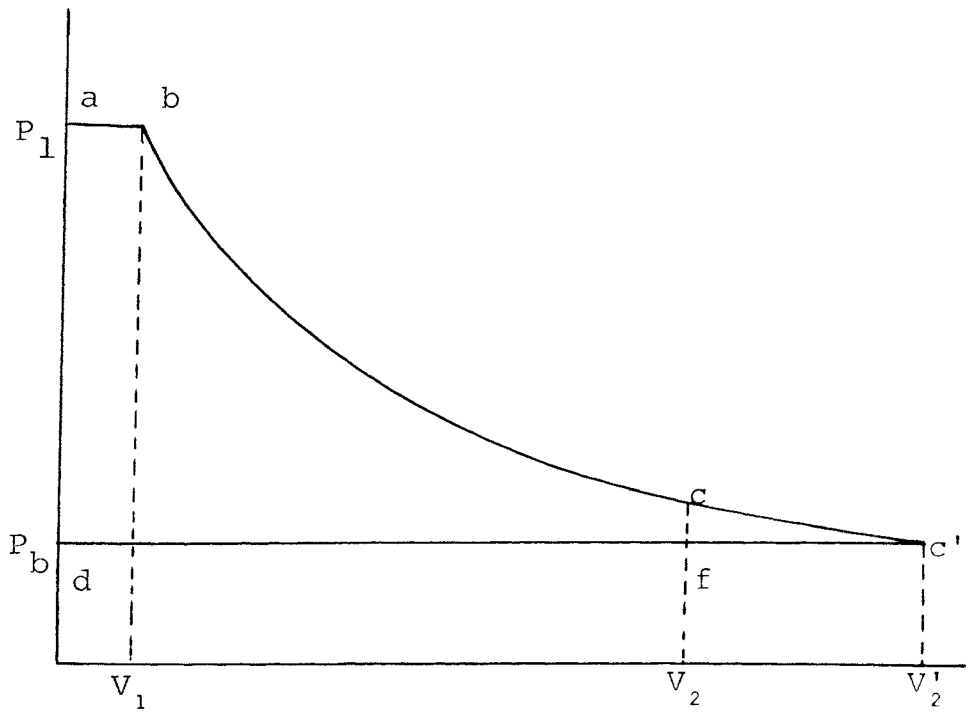

Figure 26. Ideal Pressure Volume Diagram for Reciprocating Steam Engine With no Clearance Volume and Complete Steam Expansion and Exhaust.

P_1 = Inlet Steam Pressure to the Engine

P_b = Back Pressure

a = Admission Valve Opens

ab = Steam Admission

b = Admission Valve Closes

bc' = Steam Expansion

c' = Exhaust Valve Opens

c'd = Exhaust

d = Exhaust Valve Closes

V_1 = Volume of Steam Admitted

V'_2 = Volume of Steam After Complete Expansion closes at b, when the volume of steam is V_1. The steam is then expanded along bc', and expansion ceases when the forward pressure becomes equal to the backward pressure P_b, at volume V_2'. Then the ratio of expansion will be given by

$$\frac{V_2'}{V_1} .$$

At c' the exhaust valve opens and exhaust c'd takes place.

However as the end of the stroke is approached the "toe" of the P-V diagram (cfc') becomes very narrow and infact work obtained by expansion of steam between volumes c and c' is not sufficient to overcome the friction due to piston movement required to provide this volume. In addition, at low pressures the specific volume of the steam increases rapidly and the expansion cc' will require a large engine volume. Hence, at c' the exhaust valve opens and the steam release takes place to back pressure P_b along the constant volume line cf. The point "c" or a suitable expansion ratio $\frac{V_2}{V_1}$ can thus be determined by adding a pressure equivalent (fc) to the back pressure to account for engine friction. A back pressure of 16.0 psia is selected for exhaust of steam into the condenser. This value was selected to limit engine displacement to a reasonable size and to maintain a positive pressure in the condenser. For an ideal engine the ratio of expansion with dry saturated steam at an inlet pressure of 500 psia will be

$$\text{Ratio of expansion} = \frac{V_2'}{V_1} = \frac{P_1}{P_b} = \frac{500.0}{16.0}$$

$$= 31.3.$$

The equivalent friction pressure drop can be assumed to be 9.0. This is about 50% higher than the values suggested by reference [19]. However this assumption is necessary for the rotory engine because:

(a) the inlet steam pressure is higher;

(b) the maximum engine speed is much higher (1000 rpm VS 400 rpm);

(c) sealing problem for rotory engine is not quite solved.

So the release pressure at c will be:

$$P_r = P_b + \Delta P = 25.0 \text{ psia},$$

where

$$P_b = 16.0 \text{ psia},$$

$\Delta P = 9.0$ psia

The ratio of expansion is then given by:

$$r = \frac{P_1}{P_r} = 20.0.$$

(4) Determination of engine volume: The work done in each cycle is represented by the area of the PV diagram. Theoretical and actual PV diagrams for a conventional single acting reciprocating engine are as shown in Figure 27. The clearance volume V_c of the engine is necessary to cushion the piston against unexhausted steam. The clearance volume is typically 5 to 10% of the total volume [6,19].

The actual PV diagram is different for the following reasons:

(a) During admission of steam the valve opening and closing are not instantaneous. Due to this the steam is throttled and its pressure drops. The steam admission occurs on 1'-2' instead of 1-2.

(b) At point 3', when the displacement reaches its maximum again the exhaust valve opening is not instantaneous, and so the release takes place along line 3'-4' instead of 3-4.

(c) When exhaust stroke terminates the

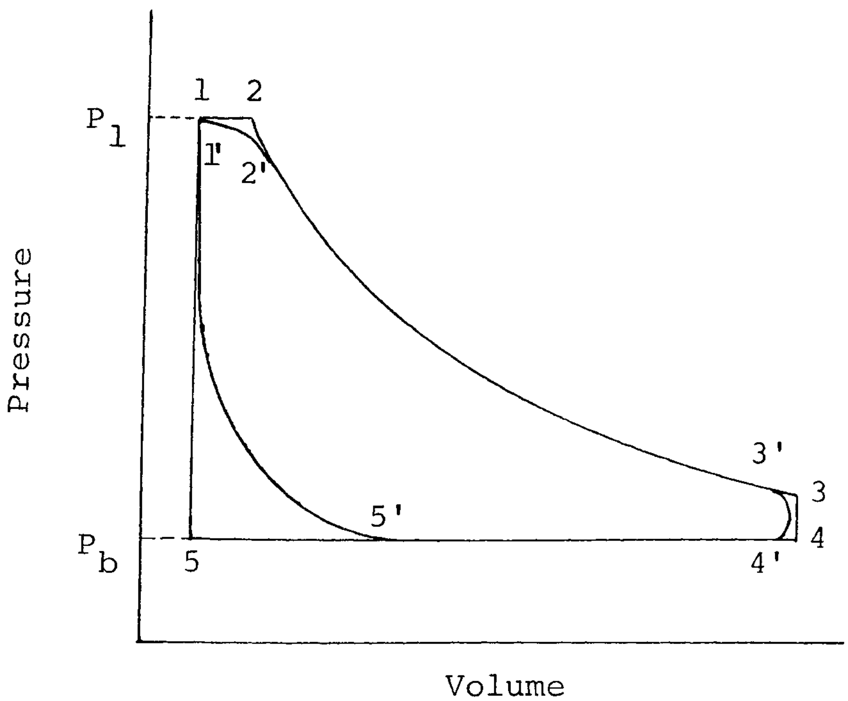

Figure 27. Ideal and Actual Pressure Volume Diagram for Reciprocating Engine With Clearance Volume.

123451 Ideal P-V Diagram

1'2'3'4'5'1' Actual P-V Diagram

1'2' Actual Steam Admission With Throttling

3'4' Actual Steam Release With Throttling

5'1' Actual Closing of Exhaust Valve

exhaust valve closing is not instantaneous; since some volume is necessary to accumulate steam for cushioning the piston, incomplete exhausting of steam occurs. The steam cushion is compressed to point 1', where the inlet steam valve opens and the cycle is repeated. Thus in a conventional reciprocating engine the actual PV diagram differs from the theoretical PV diagram at six points, the last four of which are due to the performance of exhaust valve [19]. In the rotory engine described earlier, there is an exhaust port rather than an exhaust valve. The pressure-volume characteristics of the rotory engine will now be examined.

In the actual P-V diagram of the rotory engine, the inlet valve opening and closing will have the same effect as the valve in a reciprocating engine. At the point when the exhaust port will be exposed, the release pressure will take place more rapidly than in a reciprocating engine. Furthermore total exhaust of steam will occur because no clearance volume is required.

The diagram efficiency of an engine is defined as the ratio of the area of the actual PV diagram to the theoretical PV diagram [6]. This is an important factor for selecting the engine volume. For the reciprocating, high speed (rpm $\geq$ 400) double acting steam engine it is expected to average 0.6 to 0.7 over the life of the engine. From the above discussion, since the deviation between the actual and theoretical PV diagrams for the rotory engine is less than that in the reciprocating engine, a higher diagram efficiency for the rotory engine can be expected. However since the amount of steam leakage is unknown the efficiency is estimated to be 0.7.

The area of the theoretical PV diagram represents work done per cycle. The area of the diagram 12345 (Figure 2°) for hyperbolic steam expansion* is given by

$$A_V = P_1V_1 \; [1 + \ln \frac{V_2}{V_1}] - P_bV_2 \qquad [6,19].$$

Then the indicated horse power is expressed by:

---

*Since the dry saturated steam is used the hyperbolic expansion is most likely. Mathematically it is expressed as PV = constant [6,19].

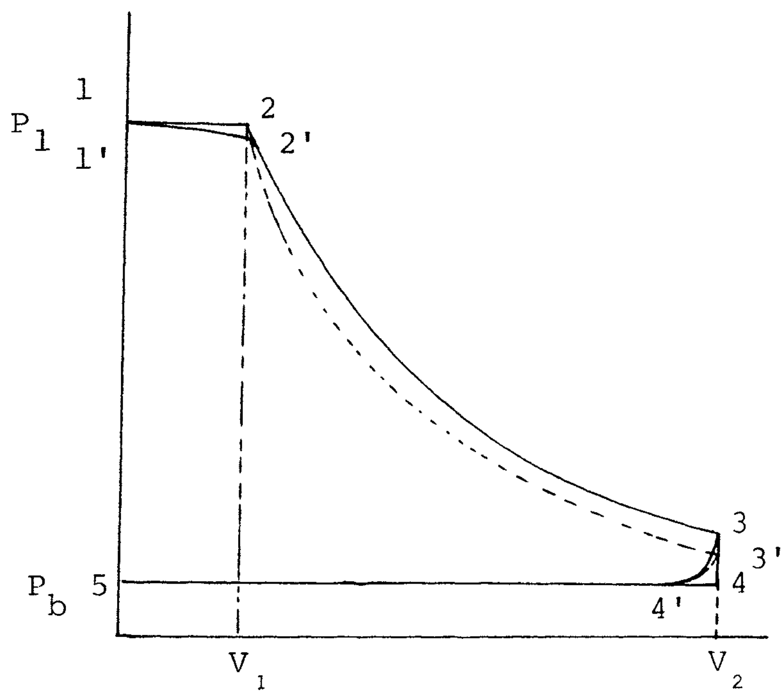

Figure 28. Ideal and Expected Actual Pressure-Volume Diagram for Rotory Engine.

P_1 = Inlet Steam Pressure

P_b = Back Pressure

V_1 = Volume of Steam Admitted

V_2 = Volume of Steam When Exhaust Port Opens

12 = Ideal Steam Admission (Constant Pressure)

1'2' = Actual Steam Admission (Pressure Drop Due to Throttling)

23 = Hyperbolic Steam Expansion

34 = Ideal Steam Release (Constant Volume)

34' = Actual Steam Release (Volume Decreases due to Rotor Movement)

45 = Ideal Exhaust

4'5 = Actual Exhaust (No Closing of Exhaust Port Occurs)

2'3' = May Occur due to Improper Sealing

$$hp = \frac{[P_1V_1(1 + \ln \frac{V_2}{V_1}) - P_bV_2] \times 2N \times \eta_d}{33000.0 \times 12.0} \qquad (5.4)$$

where

ihp = Indicated horse power,

P_1 = Inlet steam pressure psia,

V_1 = Housing volume when steam admission valve closes, in cubic inches,

V_2 = Housing volume when steam exhaust begins, in cubic inches,

P_b = Back pressure in psia,

N = Engine rpm (multiplied by two since the engine is double acting),

η_d = Diagram efficiency.

After substituting the following values in equation 5.4 the housing volume when steam exhaust begins can be calculated.

$ihp = 15.0$,

$P_1 = 500.0$ psia,

$\frac{V_2}{V_1} = 20.0$,

$N = 1000.0$ rpm,

$\eta_d = 0.7$.

The value of V_2, the maximum housing volume is found to be

$$V_2 = 50.5 \text{ cubic inches.}$$

Since $V_2 = 0.795\ R^2B$ (equation 5.3), for $R = B$, the engine radius and width for 50.5 cubic inches swept volume is found to be almost 4.0 inches.

Thus the rotory engine with radius 4.0 inches, width 4.0 inches and running at 1000.0 rpm should develop 15.0 ihp when supplied with dry saturated steam at 500.0 psia. The swept volume in this case is

$$V_2 = 0.795\ R\ B$$

$$= 51.0 \text{ cubic inches.}$$

F. Theoretical Engine Performance

(1) PV diagram: A theoretical PV diagram can be plotted using the equation

$$PV = C$$

where C is a constant. The value of C can be determined by considering the steam pressure and volume at point 3 on the theoretical PV diagram, as shown in Figure 28.

$$PV = P_b V_2 = C$$

Substituting

P_b = 25.0 psia,

V_2 = 51.0 cubic inches,

the constant is found to be

C = 1275.0 Pound-inches.

The values of pressure are tabluated for corresponding values of volume in Table 5.2, and a theoretical PV diagram is plotted in Figure 29.

(2) Power variation: The power output of a steam engine can be varied by increasing the supply of steam i.e. by delaying cut-off. Engine volume, at any shaft angle β is given by equation 5.2 as:

$$V(\beta) = V_2 R^2 B[\pi - 2\alpha - \mathrm{Sin}(\pi - 2\alpha) - (2\theta - \mathrm{Sin}2\theta)]$$

and $\alpha = \mathrm{Arc\ Sin}(0.2\mathrm{Cos}\beta)$,

and hence the ratio of expansion is obtained from

$$R.E = \frac{V_2}{V(\beta)},$$

where

R.E = Ratio of Expansion,

V_2 = Maximum volume,

$V(\beta)$ = Volume of steam at cut-off angle β.

TABLE 5.2

PRESSURE VOLUME RELATION

V'	P'
5.0 IN^3	255.0 P.S.I.
10.0	127.5
15.0	85.0
20.0	63.7
25.0	51.0
30.0	42.5
35.0	36.5
40.0	31.9
45.0	28.4
50.0	25.5
51.0	25.0 Release

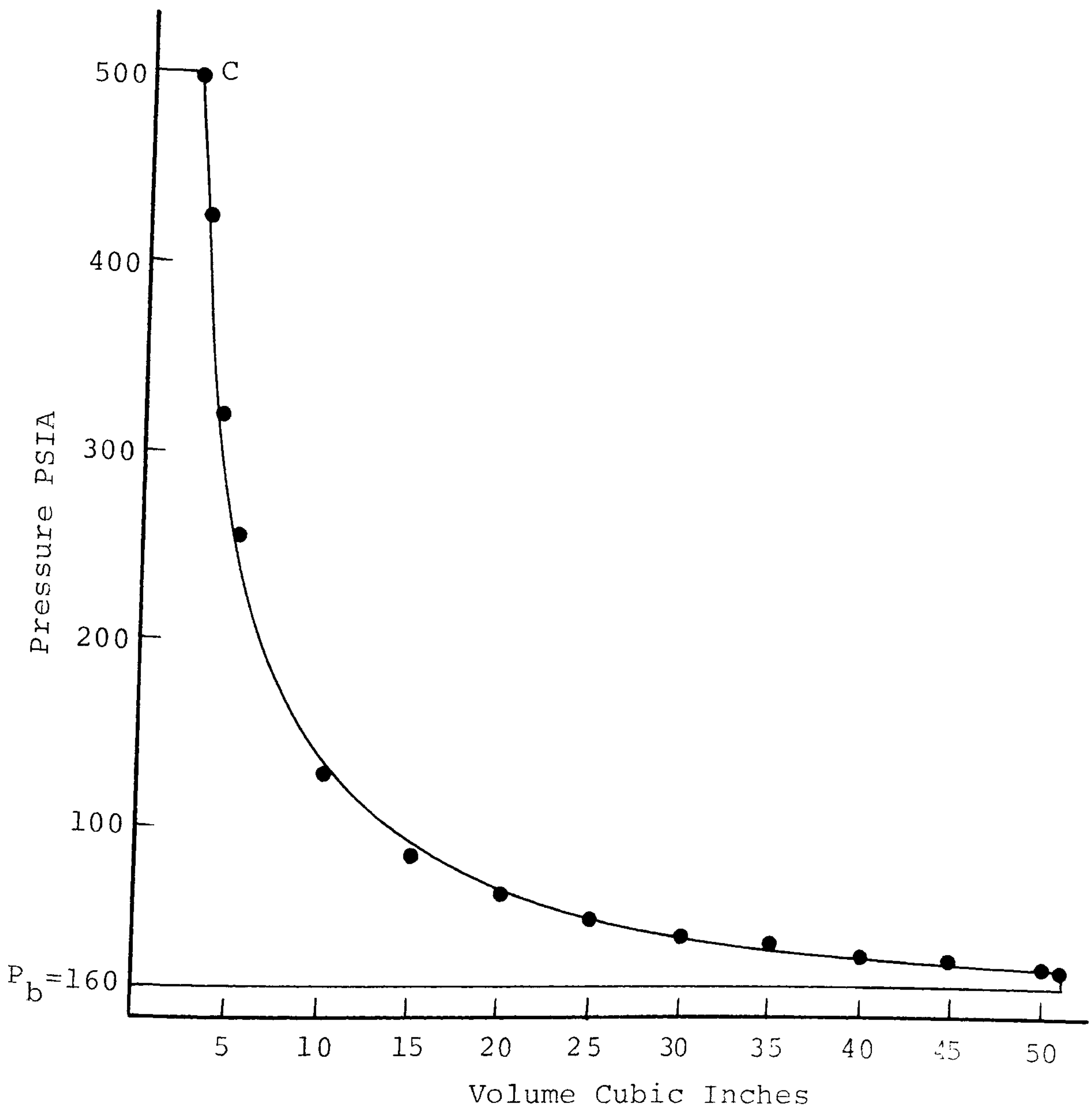

Figure 29. Theoretical Pressure Volume Diagram for Rotory Engine.

C = Point of Cut-off

The ratio of expansion for various cut-off angles was calculated with the aid of a computer and the results are tabulated in Table 5.3. As the cut-off increases, the power developed also increases. With the aid of the computer, power developed was calculated for various cut-off angles β from equation 5.4.

$$\text{ihp} = \frac{[P_1 V(\beta)(1 + \ln \frac{V_2}{V(\beta)}) - P_b\ V_2] \times 2N \times \eta_d}{33000.0 \times 12.0}$$

using

P_1 = 500.0 psia,

V_2 = 51.0 cubic inches,

P_b = 25.0 psia,

N = 1000.0 rpm,

η_d = 0.7.

Results are tabulated in Table 5.3 and a graph of cut-off angle β VS ihp is plotted in Figure 30.

(3) Theoretical steam consumption: The steam consumption in lbs per hour is expressed by:

$$w = \frac{2NV_c\ \rho}{1728}$$

where

w = Weight of steam in lbs

N = rpm

V_c = Volume of steam at cut-off in cubic inches

σ = Density of steam in lbs/cubic ft.

The volume of steam admitted when cut-off occurs (V_c) is a function of β, expressed by equation 5.2. Substituting the following values in the above equation:

N = 1000.0 rpm

σ = 0.9 lbs/cubic ft (corresponding to 500 psia steam inlet pressure).

The steam consumption is calculated to be $w = 62.5\ V(\beta)$ and which is tabulated in Table 5.3 for various values of β. The specific steam consumption per horsepower hour can be obtained by dividing w by corresponding ihp. These results are also tabulated in Table 5.3, and a graph of specific steam consumption VS angle of cut-off is plotted as shown in Figure 30.

From Figure 30 the following theoretical performance characteristics can be predicted:

(a) Power developed by the engine is increasing linearly with the increase in

TABLE 5.3

THEORETICAL ENGINE PERFORMANCE

ANGLE OF CUT-OFF β	RATIO OF EXPANSION	VOLUME AT CUT-OFF CUBIC INCHES	INDICATED HORSE POWER	STEAM CONSUMPTION LBS/HR	SPECIFIC STEAM CONSUMPTION LBS/HP-HR
26	19.7	2.59	15.32	162.0	10.6
30	14.9	3.41	19.42	212.0	10.9
35	11.0	4.60	23.92	288.0	12.0
40	8.6	5.94	29.32	372.0	12.7
45	6.8	7.43	35.62	465.0	13.0
50	5.6	9.07	40.87	567.5	13.9
55	4.7	10.83	45.72	670.0	14.65
60	4.0	12.70	50.62	790.0	15.60
70	3.0	16.73	59.62	1010.0	17.0
80	2.4	21.03	67.12	1350.0	20.0
90	2.0	25.50	72.12	1620.0	22.5

cut-off angle. By increasing cut-off to 90°, 72 hp can be developed.

(b) The theoretical specific steam consumption increases linearly with increase in angle of cut-off. However, this increase is not appreciable; the steam consumption for 15.0 hp is 10.5 lbs/hp-hr and for developing 72.0 hp it is 23.0 lbs/hp-hr. The actual steam consumption will then be 1620.0 lbs/hr. Since the boiler capacity is only 225.0 lbs/hr, the engine cannot develop more than 20.0 continuous hp. In the event of a power requirement for 30 hp the cut-off angle must be increased to 41° and steam demand will rise to 360.0 lbs/hr. In a short time the steam pressure in the boiler will fall and the engine will fail to meet the power demand. But unlike the i.c. engine, the steam engine developes large torque at zero speed which remains fairly constant in lower speed range (Figure 4). So when heavy tractive load is encountered the engine speed will fall and by delaying the cut-off higher mean effective pressure and torque can be developed at the same

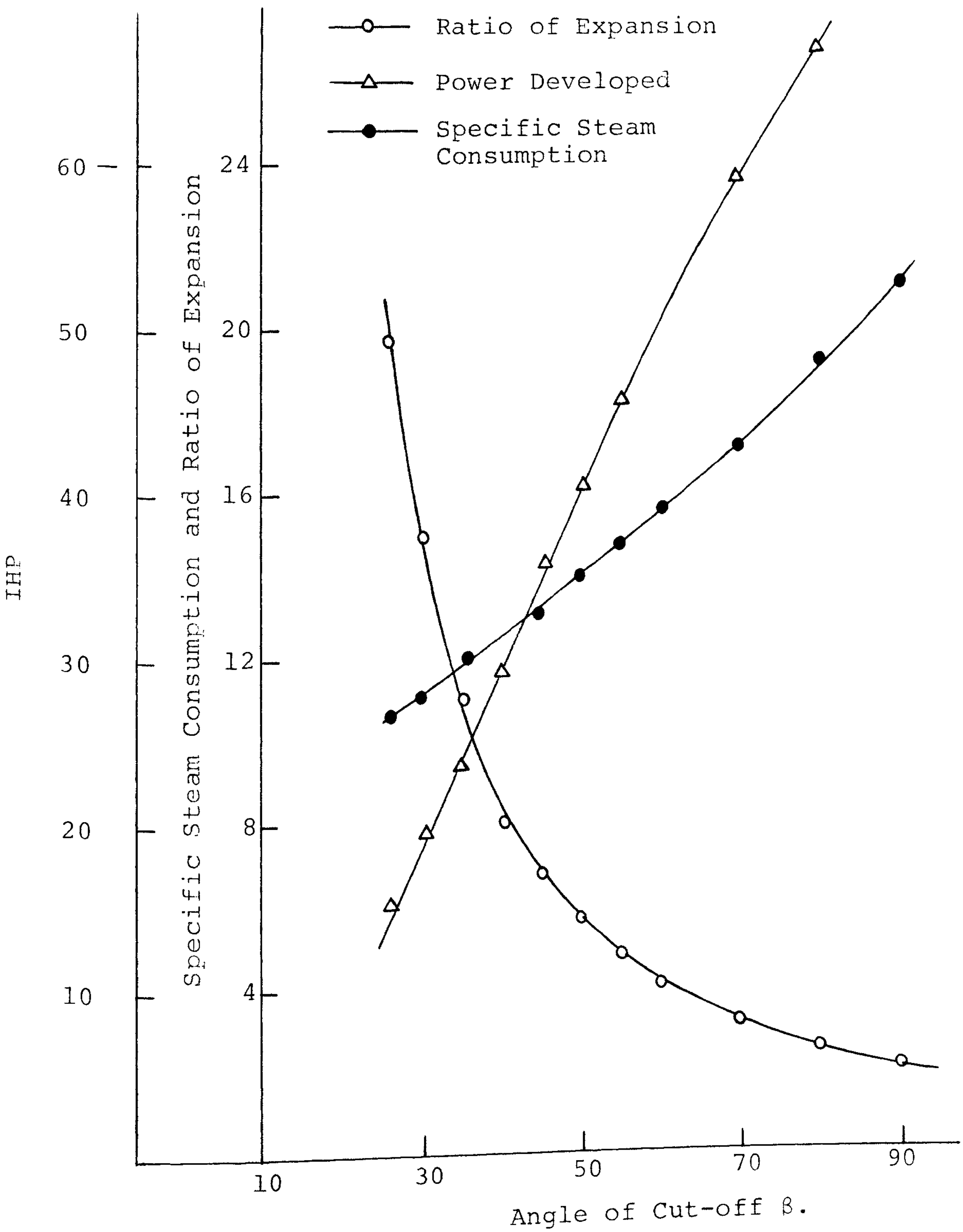

Figure 30. Theoretical Engine Performance.

steam consumption. This is one of the main advantages of steam engines compared to the i.c. engines.

G. Torque Analysis

Referring to Figure 24, the minor axis of the rotor passes at a distance O_2O_3 from the shaft center. The shape filled with steam can be assumed to be symmetrical about the minor axis, i.e. assuming the gap cm bridged by seal is zero,* and hence the total steam load acts along the minor axis with the torque arm O_2O_3. From Figure 24,

$$O_2O_3 = O_2O_4 \ \mathrm{Sin}\beta,$$

where β is the shaft angle and for $O_1O_2 = R/5$, the value of O_2O_4 can be determined as follows:

$$O_2O_4 = O_2O_1 - O_1O_4$$

$$= \frac{R}{5} - [R - \frac{\sqrt{24}}{5} R]$$

$$= 0.1798 \ R.$$

Hence

$$O_2O_3 = 0.1798 \ R \ \mathrm{Sin}\beta.$$

The effective rotor area over which the steam pressure acts is:

*In the Section I of this chapter this effect is calculated.

$$A = 2.0(\text{Sin}\theta)RB,$$

where

A = Effective area,

2θ = Included angle of rotor arc (Figure 23),

R = Housing radius,

B = Housing width.

For $O_1O_2 = \frac{R}{5}$, the value of θ is fixed and the effective area is expressed as $A = 1.96RB$.

Therefore, if $P(\beta)$ is the steam pressure at any angle β, the torque exerted on the output shaft will be:

Torque = (steam pressure) X (effective area) X (arm)

$$T = P(\beta) \times (1.96RB) \times (0.1798R\ \text{Sin}\beta) \qquad (5.5)$$

The steam pressure $P(\beta)$ is constant during the admission period, and after the admission valve closes i.e. after cut-off occurs at angle β_c, the expansion follows in hyperbolic fashion. This can be expressed as follows:

$$P(\beta) = p_1 \qquad \beta \leq \beta_c \qquad (5.6A)$$

$$P(\beta) = \frac{p_1 V_c}{V(\beta)} \qquad \beta \geq \beta_c \qquad (5.6B)$$

where

p_1 = Effective inlet steam pressure,

β = Shaft angle,

β_c = Angle of steam cut-off,

V_c = Housing volume at steam cut-off

$V(\beta)$ = Housing volume at any angle β expressed by equation 5.2.

The equations 5.6A and B were computed for various values of β, using

$$p_1 = 484.0 \text{ psi}$$

$$\beta_c = 26° \quad \text{(Design angle of cut-off)}$$

$$V_c = \frac{V_2}{V(26)} = 19.62 \text{ cubic inches}$$

$$R = 4.0 \text{ inches}$$

$$B = 4.0 \text{ inches}$$

Results are tabulated in Table 5.4 and torque VS β is plotted in Figure 30. The torque displacement diagram is utilized in Chapter VII to determine the necessary flywheel inertia.

Because of the peculiar motion of the rotor, rotating about its own axis and as well about a fixed point, a motion analysis is performed to investigate the inertia torque of the rotor.

H. Inertia Torque Analysis

(1) Locus of rotor center: In section D of this chapter it was assumed that the path of rotor center is a circle. The validity of this assumption is checked here by plotting the actual path of the rotor center. The

TABLE 5.4

TORQUE-ANGLE RELATION

(IN ABSENCE OF ROTOR INERTIA)

ROTATION °	TORQUE IN FT-LBS.
0	0.0
10	158.0
20	311.2
26 (Angle of cut-off)	398.8
30	344.6
40	254.5
50	198.7
60	160.4
70	132.1
80	110.1
90	92.3
100	77.4
110	64.5
120	53.2
130	43.0
140	33.5
150	24.7
160	16.2
170	8.0
180	0.0

geometric constraints and the locus of the rotor center are equivalent to the simplified construction shown in Figure 31A. The circle is equivalent to the housing and line a_1b_1 is equivalent to the semi-major axis of the rotor. O_1 is equivalent to the housing center and O_2 is equivalent to the shaft center. The horizontal position of line a_1b_1 is equivalent to rotor position at $\beta = 0$.

The locus of point b_1 is investigated, subject to the following two constraints.

(a) Point a_1 has to travel on the circle abcd.

(b) The line a_1b_1 has to pass through the point O_2.

For a circle of radius R = 4.0 inches and $O_1O_2 = \frac{R}{5.0}$, the path of point b_2 was calculated and plotted with the aid of a computer, as shown in Figure 31B. Also the assumed path, a circle, is drawn and the maximum deviation is found to be 0.0125 in. representing an error of 3.4% for the assumed circle of diameter 0.719 inches. Hence the path can be assumed to be a circle.

(2) Acceleration of rotor center: The absolute acceleration of any point p in the general system shown in Figure 32 is obtained from the equation:

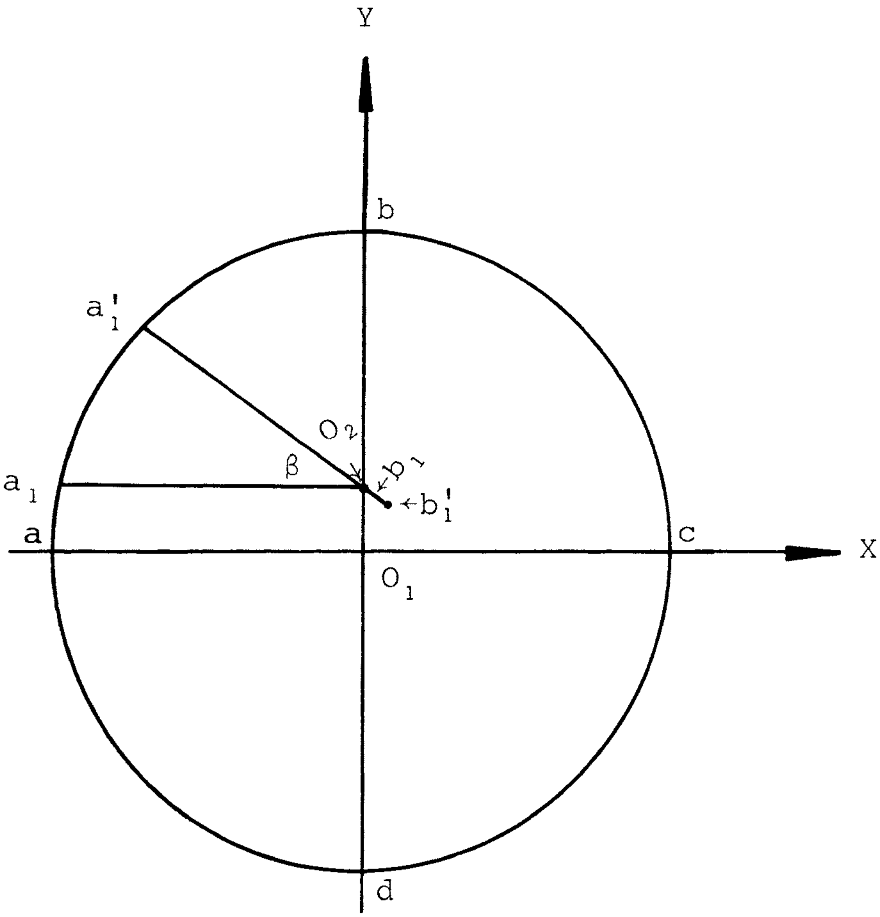

Figure 31A. Simplified Geometric Construction for the Locus of Rotor Center.

abcd = Circle with center at origine O_1,

a_1b_1 = Straight line passing through point O_2 on vertical diameter bd, and b_1 coincides with O_2 when a_1b_1 is horizontal,

$a_1'b_1'$ = A position of straight line a_1b_1 after $\beta°$ of rotation.

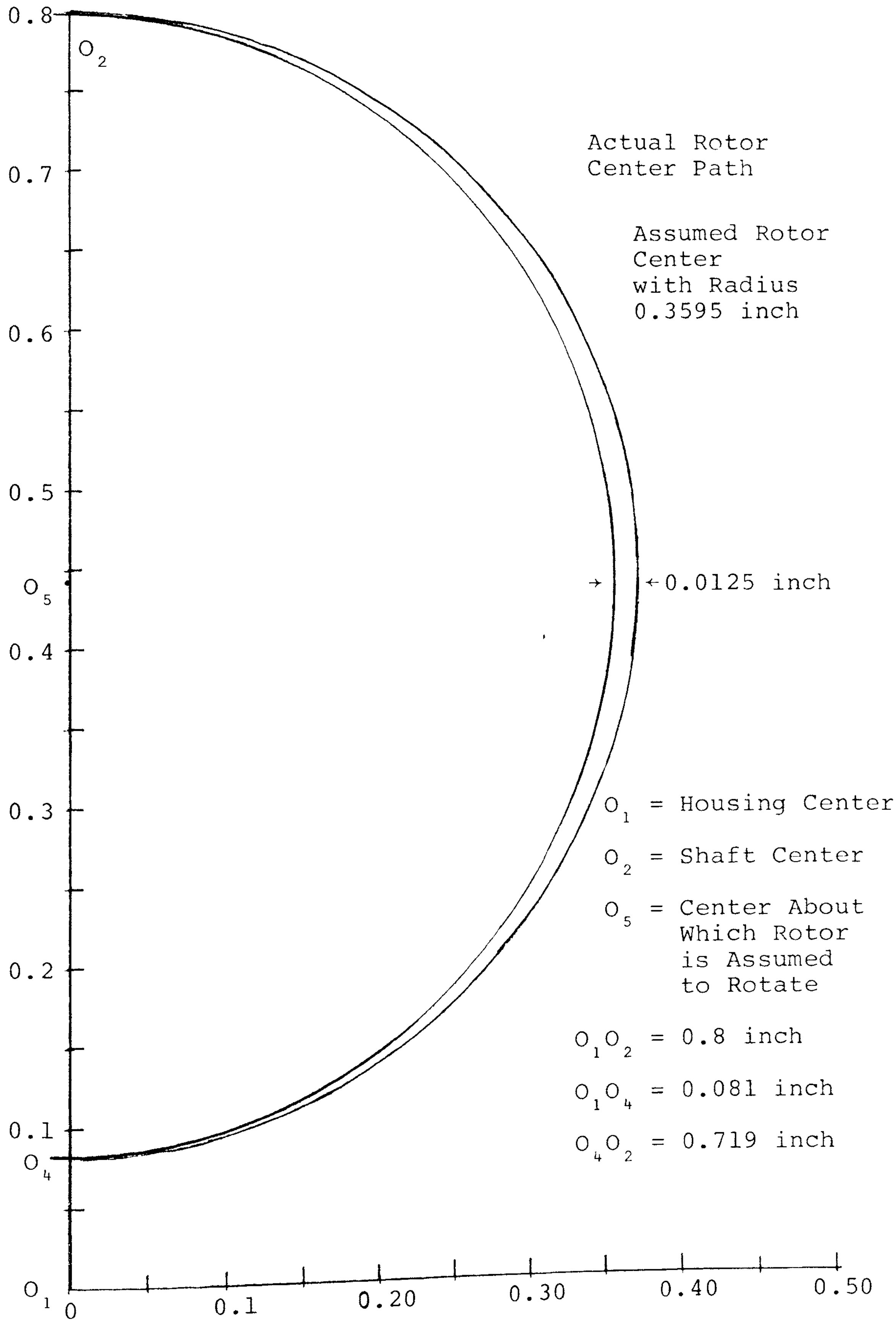

Figure 31B. Actual and Assumed Path of Rotor Center O_3.

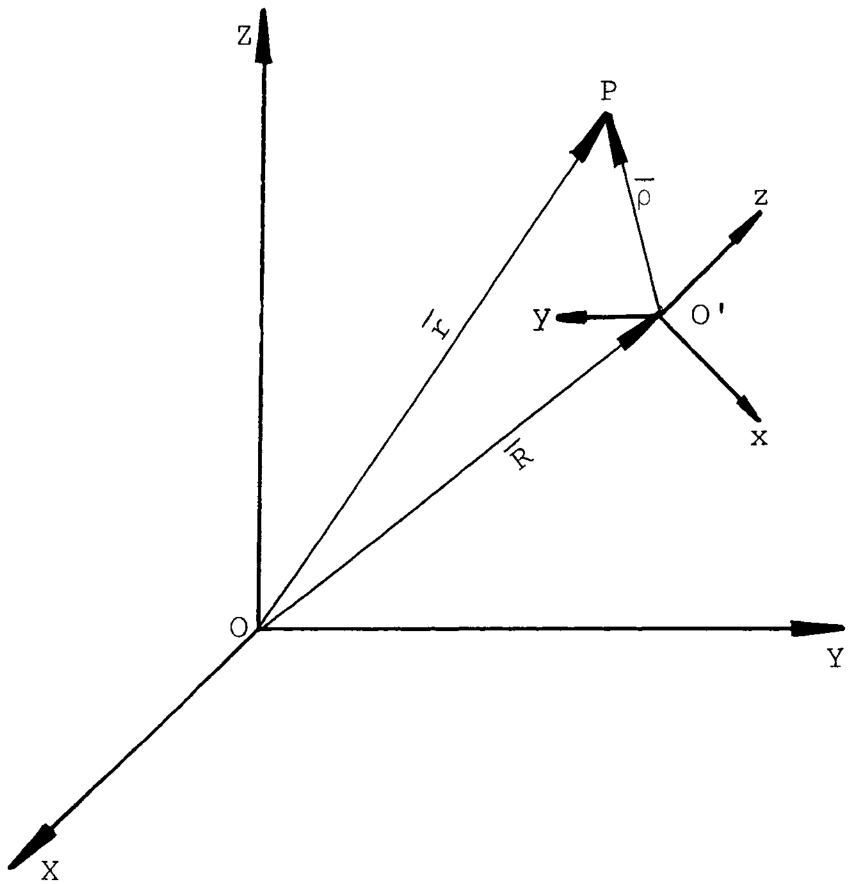

Figure 32. General Acceleration Equation.

XYZ = Fixed Reference System

xyz = Translating and Rotating System

P = Any Point in Space Under Investigation

$\bar{\rho}$ = Position Vector of Point P with Reference to xyz

$\bar{R}$ = Position Vector of Origine O' of System xyz

$\bar{r}$ = Position Vector of Point P with reference to XYZ.

$$\bar{A}_p = \ddot{\bar{R}} + \ddot{\bar{\rho}} + (2\bar{w} \text{ X } \dot{\bar{\rho}}) + (\dot{\bar{w}} \text{ X } \bar{\rho}) + w \text{ X } (w \text{ X } \rho) \tag{5.7}$$

where

$\bar{A}_p$ = Absolute acceleration of point P,

$\ddot{\bar{R}}$ = Absolute acceleration of O',

$\ddot{\bar{\rho}}$ = Acceleration of point ρ relative to xyz system,

$2\bar{w} \text{ X } \ddot{\bar{\rho}}$ = Coriolis acceleration,

$\dot{\bar{w}} \text{ X } \bar{\rho}$ = Tangential acceleration,

$\bar{w} \text{ X } (\bar{w} \times \bar{\rho})$ = Centrepital acceleration.

This equation can also be applied to the rotor housing assembly as shown in Figures 33 and 34.

R_c = Position vector of the rotor center relative to xyz coordinate system,

$\bar{r}$ = Position vector of any point P on rotor relative to xyz coordinate system,

ρ = Position vector of point P, relative to $x_2y_2z_2$ coordinate system.

Hence the absolute acceleration of point P can be calculated from equation 5.7.

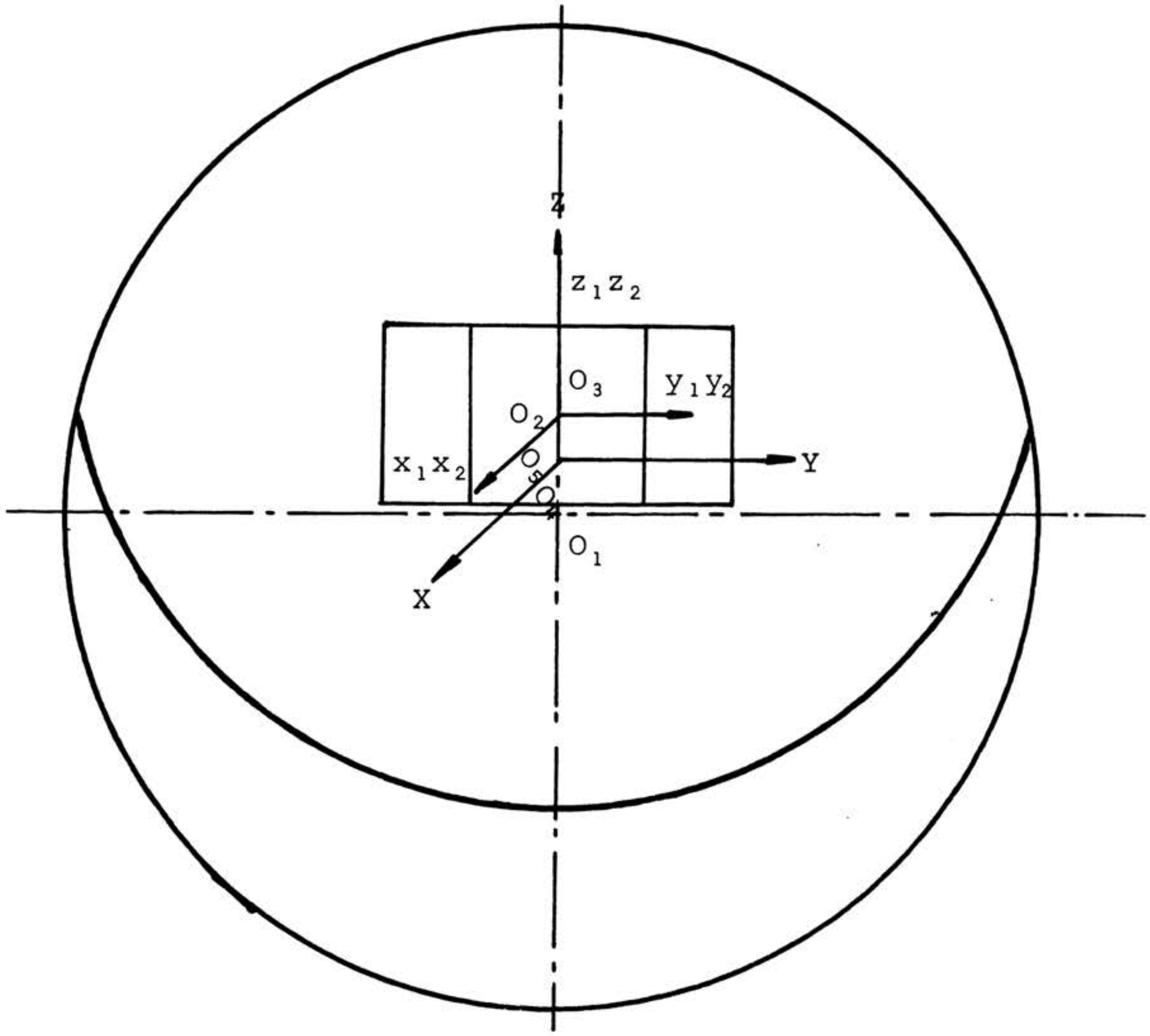

Figure 33. Zero Degree Rotor Position.

O_1 = Housing Center

O_2 = Shaft Center and Origine for $x_1y_1z_1$ System Fixed on Shaft

O_3 = Rotor Center (Coinciding with Shaft Center for 0° Position) and Origine for $x_2y_2z_2$ System Fixed on Rotor

O_4 = Point Through Which Minor Axis is Always Passing

O_5 = Mid-point of O_2O_4, the Diameter of Circle on Which Rotor Center O_3 is Assumed to be Traveling

$x_1y_1z_1$ = Fixed Reference System on Shaft

$x_2y_2z_2$ = Fixed Reference System on Rotor

XYZ = Absolute Fixed Reference System on O_5.

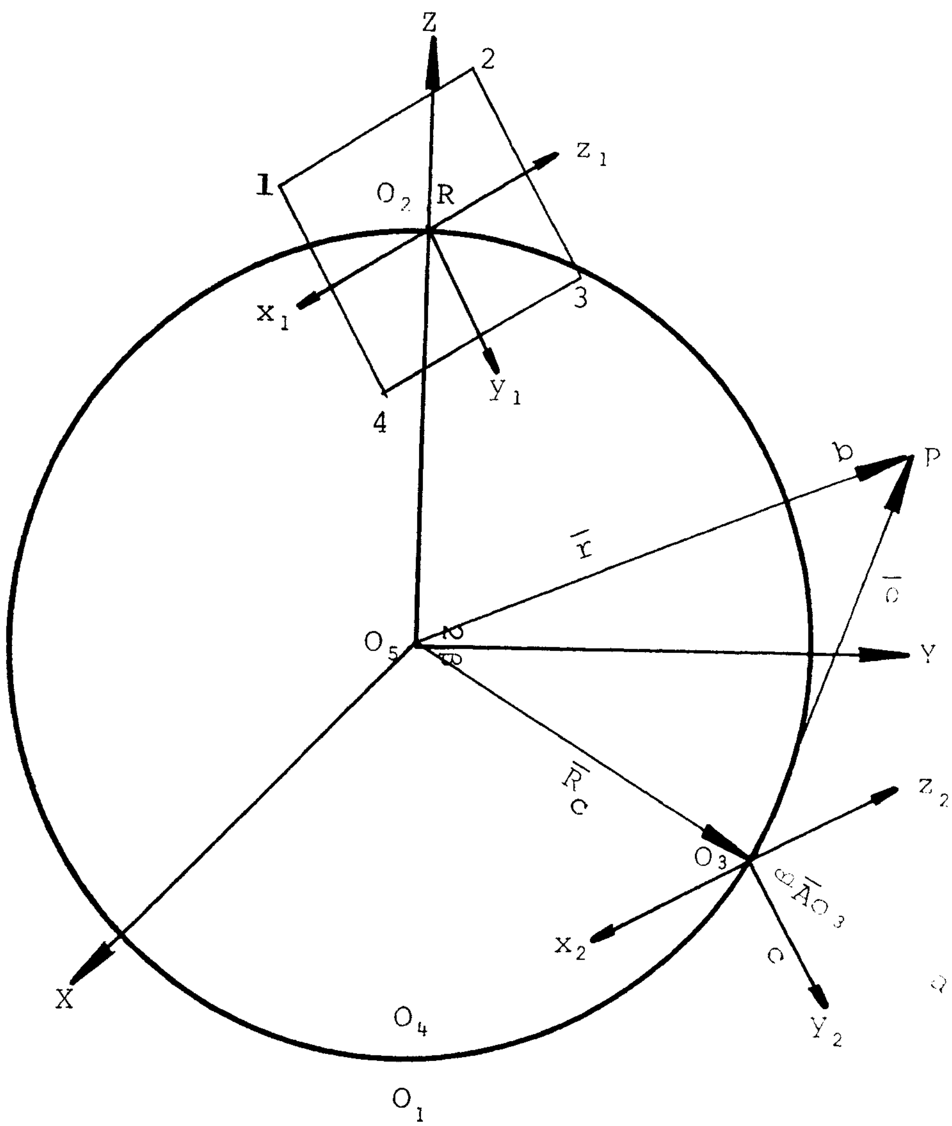

Figure 34. Assumed Path of Rotor Center and General Acceleration of any Point P on the Rotor.

O_1 = Housing Center

O_2 = Shaft Center (Origine for $x_1y_1z_1$ Shaft Fixed System)

O_3 = Rotor Center (Origine for $x_2y_2z_2$ Rotor Fixed System)

O_4 = Point Through Which Minor Axis is Assumed to Pass Through.

O_5 = Center of the Circle on Which Rotor Center is Assumed to Travel (Origine for Absolute Reference Frame XYZ

YZ, y_1z_1, y_2z_2 are in the Plane of Paper.

$$\ddot{\bar{A}}_p = \ddot{\bar{R}}_c + \ddot{\bar{\rho}} + 2\bar{w}_r \times \dot{\bar{\rho}} + \dot{\bar{w}}_r \times \rho + w_r \times (w_r \times \bar{\rho})$$

where

w_r = The absolute angular velocity of rotor (The angular velocity of $x_2 y_2 z_2$ relative to xyz system).

When point P is the rotor center, i.e. when $\bar{\rho} = 0$, equation 5.7 becomes:

$$\ddot{\bar{A}}_p = \ddot{\bar{R}}_c \; .$$

The vector $\bar{R}_c$ can be expressed in terms of the shaft rotation β as follows:

$$\bar{R}_c = R_c \mathrm{Cos}(2\beta)\hat{K} + R_c \mathrm{Sin}(2\beta)\hat{j} \; .$$

Since the path of the rotor center is assumed to be circular, the deviations of $\bar{R}_c$ with respect to time will be zero. Therefore,

$$\dot{\bar{R}}_c = -2R_c(\mathrm{Sin}2\beta)(\dot{\beta})\hat{K} + 2R_c \mathrm{Cos}(2\beta)(\dot{\beta})\hat{j} \qquad (5.8)$$

and

$$\ddot{\bar{R}}_c = -4\dot{\beta}^2\bar{R}_c - 2\ddot{\beta}(R_c \mathrm{Sin}2\beta\hat{K} - R_c \mathrm{Cos}2\beta\hat{j}) \; .$$

If there is no angular acceleration of the shaft, i.e. $\ddot{\beta} = 0$, the acceleration of the rotor center is given by:

$$\ddot{\overline{R}}_c = -4\beta^2 \dot{\overline{R}}_c$$

$$= -4w^2 \overline{R}_c$$

where

w = Angular velocity of output shaft.

This means that the direction of acceleration is radial and directed towards the center of rotation of O_3. This is indicated by vector AO_3 in the Figure 34.

If the rotor mass is m then the inertia force due to the radial acceleration AO_3 will be

$$\overline{aO}_3 = -4mw^2 \overline{R}_c \ .$$

The tangential and radial components are

$$\overline{bO}_3 = \overline{aO}_3 \ \mathrm{Cos}\beta$$

$$\overline{cO}_3 = \overline{aO}_3 \ \mathrm{Sin}\beta \ .$$

$\overline{bO}_3$ is the force causing torque on the shaft as given by:

$$\overline{T}_i = (-bO_3 \hat{K}) \ X \ (-O_3 O_2 \hat{j})$$

$$\overline{T}_i = -(bO_3 \ X \ O_2 O_3)\hat{i}$$

and torque due to the steam load will be

$$\overline{T}_s = -(bO_3 \times O_2O_3)\hat{i}$$

where

T_s = Torque due to steam load

P = Steam load.

Hence the effective torque will be

$$\overline{T}_e = -(P \times O_2O_3)\hat{i} - (bO_3 \times O_2O_3)\hat{i} .$$

But since,

$$bO_3 = aO_3 \ \text{Cos}\beta$$

$$O_2O_3 = O_2O_4 \ \text{Sin}\beta, \text{ (Figure 34)}$$

$$aO_3 = -4mw^2\overline{R}_c$$

$$O_2O_4 = 2R_c$$

$$T_e = -(P \times 2R_c \ \text{Sin}\beta)\hat{i} - (4mw^2R_c^2 \ \text{Sin } 2\beta)\hat{i} . \qquad (5.9)$$

The value of R_c is given in Figure 24,

$$2R_c = O_2O_4 = O_2O_1 - O_1O_4$$

$$= \frac{R}{5} - [R - \frac{\sqrt{24}}{5} R]$$

$$= 0.1798 \text{ R.}$$

The first part of equation 5.9 has been evaluated and tabulated as shown in Table 5.4. The second part represents the inertia effect of rotor. Assuming the rotor weight to be

20.0 lbs and the angular velocity to be 1000 rpm, equation 5.9 was evaluated for different values of β. Results are given in Table 5.5 and a graph of torque VS shaft angle is plotted in Figure 35.

The radial component of the force vector $\overline{aO}_3$, i.e. $\overline{cO}_3$ does not cause any inertia torque on the shaft because its line of action always passes through the shaft center. But it will cause the inertia force on the shaft which will tend to bend the shaft. The magnitude of this force

$$\overline{cO}_3 = -4mw^2R_c \operatorname{Sin}\beta$$

The maximum value of which will be

$$= 4mw^2R_c \ .$$

Substituting the following values in above equation the maximum inertia is evaluated

$m = 0.62$ lb-sec^2/ft (rotor weight = 20.0 lbs),

$w = 104$ rad/sec (rotor speed = 1000 rpm),

$R_c = 0.1798$ R, where R = 4.0 inches.

The inertia force is 4 lbs which can be neglected.

TABLE 5.5

TORQUE-ANGLE RELATION

(WITH INERTIA EFFECT)

ROTATION OF OUT-PUT SHAFT IN DEGREES	STEAM TORQUE IN FT-LBS	INERTIA TORQUE FT-LBS	EFFECTIVE TORQUE FT-LBS
0	0	0	0
10	157.99	8.38	166.37
20	311.17	+15.74	326.91
26-(Cut-off)	398.83	19.30	418.13
30	344.63	21.21	365.84
40	254.54	24.12	278.86
50	198.74	24.11	222.85
60	160.38	21.19	181.57
70	132.08	15.72	147.80
80	110.07	8.35	118.42
90	92.26	0.00	92.26
100	77.35	-8.41	68.94
110	64.52	-15.77	48.75
120	53.19	-21.23	31.96
130	42.96	-24.12	18.84
140	33.53	-24.10	9.43
150	24.68	-21.17	3.54
160	16.23	-15.69	0.54
170	8.02	-8.32	-0.20
180	0.00	0.00	0.00

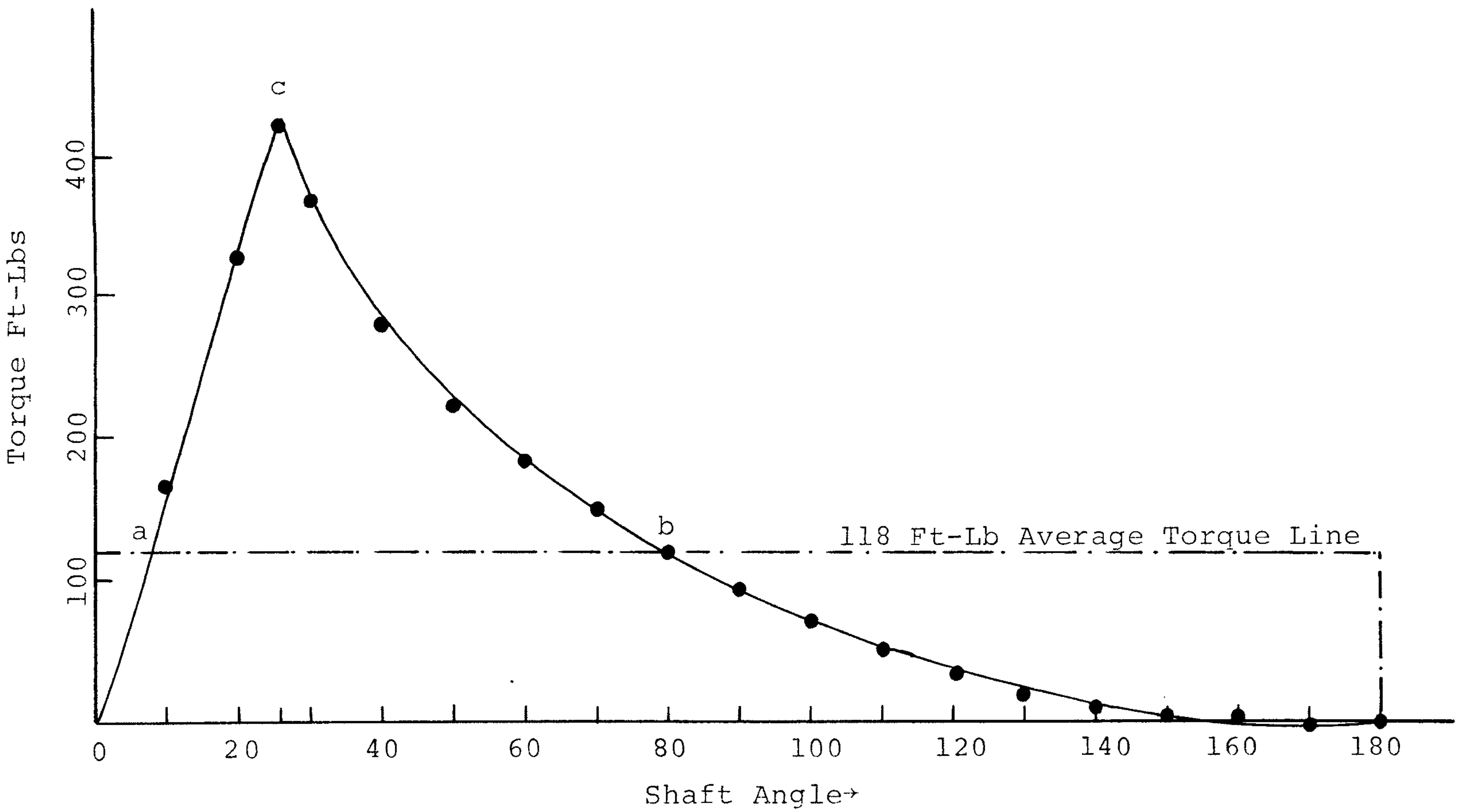

Figure 35. Torque-Angle Relationship.

c = Steam Cut-off at 26°

I. Sealing, Friction Losses and Lubrication

(1) Sealing: Sealing the flow of steam, from the high pressure side to the low pressure side, presents a difficult problem in rotary engines. The problem in this case is similar to that encountered in the Wankel engine. Since it now appears possible to seal the Wankel engine satisfactorily, it should be possible to accomplish the same result with the engine proposed here.

The two areas that must be sealed are:

(a) between the housing walls and rotor ends, and

(b) between the cover plates and rotor sides.

The seals are called apex seals and face or side seals respectively. The apex seals developed for the Wankel engine should perform satisfactorily. Figures 39 and 40 show this type of seal. It is interesting to analyze the apex seal movement with respect to shaft rotation (cm in Figure 24).

$$cm = am - ac$$

From triangle aO_1m:

$$am = 2R \text{ Cos}\alpha,$$

and

$$ac = 2R \text{ Sin}\theta \text{ (Major axis)}$$

Substituting for θ (From Section E):

$$cm = 2R[\mathrm{Cos}\alpha - 0.979], \qquad (5.11)$$

where

$$\alpha = \mathrm{Arc\ Sin}\ (0.2\ \mathrm{Cos}\beta),$$

and

$$\beta = \text{Shaft rotation.}$$

In Section G this seal movement was assumed to be negligible in calculating steam torque on the output shaft. Referring to Figure 24, it is obvious that high pressure steam will cause some force on seal and an additional torque on the shaft. This torque can be calculated as follows:

$$T_{seal} = (B \times cm) \times P(\beta) \times (O_3c + \frac{1}{2}cm) \qquad (5.12)$$

where

T_{seal} = Torque due to steam pressure on seals,

B = Seal width (4.0 inches),

cm = Seal length,

$P(\beta)$ = Effective steam pressure on seal,

$O_3c + \frac{1}{2}cm$ = Torque arm.

Values of cm for different values of β can be calculated from equation 5.11. For hyperbolic steam expansion, the value of $P(\beta)$ for any angle β is expressed by equation 5.6A and B.

$$P(\beta) = p_1 \qquad \beta \leq \beta_c ,$$

$$P(\beta) = \frac{p_1 V_c}{V(\beta)} \qquad \beta \geq \beta_c ;$$

where

p_1 = Inlet steam pressure

V_c = Volume of steam at cut-off

β_c = Angle of steam cut-off

$V(\beta)$ = Housing volume at any angle expressed by equation 5.2

O_3c = Semi major axis (3.92 in.)

Values of T_{seal} for various shaft positions are calculated and tabulated in Table 5.6.

The area between the cover plates and adjacent rotor surfaces is sealed by face or side seals. Piston ring type face seals similar to those developed for the Wankel engine (Figures 39, 40) are recommended. Table 5.7. obtained from reference [21], suggests various material combinations for seals and mating surfaces.

(2) Friction losses: At this stage of design it is difficult to estimate accurately the friction losses due to the apex and face seals. However a preliminary analysis will indicate the order of magnitude of seal friction losses.

The average rubbing velocity for the apex

TABLE 5.6

SEAL MOVEMENT AND TORQUE DUE TO STEAM PRESSURE ON SEAL

SHAFT ROTATION β, DEGREES	PRESSURE, PSI (EFFECTIVE)	SEAL MOVEMENT CM, INCHES	SEAL EFFECTIVE AREA (B X CM), SQ INCHES	TORQUE ARM, IN.	TORQUE, FT/LBS.
0	0	0	0	3.920	0
10	489.0	0.005	0.02	3.924	3.1
20	484.0	0.019	0.076	3.930	12.1
26	484.0	0.031	0.124	3.936	19.8
30	359.0	0.058	0.232	3.940	27.0
40	200.0	0.067	0.268	3.954	17.7
50	125.0	0.102	0.408	3.971	16.7
60	84.0	0.122	0.488	3.981	13.5
70	50.0	0.143	0.472	3.991	9.5
80	44.5	0.157	0.628	3.998	9.3
90	34.0	0.162	0.648	4.008	7.4
100	26.5	0.157	0.628	3.998	5.5
110	21.2	0.143	0.472	3.991	4.0
120	17.3	0.122	0.488	3.981	2.8
130	14.5	0.102	0.408	3.971	2.5
140	12.3	0.067	0.268	3.954	1.1
150	10.8	0.058	0.232	3.948	0.825
160	9.8	0.019	0.076	3.930	0.242
170	9.3	0.005	0.02	3.924	0.06
180	0.0	0.00	0.0	3.920	0.0

TABLE 5.7

PROPER COMBINATIONS FOR BEST SEALING RESULTS

HOUSING INSIDE SURFACE	APEX SEALS	SIDE COVERS	FACE OR SIDE SEALS
Hard chrome	Carbon	Molybdenum	Piston ring cast iron*
Cemented carbide	Cast iron	Bronze	Cast iron, steel
10% Molybdenum + 90% steel	Soft iron	Cast iron (Nitrided or induction hardened)	Piston ring cast iron*
Nickel plating and simultaneous depositing of silicon carbide particles	Piston ring cast iron	Steel, spray deposited	Piston ring cast iron*

The last combination in this table was developed in the United States and appears to be best suited for mass production at reasonable cost.

*Same composition as used for piston rings.

seals is given approximately by

$$V_s = R \times w,$$

where

R = Radius of the housing,

w = Rotor angular velocity.

Hence, the horsepower loss at each apex seal will be

$$HP_a = f \frac{V_s f_1}{550}$$

where

HP_a = Friction horsepower at apex seals,

f = Coefficient of friction,

V_s = Rubbing velocity,

f_1 = Force in lbs.

For

R = 4.0 in,

w = 104.0 rad/sec (1000 rpm),

this equation reduces to $HP_a = 0.0619ff_1$ for each of the apex seals. For both the apex seals $HP_A = 0.1238ff_1$.

There is no precise data available for the coefficient of friction between the seal and housing in the presence of steam containing a lubricant, nor it is easy to estimate the contact force f_1.

Assuming f = 0.08 [20] and apex seals width 0.1 inch, length 4.0 inch (i.e. contact area 0.4 sq inch) and mean effective steam pressure of 82 psi will have contact force of 35 lbs. Assuming spring force of 15 lbs at each seal the total contact force f_1 = 50 lbs and hp lost will be:

$HP_a = 0.5.$

It is difficult to estimate rubbing velocity of face seals because the rotor is rotating as well as reciprocating. However a fair approximation can be obtained by assuming that the rotor is not reciprocating on the shaft and that the face seals are circular of 8.0 inch diameter. At the normal running speed of 1000 rpm these approximations will yield a rubbing velocity of 30 ft/sec. The cross section of each seal is assumed to be rectangular with width of 1/16 inch, total length of all four pieces will be 40.0 inches based on Figure 39. The pressure on each seal is assumed to be 82.0 psi (mean effective steam pressure and spring force is neglected). Hence, the seal friction losses will be

$$HP_f = \frac{f\ V_s P w l^1}{550} \qquad (5.13)$$

where

HP_F = Friction horsepower at face seals,

f = Coefficient of fraction,

V_s = Rubbing velocity in ft/sec,

p = Sealing pressure (mean effective steam pressure),

w = Width of the seal,

l^1 = Half the total seal length.

Substituting in equation 5.13:

V_s = 30 ft/sec,

p = 84.0 psi,

w = 1/16 inch,

l^1 = 20 inches,

yields $HP_F = 5.7\ f$.

For a coefficient of fraction $f = 0.08$, HP_F = 0.456 hp, and the total friction losses from face and apex seals will be

$$HP_F = 0.96 \text{ hp}.$$

Friction losses between the shaft and rotor can be calculated on the basis of average rotor velocity with respect to the shaft and mean effective pressure.

Equation 5.8 ($\dot{\bar{R}}_c = -2R_c \mathrm{Sin}(2\beta)(\dot{\beta})\hat{k} + 2R_c \mathrm{Cos}(2\beta)(\dot{\beta})\hat{j}$) represents the absolute velocity of the rotor center; and the relative sliding velocity of the rotor on the shaft is then

$$\bar{v} = 2R_c \operatorname{Cos}(2\beta)\dot{\beta}j.$$

The maximum sliding velocity occurs when $\beta = 0$ and decreases to zero at $\beta = 90°$. Hence the average velocity can be obtained by integrating the velocity function from 0 to $\pi/4$ and dividing the result by $\pi/4$:

$$V_{avg} = \frac{\int_0^{\pi/4} 2R_c\, w \operatorname{Cos}(2\beta)\, d\beta}{\pi/4}$$

$$= \frac{4R_c\, w}{\pi} \quad .$$

For

$$R_c = 0.1798R,$$

$$R = 4.0 \text{ in},$$

$$w = 104 \text{ rad/sec (1000 rpm)},$$

$$V_{avg} = 7.9 \text{ ft/sec}.$$

For the mean effective pressure of 82.0 psi and an effective rotor area of 29.5 sq in (For R = β = 4.0), the total steam load on the rotor will be 2475.0 lbs.

The corresponding horsepower lost in friction between the rotor and shaft is given by

$$HP_R = f\,\frac{PV}{550} \; .$$

For

$$P = 2475 \text{ lbs},$$

$$V = 7.9 \text{ ft/sec},$$

$$HP_R = 35.18 \; f,$$

where

$$f = \text{Coefficient of friction.}$$

Again the value of coefficient of friction is difficult to estimate. However, as mentioned later, it is possible to provide adequate lubrication at the shaft rotor surface; the coefficient of friction is therefore assumed to be 0.08 [20]. The resulting horsepower loss is 2.8 at maximum engine speed and design cut-off.

The total friction losses inside the engine are obtained by adding HP_F and HP_R. The maximum value of these losses is 4.26 hp, and brake horsepower is thus 10.74 at 1000 rpm. This will give a mechanical efficiency of 71.5% which is relatively poor compared to the 85% efficiency of reciprocating internal combustion engines.

(3) Lubrication: The usual practice in conventional reciprocating steam engines is to provide forced lubrication of the cross head and crankpin connections. Piston and cylinder lubrication are achieved by introducing a small amount of oil into the steam [6]. The same practice can

be used here.

(a) Oil can be supplied under pressure to the shaft-rotor contact surface through a passage drilled in the shaft.

(b) The seals can be lubricated by introducing oil into the steam. However, complete removal of the lubricant from the condensate is essential to prevent oil deposition on boiler tubes and eventual failure through cracking [3]. Although no method is currently available for completely removing all lubricant from the condensate, oil injection appears to be the only method for lubricating the seals. If a self-lubricating material can be used for the seals, the problem of lubricant removal will be eliminated. Until a satisfactory material is developed a lubricating pump and oil separator will be required.

J. Engine Housing, Shaft, Bearings and Coverplate Design

(1) Housing design: The engine housing can be considered to be a thick walled cylinder for purposes of stress analysis. When a closed cylinder is filled with pressurized fluid, it is subjected to three mutually perpendicular stresses: (away from ends) radial, tangential

and longitudinal. The radial stress at some distance from the ends varies from $-p$ at inside to 0 at outside. The tangential and longitudinal stresses are given by:

$$S_t = \frac{pr_1^2}{(r_2^2 - r_1^2)} \left(\frac{r_2^2}{r_1^2} + 1\right) \tag{5.14}$$

and $$S_l = \frac{pr_1^2}{(r_2^2 - r_1^2)}$$

where

S_t = Tangential stresses,

S_l = Longitudinal stresses,

p = Maximum fluid pressure,

r_1 = Inside radius,

r_2 = Outside radius.

Cast steel has been widely employed for steam engine cylinders and has a tensile strength ranging from 60 to 80 kpsi. Cast steel has a fatigue endurance limit ranging from 24 to 32 kpsi. The stresses developed are calculated assuming a cylinder thickness of 0.5 inches.

Substituting

p = 500 psi,

r_1 = 4.0 inch,

r_2 = 4.5 inch,

the tangential and longitudinal stresses are found to be 4300 psi and 2000 psi, respectively. The maximum shear stress is 2400 psi; thus all stresses in the housing are well within safe limits.

In the above analysis it was assumed that the entire housing is filled with high pressure steam. But actually only the inlet side of the housing is subjected to this pressure, while exhaust side is subjected to 16 psia. It is very difficult to calculate the exact stress distribution under these conditions, but the above analysis should provide a reasonable, yet conservative estimate.

(2) Shaft design: The shaft is subjected to combined loading and should be carefully designed since there is a change in section and loading is cyclic. The shaft will be supported in journal bearings as is done in usual practice.

The shaft is subjected to both steam torque and steam load. The maximum steam torque will occur at a 90° shaft position, as seen from equation 5.5, when there is no cut-off applied. This condition may prevail when starting under heavy load. The maximum steam torque will be 10,800 lbs-in. The direct maximum steam load is the product of steam pressure and the effective rotor area. During normal operation maximum steam load occurs up to design cut-off (26°) and reduces to 0 at 180° of rotation. Since there are two cycles in each revolution the shaft is subjected to bending stresses which are reversed. For a net steam pressure of 484 psi and 314 sq inches projected area, the maximum steam load is 15,200 lbs. Since the shaft is supported in journal bearings the end conditions are neither simply supported nor fixed. However, to make a conservative analysis the shaft is treated as a simply supported beam. The shaft material is AISI 3250 steel drawn at 600°F, with a yield strength of 200 kpsi in tension, 100 kpsi in shear, and a fatigue endurance limit of 80 kpsi in tension [20].

The maximum bending moment to which the shaft is subjected can be calculated from Figure 36 as follows:

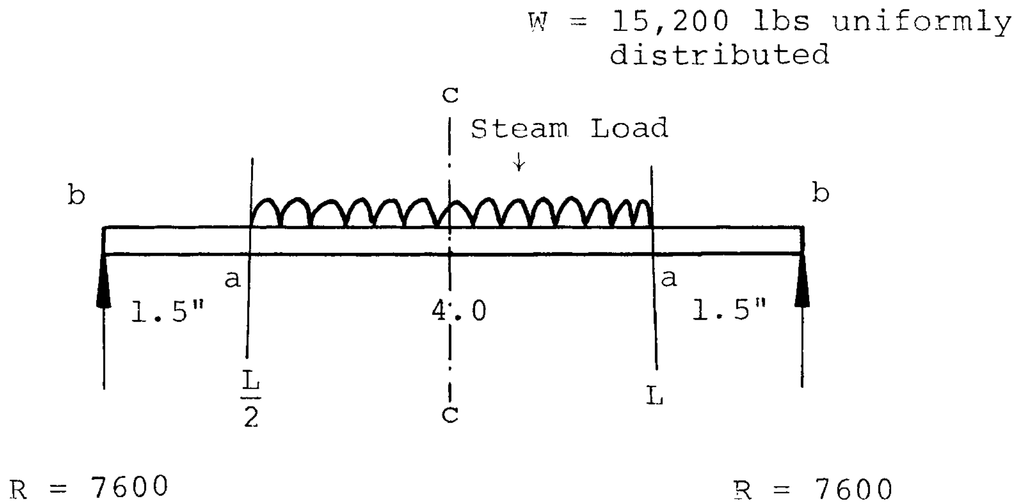

Figure 36. Shaft Loading.

aa = Square section of shaft subjected to uniformly distributed load of 15,200 lbs,

= 4.0 inches.

bb = Total shaft length from center to center of bearings,

= 7.0 inches (It is assumed that bearing length is 3.0 inches which is verified later.)

The maximum bending moment occurs at cc and is given by

$$M_v = R\left(\frac{L}{2}\right) - \left(\frac{W}{2}\right)\left(\frac{L}{2} - ab\right)\frac{1}{2}$$

where

R = Bearing reaction.

Substituting from Figure

R = 7600 lbs,

L = 7.0 in,

W = 15,200 lbs,

$ab = 1.5$ in,

$M_v = 19{,}000$ lb-in,

and assuming that the shaft is circular, the minimum diameter is given by

$$d = 2.17\ [\eta\{0.422(\frac{T_o}{\sigma_y})^2 + (\frac{K_{tt}\ M_v}{\sigma_e})^2\}^{\frac{1}{2}}\ ]^{\frac{1}{3}}$$

(5.15) [20]

where

d = Diameter,

η = Factor of safety,

T_o = Steady torque,

M_v = Completely reversed bending moment,

σ_y = Yield shear stress,

σ_e = Yield bending stress,

K_{tt} = Notch and fatigue factor.

The value of K_{tt} is given by:

$$K_{tt} = q(K - 1) + 1 \qquad (5.16)\ [20]$$

where

q = Notch sensitivity factor,

K = Stress concentration factor.

The value of q depends on the fillet radius where the shaft section changes, up to a maximum value of unity. Since no data are available on the section change from square to to circular, the square section is assumed to be circular with diameter equal to the diagonal, as shown in Figure 37A. The dimensions given in Figure 37A are assumed and verified later.

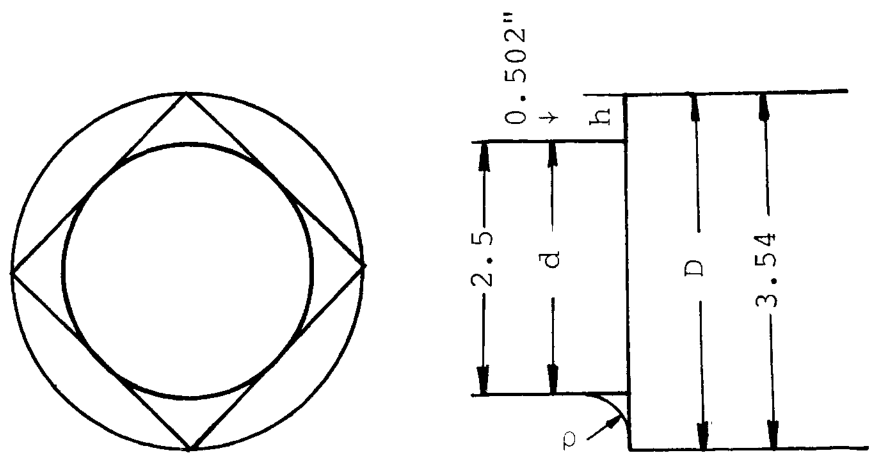

Fillet
Radius ρ = 0.25 inch

Figure 37A. Shaft Details.

For a fillet radius greater than 0.2, the value of q is unity [20].

The stress concentration factor is plotted as function of sharpness of fillet (h/ρ) and the ratio h/d in reference [20]. In this case values of

$$\frac{h}{\rho} = 2.0$$

and

$$\frac{h}{d} = 0.2$$

are obtained.

For these values, the stress concentration factor (K) is found to be 1.4. But to account for oil hole which may weaken the shaft [page] the stress concentration factor is assumed to be 2.0. Hence, value of K_{tt} in equation 5.16:

$$K_{tt} = 2.0.$$

The factor of safety η in equation 5.15 is recommended by reference [20]. Substituting the following values in equation 5.15:

$$\eta = 4.0,$$
$$T_o = 10{,}800 \text{ lbs-in},$$
$$\sigma_y = 100{,}000 \text{ psi},$$
$$K_{tt} = 2.0,$$
$$M_v = 19{,}000 \text{ lbs-in},$$
$$\sigma_e = 214{,}000 \text{ psi},$$

the shaft diameter is found to be 2.3 in, therefore, a diameter of 2.5 in should be adequate.

Next the maximum stresses produced in the square section will be calculated:

the bending stresses are given by;

$$S_{t,c} = \frac{6M_v}{a^3} \quad [20]$$

where

$S_{t,c}$ = Stresses, tensile and compressive,

M_v = Maximum bending moment

a = Side of the square section.

Substituting

M_v = 19,000 lb-in,

a = 2.5 in,

yields

$$S_{t,c} = 7300 \text{ psi.}$$

The torsional shear stresses are given by

$$T_t = \frac{9}{2} \frac{T_o}{a^3} \quad [20]$$

where

T_t = Maximum torsional shear stresses ,

T_o = Maximum torque,

a = Side of the square.

Substituting

T_o = 10,800 lb-in,

a = 2.5 in,

gives

T = 3140 psi.

These shear stresses are maximum values and occur at the mid point of each side of the square section; the stresses vanish at the corners and center of the section. The resulting stress distribution on the shaft surface is parabolic in nature [20]. The direct average shear stresses are

$$T_s = \frac{W}{a^2}$$

where

T_s = Direct average shear stresses

W = Direct load

a = Side of the square.

For

W = 15,200 lbs

a = 2.5 in

T_s = 2440 psi,

the maximum direct shear stresses occur at center of the section and is given by:

$$T_{smax} = 1.5\ T_s$$

$$= 3660 \text{ psi.}$$

Therefore torsional and direct shear stresses occur in different planes and have maxima at different locations. Stresses at different locations on the shaft section are shown in Figure 37B.

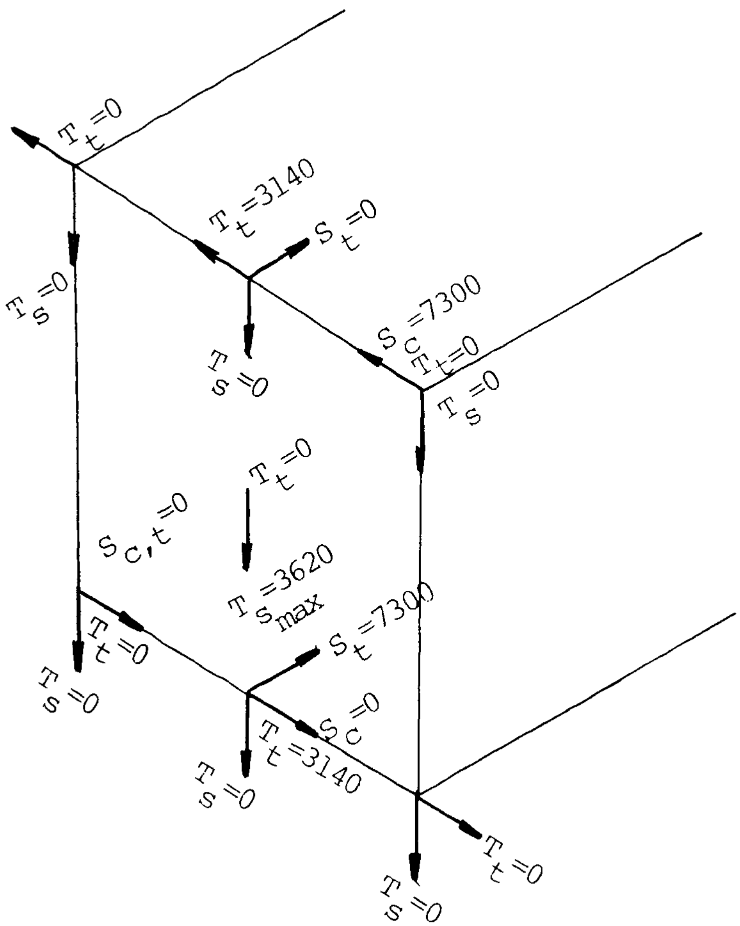

Figure 37B. Stresses at Different Locations in the Shaft.

Since the maximum direct shear stress is not accompanied by any other stresses, it is neglected in calculating principle stresses.

The principle stresses based on torsional and direct bending stresses are given by:

$$\sigma_{t,c} = \frac{S_{t,c}}{2} \pm \sqrt{\frac{S_{t,c}^2}{4} + T_t^2} \qquad (5.17)$$

Substituting the following values in equation 5.17:

$$S_{t,c} = 7300 \text{ psi}$$

$$T_t = 3140 \text{ psi}$$

$$\sigma_{t,c} = 3650 \pm 4900 \text{ psi}$$

to summarize

Maximum principle tensile stresses = 8550 psi.

Maximum principle compressive stresses = 1250 psi.

Maximum shear stresses = 4900 psi.

These values are far less than the corresponding endurance limits given earlier.

(3) Bearing design: As mentioned previously, journal bearings are commonly used for automotive applications. Journal bearings are reliable when radial loads are large and shaft speed is greater than 600 rpm. However, special arrangements are necessary to lubricate these bearings. A lubricating pump is usually employed which supplies sufficient lubricant to form a lubricating oil film; the shaft is supported on this film.

The design pressure (load/projected area) that a journal bearing can withstand depends on the bearing alloy used. The current practice for permissible pressures on the journal bearing in marine steam engines is about 1200 psi [20], when copper-lead alloy is used. As discussed previously in shaft design, the steam load on the shaft is about 16,000 lbs and so on each bearing the maximum steam load will be approximately 8000 lbs. For a bearing 3.0 in long and 3.0 in in diameter, the bearing pressure for load of 8000 lbs will be 880 psi.

Because of higher running speed and heavy radial load an RC 5 or RC 6 class of journal bearing fit is recommended by reference [20]. The clearance for this class will be 0.002 in for a 1.5 in radius. The oil selected is SAE 20 oil, and the necessary oil pressure and flow rate can be calculated from

$$P_i = \frac{F_1}{BC^3(1 + 1.5\varepsilon^2)} \qquad (5.18A)\,[22]$$

where

$$B = \frac{23340\ \gamma\ (t_o - t_i)}{\mu l^{12} \eta} \qquad (5.18B)\,[22]$$

P_i = Pressure under which oil should be supplied

F_1 = Tangential force on the journal,

C = Radial clearance,

ε = Eccentricity ratio of the bearing,

γ = Specific gravity of oil,

$t_o - t_i$ = Temperature rise in oil,

μ = Viscosity of oil in lb-sec/in^2,

l^1 = Semi-bearing length,

η = RMP of the shaft.

It is assumed that inlet and outlet temperatures of oil are 160°F and 175°F respectively. Hence, the temperature rise of the oil is 15°F. The viscosity of oil and specific gravity should be determined at an average temperature of 167.5°F.

Substituting the following values in equation 5.18B:

γ = 0.03053 lb/in^3 [22],

μ = 19.4 X 10^{-} lb-sec/in^2 [22],

l^1 = 1.5 in,

$t_o - t_i$ = 15°F,

η = 1000 rpm,

the value of B is found to be

$B = 240 \times 10^4$.

The value of the eccentricity ratio, ε, can be determined by using data presented in graphical form in reference [22] where ε is plotted as a function of

$$\frac{W_1}{\mu u}\left(\frac{C}{\gamma}\right)$$

for different values of ratio l/d (bearing length/diameter),

where

W_1 = Radial load,

μ = Viscosity in lb-sec/in^2,

u = Rubbing velocity,

C = Radial clearance,

γ = Radius of the journal.

Substituting:

W_1 = 8000 lbs,

$\mu = 19.4 \times 10^{-7}$,

$u = \frac{\pi d\eta}{60} = 157$ in/sec,

$C = 0.002$ in,

$\gamma = 1.5$ in,

$$\frac{W_1}{\mu u}\left(\frac{C}{\gamma}\right)^2 = 46.5.$$

From the graphical data presented in [22] the value of ε for

$$\frac{W_1}{\mu u}\left(\frac{C}{\gamma}\right)^2 = 46.5$$

and $l/d = 1.0$ is $\varepsilon = 0.95$.

Corresponding to this value of ε the value of parameter

$$\frac{\mu u}{F_1}\left(\frac{\gamma}{C}\right)$$

can be estimated from data presented in reference [22], and for $\varepsilon = 0.95$ and $l/d = 1.0$,

$$\frac{\mu u}{F_1}\left(\frac{\gamma}{C}\right) = 0.038,$$

$$F_1 = \frac{\mu u}{0.038}\left(\frac{\gamma}{C}\right),$$

$$F_1 = 6.025 \text{ lbs.}$$

Now substituting the following values in equation 5.18A

$$F_1 = 6.025 \text{ lbs},$$

$$B = 240 \times 10^4,$$

$$C = 2 \times 10^{-3},$$

$$\varepsilon = 0.95,$$

the inlet oil pressure is found to be

$$P_i = 132 \text{ psi.}$$

The quantity of oil in each side is given by

$$Q = \frac{\pi \gamma C^3 P_i}{6\mu l^1}(1 + 1.5\varepsilon^2) \qquad [22]$$

For

$$\gamma = 1.5 \text{ in},$$

$$C = 0.002 \text{ in},$$

$$P_i = 132 \text{ psi},$$

$$\mu = 19.4 \times 10^{-} \text{ lb-sec/in},$$

$$l^1 = 1.5 \text{ in},$$

$$\varepsilon = 0.95,$$

the quantity of oil on each side is found to be

$$Q = 0.168 \text{ in}^3/\text{sec}.$$

Total oil flow is therefore 0.087 gpm.

The horsepower consumed by the pump is given by

$$HP = \frac{\text{psi} \times \text{gpm}}{\eta \times 1714}$$

where

psi = delivery pressure in psi,

gpm = Flow in gallons per minute,

η = Mechanical efficiency.

For

psi = 132.0,

gpm = 0.087,

η = 50%,

the horsepower required is found to be 0.0134, which can be ignored.

The bearing friction hp will be

$$HP = \frac{F_1 lu}{12 \times 550} .$$

For

$$F_1 = 6.025 \text{ lbs},$$

$$l = 6.0 \text{ in (both the bearings)},$$

$$u = 157 \text{ in/sec},$$

$$HP = 0.85.$$

This value is relatively large, but in normal running there will not be a steady load of 8000 lbs (average load of 1340 lbs corresponds to 84.0 psi mean effective pressure). Thus the friction horsepower can be expected to be significantly less. It should be noted here that the bearing design requires more investigation since the bearing load will be a steady 8000 lbs during starting or stalling conditions. Due to such conditions the oil film may rupture and metal to metal contact will increase friction and wear. In these circumstances it may become necessary to increase the oil inlet pressure to achieve hydrostatic lubrication.

(4) Cover plates and bolts: The maximum loading that can occur is shown by the shaded area (Figure 38). This may occur during starting period when there is no cut-off applied.

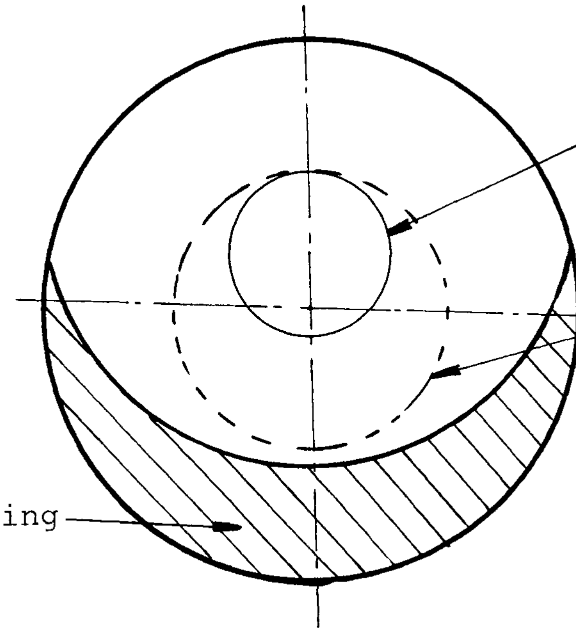

Figure 38. Cover Plate.

The plate thickness is assumed to be 0.5 inch and stresses developed are calculated assuming:

(a) The plate is simply supported.

(b) The hole is in the center but of 4.0 inch in diameter to compensate for the actual 2.5 inch diameter hole being off center.

(c) The load on the plate is uniformly distributed over the entire plate.

In the actual case there will be eight bolts used in fixing the plate to the rotor housing; this will provide some fixity and help to reduce deflection and bending stresses. The hole diameter is assumed to be almost twice as large to compensate for its shift from the center. This shift is only 10% of the cover diameter; hence the hole dimensions assumed should give a fairly conservative design. The 500 psia load is assumed to be acting over the entire plate but infact is acting only on about 30% of the plate area and also in the vicinity of the plate edge. It should be noted that these assumptions should result in a conservative design.

The maximum stresses developed are given by:

$$S_m = K \frac{Wr^2}{t^2} \quad [20]$$

where

S_m = Maximum bending stresses,

K = Coefficient depending on ratio of plate and hole diameter,

W = Uniformly distributed load,

r = Outside radius of the plate,

t = Thickness of the plate.

The value of K for the ratio of plate diameter to hole diameter of (9.0/4.0) is found to be 2.05 [20].

Substituting:

W = 485 psig,

r = 4.5 inch,

t = 0.5 inch,

the stresses developed are calculated to be $S_m = 44{,}500$ psi. Cast steel is recommended with an endurance limit of 30 to 50 KPSI.

The deflection is given by

$$Y_m = K_1 \frac{W\eta^4}{Et^3} .$$

For

$K_1 = 0.664$ [20],

$W = 485$ psig,

$\eta = 4.5$,

$E = 30 \times 10^6$ psi,

$t = 0.5$ inch.

The maximum deflection is $Y_m = 0.088$ inch, which appears reasonable.

The bolts can be designed on the basis of 485 psig steam pressure acting on the area of the plate with 8 inch diameter and 3 inch hole in the center, i.e. 21,000 lbs. Six bolts of 7/8 nominal diameter with 95 KPSI ultimate strength are recommended.

Rotor: The rotor can be made of cast iron or aluminum and should be cast and finished in two parts, so it can be assembled on the shaft. The length of the rectangular hole in the rotor is equal to the shaft width added to rotor travel relative to the shaft. Rotor travel is

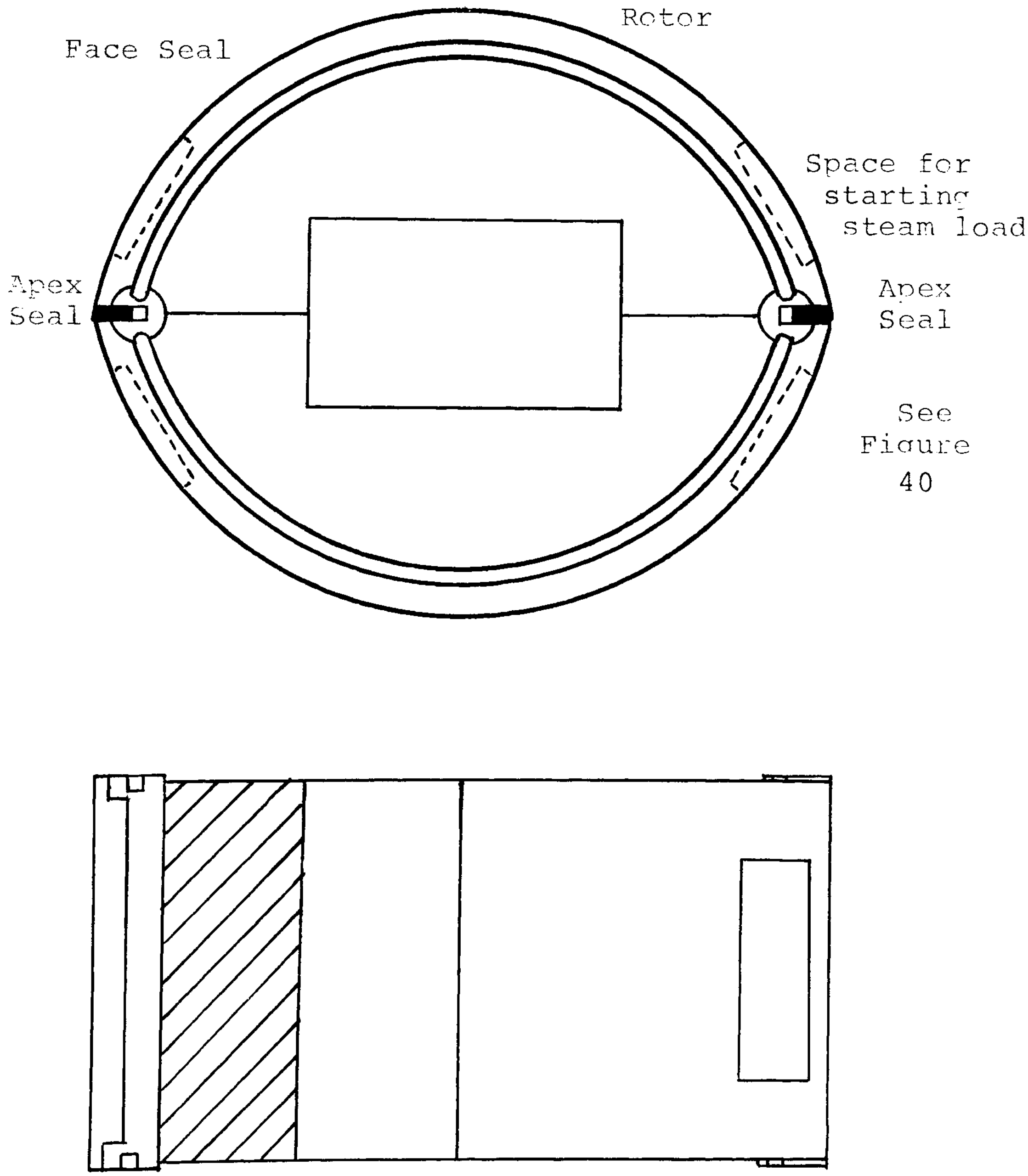

Figure 39. Rotor.

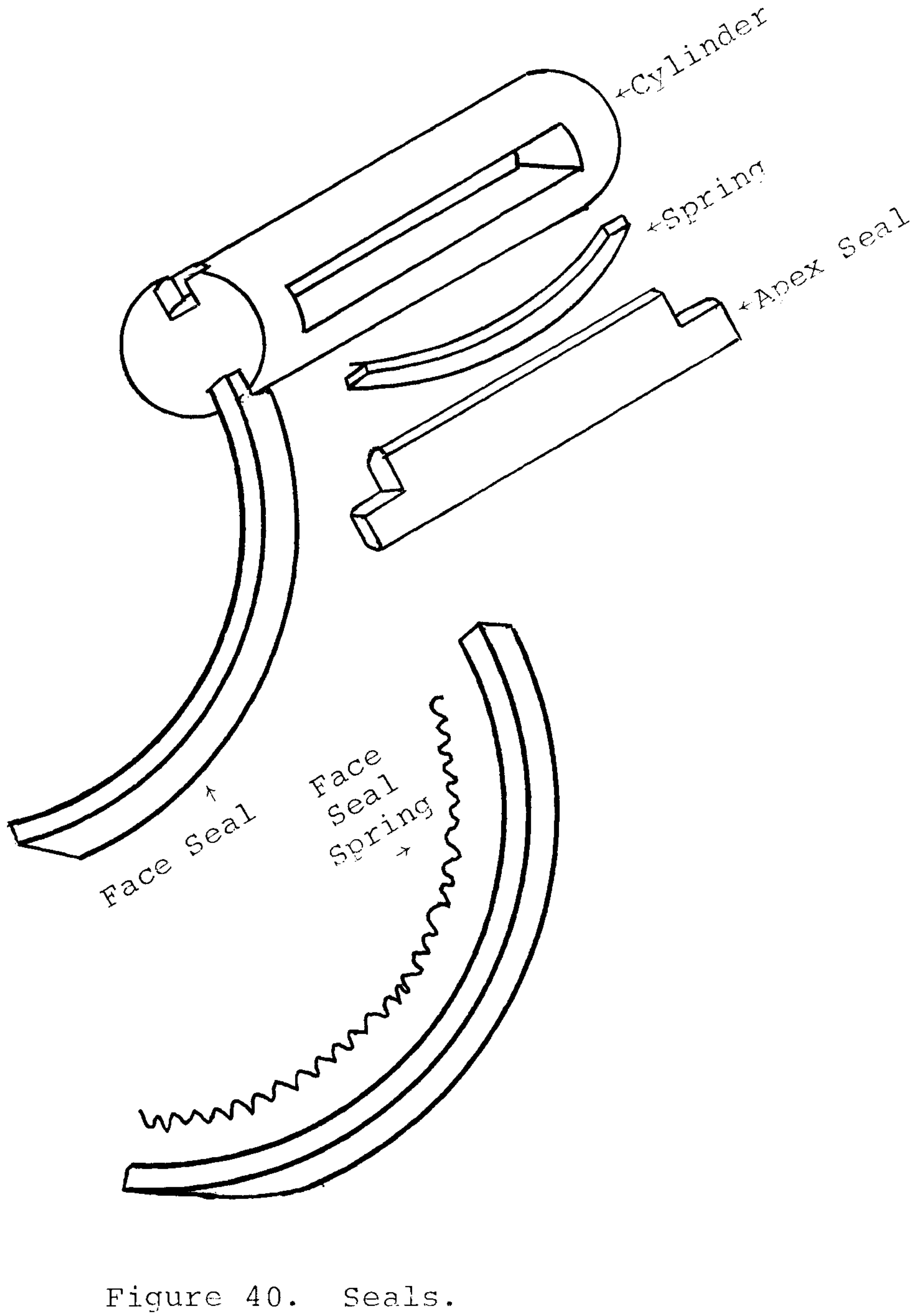

Figure 40. Seals.

the difference between the major and minor axes (1.60 inches) as shown in Figure 24. Dimensions of the rectangular holes are therefore 4.1 inches long X 2.5 inches wide.

Some metal should be removed from the rotor surface as shown in Figure 39. This will permit start-up when the rotor is in the dead center position, (Figure 18). If 1.0 square inch area is exposed to 500 psia inlet steam, the net force will be 484.0 lbs. This load will have a torque arm of about 0.8 inch and will produce a net torque of 16.0 ft-lbs, which should be sufficient to move the rotor from its dead center position.

K. Engine Governing.

The output power of a steam engine is governed by two variables:

(1) The inlet steam pressure

(2) The steam cut-off.

The inlet steam pressure is controlled by throttling. Usually this control is accomplished by an overspeed governor which operates a throttling valve whenever engine speed increases due to reduced requirements. Figure 41A indicates how the pressure-volume diagram changes with inlet steam throttling. As the inlet pressure is reduced, the steam expands more nearly to the condenser pressure and diagram efficiency increases. However, the indicated engine efficiency decreases because of losses due to throttling. As a result when engine speed is controlled by throttling, the overall efficiency decreases slightly. As the engine load increases the degree of throttling is reduced accordingly. If more power is needed than is available with no throttling, the steam admission period is increased. This is known as cut-off control. Figure 41B indicates how the pressure-volume diagram changes. Since the steam expansion becomes less complete engine efficiency is reduced. Also, for a given load, specific steam consumption for cut-off control is found to be more than for throttle control [Figure 42]. At the designed conditions (i.e. no throttling) and designed cut-off the engine operates at maximum efficiency. The low load conditions should be met by throttle control because it does not affect the engine efficiency appreciably. However at the overload conditions (and in starting) increased cut-off is essential to develop higher mean effective pressure and torque. Thus both the controls are necessary for automotive applications [2]. The effect of the throttling and cut-off control on indicated engine efficiency and relative steam consumption is shown in Figure 42.

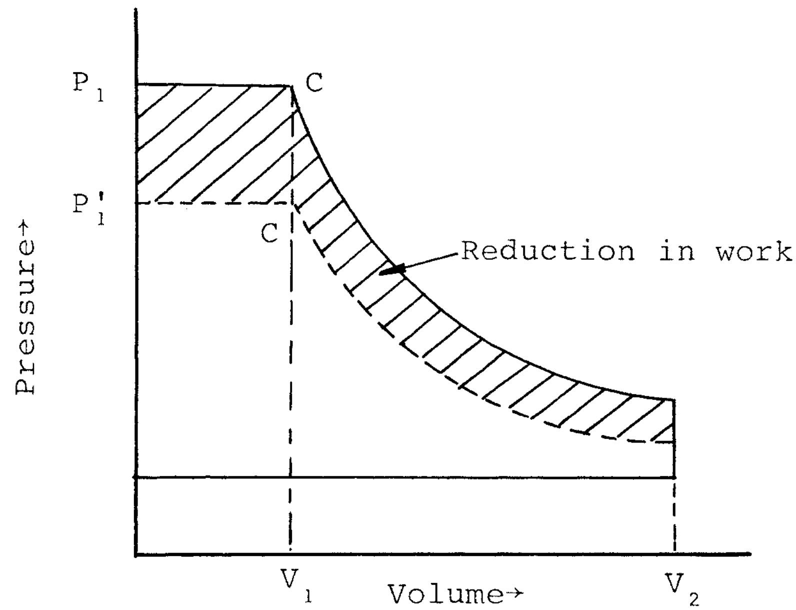

Figure 41A. Power Reduction due to Throttling.

P_1 = Inlet steam pressure

C = Point of cut-off

V_1 = Volume of steam at cut-off

V_2 = Volume of steam at end of expansion

P_1' = Pressure after throttling

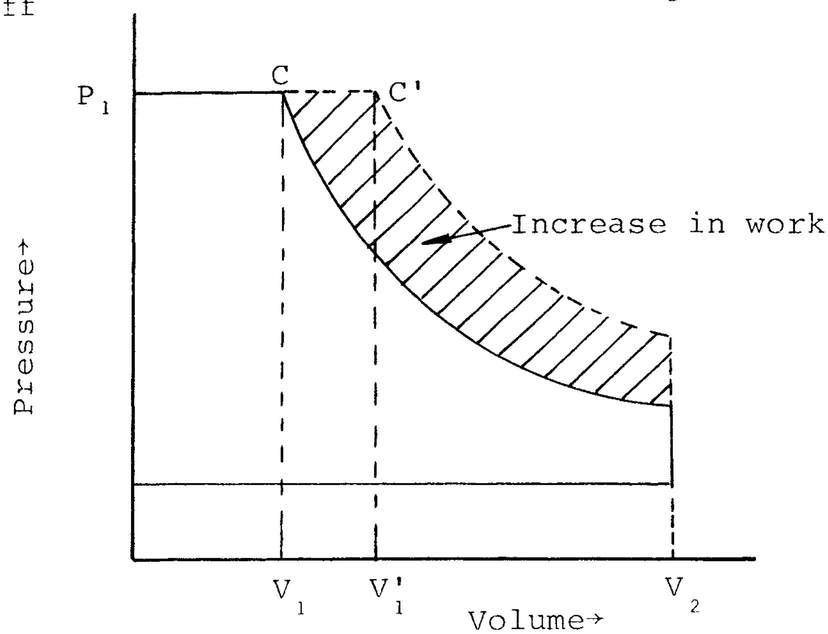

Figure 41B. Power Increase due to Late Cut-off.

C' = Increased cut-off

V_1' = Volume of steam at increased cut-off

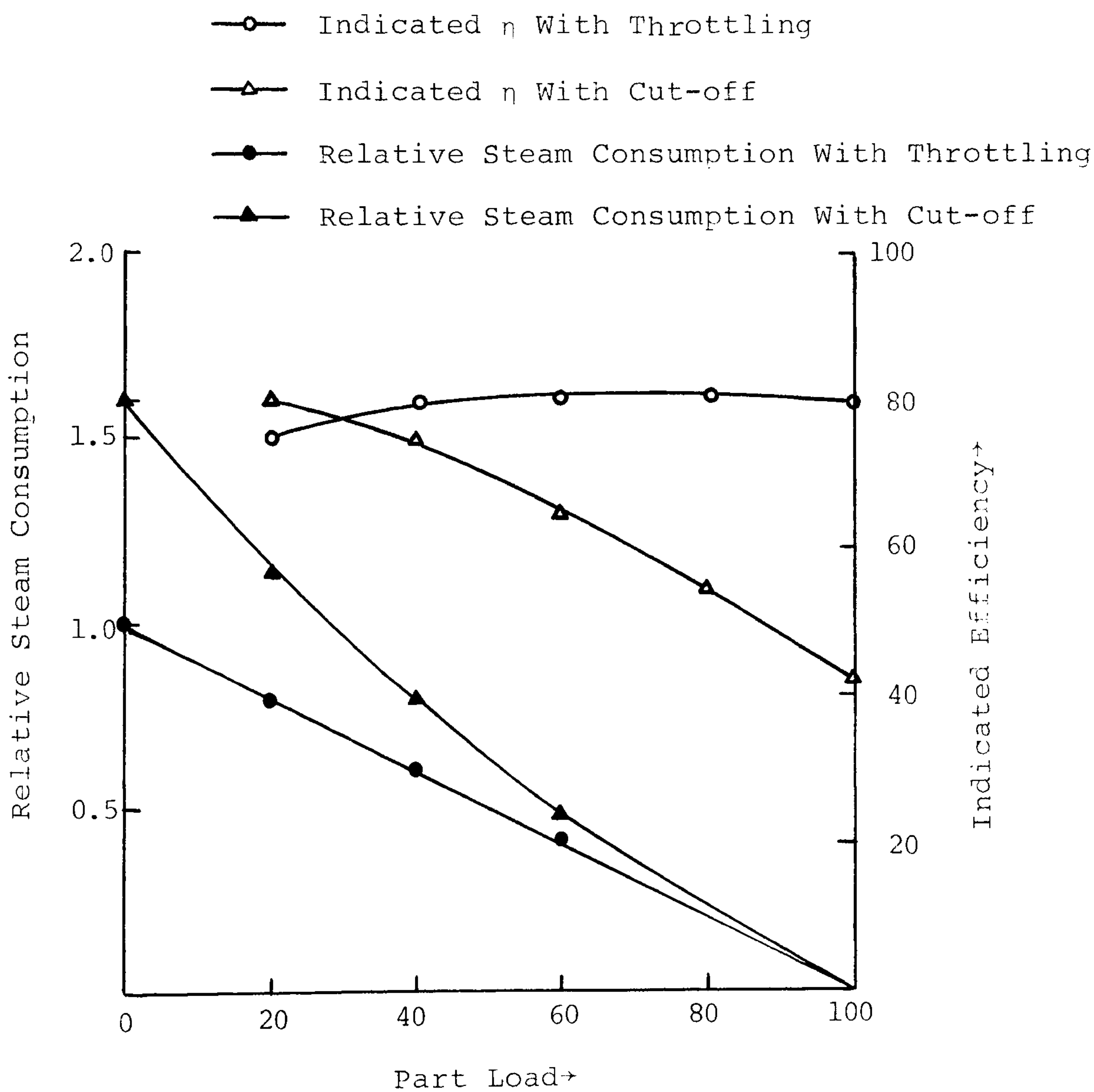

Figure 42. Effect of the Throttling and Cut-off Control on Indicated Engine Efficiency and Relative Steam Consumption [2].

L. Determination of Port Area.

It has been suggested by reference 19 that the inlet steam velocity should not exceed 150 ft/sec. Sufficient port area should be provided to keep the steam velocity within this limit. For this purpose, it is necessary to determine the rate of volume change inside the engine.

The displaced volume at any shaft angle β can be approximated by equation

$$V(\beta) = \frac{\pi}{4} d^2 r(1-\cos\beta)$$

where

β = Shaft Angle,

$V(\beta)$ = Volume displaced corresponding to shaft angle β,

$\frac{\pi}{4} d^2 r$ = Half the maximum volume.

The angle β as a function of time can be expressed as

$$\beta = \frac{2\pi N}{60} \times t$$

where

N = rpm,

t = Time in seconds after 0° position.

For the maximum volume of 51.0 cubic inches the value of

$$\frac{\pi}{4} d^2 r = 25.5 \text{ cubic inches.}$$

Hence, the volume displaced can be expressed as

$$V(t) = 25.5(1-\text{Cos}\ \frac{2\pi N}{60}\ t).$$

Thus

$$\frac{dV(t)}{dt} = 25.5\ (\frac{2\pi N}{60})\ \text{Sin}\ (\frac{2\pi N}{60}\ t),$$

the maximum value of which is

$$\frac{dV(t)}{dt}\Big)_{max} = 25.5\ (\frac{2\pi N}{60}).$$

For $N = 1000.0$ rpm,

$$\frac{dV(t)}{dt}\Big)_{max} = 2550.0 \text{ cubic inches/sec.}$$

Hence the minimum port area required will be

$$(A_p)_{min} = \frac{\frac{dV(t)}{dt}\Big)_{max}}{\text{steam velocity}}.$$

For a steam velocity of 150 ft/sec,

$$(A_p)_{min} = 1.4 \text{ sq inches.}$$

Thus the port dimensions can be selected to be 3.0 in X 0.5 in.

M. Engine Assembly.

A section view of the engine assembly is shown in Figure 43, and the following components are identified.

1. Inlet steam valve (cam operated)
2. Steam box
3. Steam inlet from boiler

4. Reversing valve
5. Reversing lever
6. Inlet steam passage
7. Rotor
8. Shaft
9. Exhaust steam passage
10. Exhaust steam passage to the condenser.

Engine reversing is accomplished by sliding valve 4, which transforms passage 6 and 9 to exhaust and inlet functions respectively.

The advantages and disadvantages of this engine compared to a reciprocating, steam engine can be summarized as follows:

Advantages of Rotory Engine

(1) Smaller overall volume, since connecting rod, crankshaft and crankcase are eliminated.

(2) Reduced clearance volume, complete exhaust and elimination of "cushion" improves engine efficiency.

(3) Equivalence to double acting reciprocating engine with fewer moving parts.

(4) Reduced reciprocating motion and inertia forces.

Disadvantages:

(1) Proper sealing may be expensive.

N. Rotary Engine Specifications.

Overall Diameter: Maximum diameter 12.0 inches

Maximum width 5.0 inches

Maximum height 14.0 inches.

Housing Bore Dimensions: Diameter 8.0 inches

Width 4.0 inches.

Shaft Dimensions: Circular section 2.5 inches diameter

Square section 2.5 X 2.5 X 4.0 inches long.

Swept Volume: 51.0 Cubic inches.

Steam Conditions: Inlet 500 psia dry saturated

Exhaust 16.0 psia.

Power Developed (at design cut-off 26°): 15.0 IHP @ 1000 rpm

10.8 BHP @ 1000 rpm.

Maximum Power Developed (cut-off 31°): 20.0 IHP @ 1000 rpm.

Specific Steam Consumption (at 26° cut-off):

10.5 LB/IHP/HR.

Specific Steam Consumption (at 31° cut-off):

11.0 LB/IHP/HR.

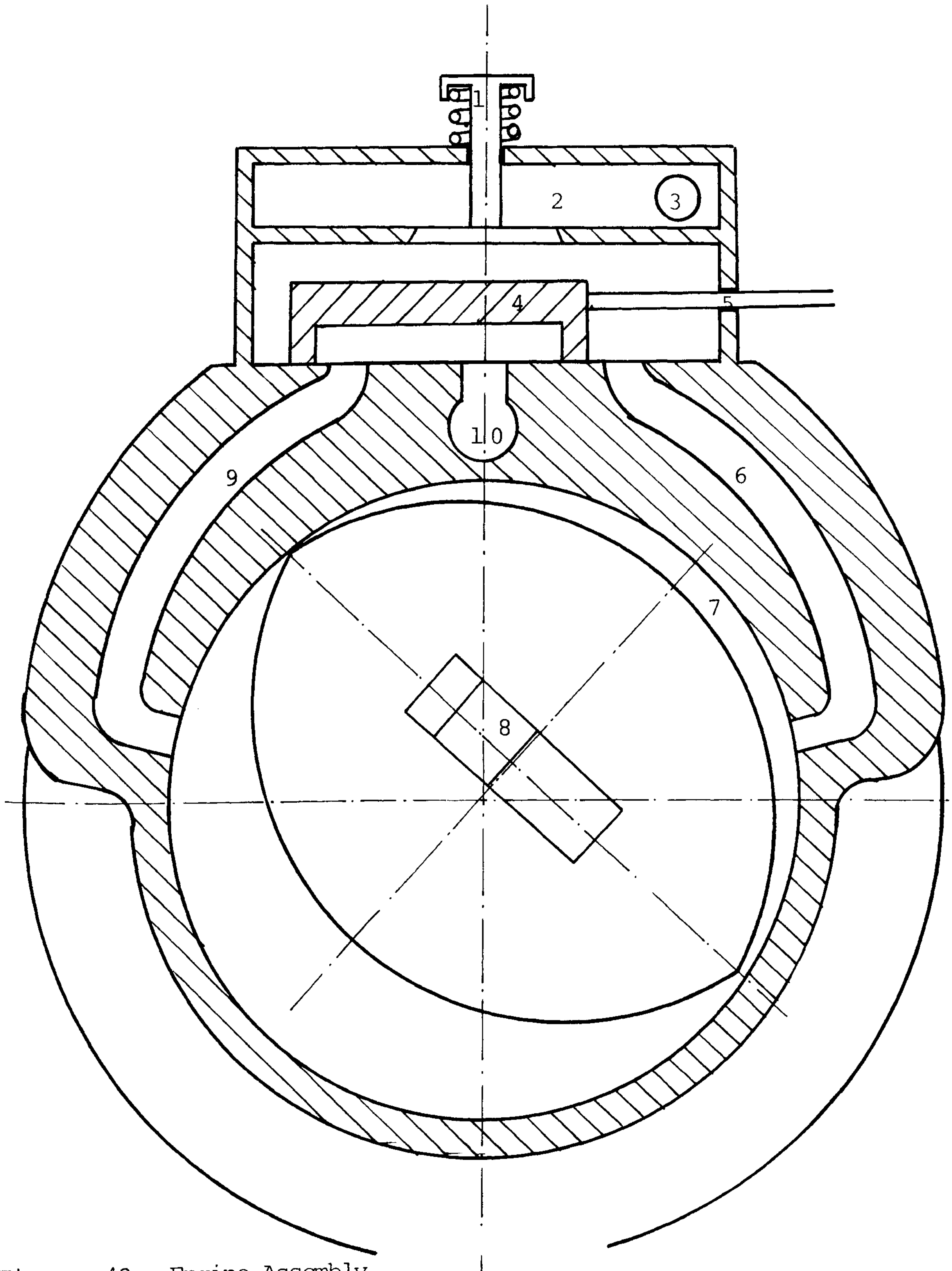

Figure 43. Engine Assembly

VI. CONDENSER DESIGN

A. Introduction.

A condenser is an essential element of steam-powered automotive engines, because the water consumption per horsepower produced is very high (10.6 lbs/1 hp-hr, Table 5.3. This rate is approximately 10 times the fuel consumption rate (page 79). In order to avoid frequent makeup of boiler feed water and reduce the reserve tank size, a condenser is essential.

In power plants, condensing of exhaust steam is carried out in a cooling tower, but for automotive applications an air cooled finned tube heat exchanger is universly employed. To accomplish the needed transfer of heat, a cooling fan is necessary.

B. Selection of Condenser Size.

The condenser size may be estimated approximately by analogy to a conventional tractor radiator. The heat transfer conditions are very similar, but the condenser will have to dissipate approximately three times more heat than a radiator [3]. The condenser size is a function of the engine efficiency, the condensing temperature and the average temperature difference between the heat transfer surface and air stream. The size can be minimized by raising the condensing temperature. However, this leads to a reduction in engine efficiency and excessive fan power requirements. In general, the largest possible condenser should be employed, consistent with available space [23]. For this design a condenser 16 inches wide, 20 inches high and 3.0 inches thick is selected [Figure 44]. In addition, a 2 inch steam and water header space is provided on top and bottom of the condenser.

C. Surface Geometry.

The surface geometry selected is shown in Figure 45 and is recommended by reference [14]. The important properties are listed in Figure 45.

D. Operating Conditions.

The assumed operating conditions are as follows,

(1) Air side:

(a) Air flow, dry

(b) Air entering temperature, 100°F

(c) Air entering pressure, 14.7 psi.

(2) Steam side:

(a) Maximum continuous steam flow rate, 225.0 lbs/hr

(b) Heat to be removed, 970.0 BTU/lb

(c) Steam Temperature, 220°F

(d) Condensate temperature, 220°F

(e) Condenser pressure, 16.0 psia.

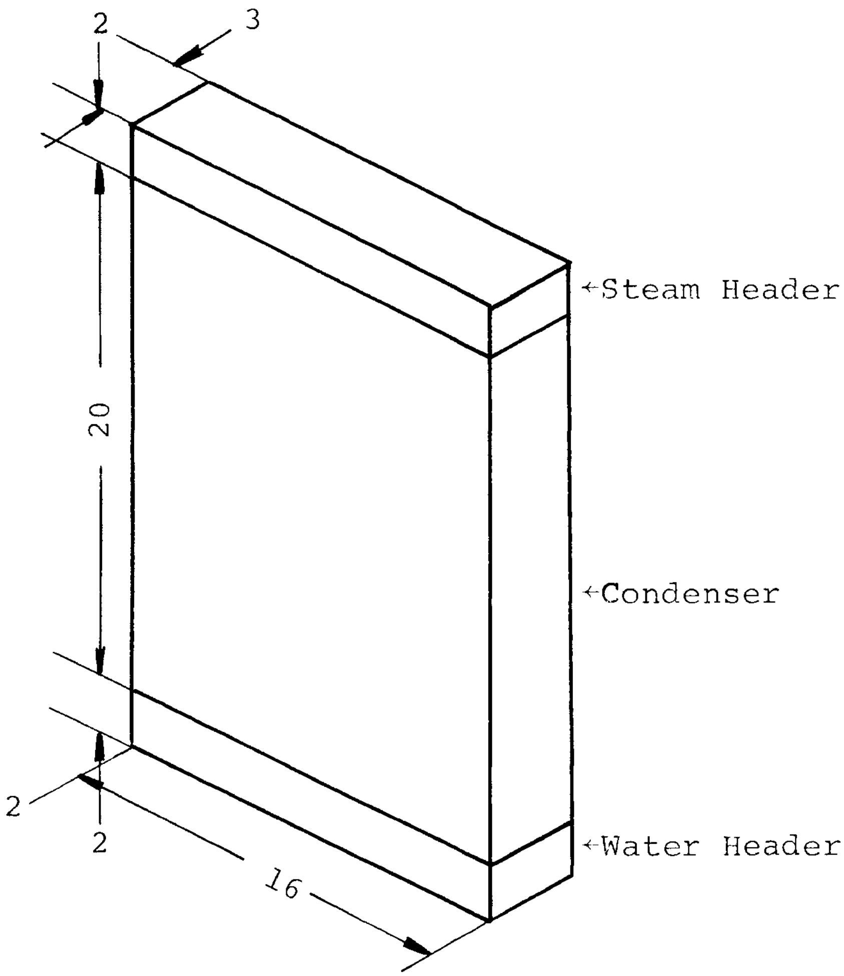

All dimensions in inches.

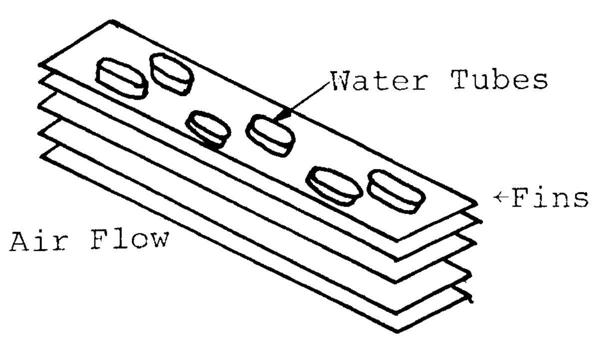

Figure 44. Condenser

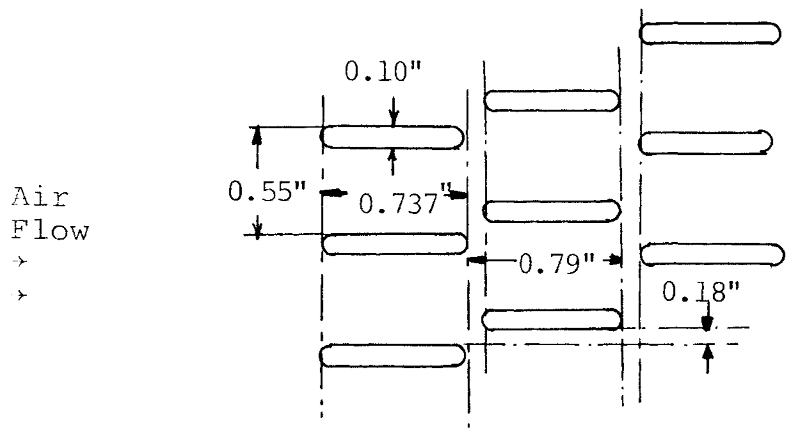

Figure 45. Condenser Configuration [14].

CONDENSER SURFACE: 1.32-0.737-SR., Flat tubes, continuous fin

TUBE ARRANGEMENT: Staggered

FIN TYPE: Ruffled

TUBE LENGTH: 0.737 inch

TUBE WIDTH: (Normal to Flow): 0.1 inch

FINS PER INCH: 11.32

HYDRAULIC DIAMETER: 0.01152 ft

FIN THICKNESS: 0.004 inch

FREE FLOW/FONTAL AREA: $\sigma = 0.78$

HEAT TRANSFER AREA/VOLUME: $= 270\ ft^2/ft^3$

RATIO OF FIN AREA TO TOTAL AREA: 0.845

E. Design Analysis.

An analysis will now be carried out to find the necessary cooling effect and fan power for the selected surface, dimensions and operating conditions. This will be carried out in the following steps.

From published data, obtain:

(1) Condenser surface characteristics

(2) Fluid properties.

From assumed operating conditions, estimate:

(3) Temperature rise in air

(4) Pressure drop on air side.

Calculate:

(5) Required mass flow rate of air

(6) Air side heat transfer coefficient

(7) Water side heat transfer coefficient

(8) Overall heat transfer coefficient

(9) Exit air temperature.

Finally, compare the assumed rise in air temperature with the calculated rise. If they do not agree, the entire process should be repeated by selecting a new value for the temperature rise. When the assumed rise equals the calculated value, calculate

(10) Air side pressure drop

(11) Fan power.

(1) Condenser surface characteristics: The surface characteristics are listed in Figure 45 [14]. From the selected core dimensions:

(a) Air side frontal area = $A_{fr,a}$ = 2.222 sq ft,

(b) Water side frontal area = $A_{fr,w}$ = 0.333 sq ft,

(c) Total volume = V_c = 0.555 cu ft.

(2) Fluid properties: The properties of the condensing vapor, water and air can be found from standard tables [14].

(3) Temperature rise in air: The ambient air temperature is assumed to be 100°F and a temperature rise of 70°F is assumed. The steam condensing temperature is 220°F, corresponding to the condenser pressure of approximately 16 psia. Figure 46 shows a schematic diagram of the heat exchanger and a representative temperature distribution, from which:

$$\Delta T_{out} = T_{sat} - T_{out} = 50°F,$$

$$\Delta T_{in} = T_{sat} - T_{in} = 120°F,$$

$$\Delta T_a = T_{out} - T_{in} = 70°F.$$

The log mean temperature difference on the air side will be

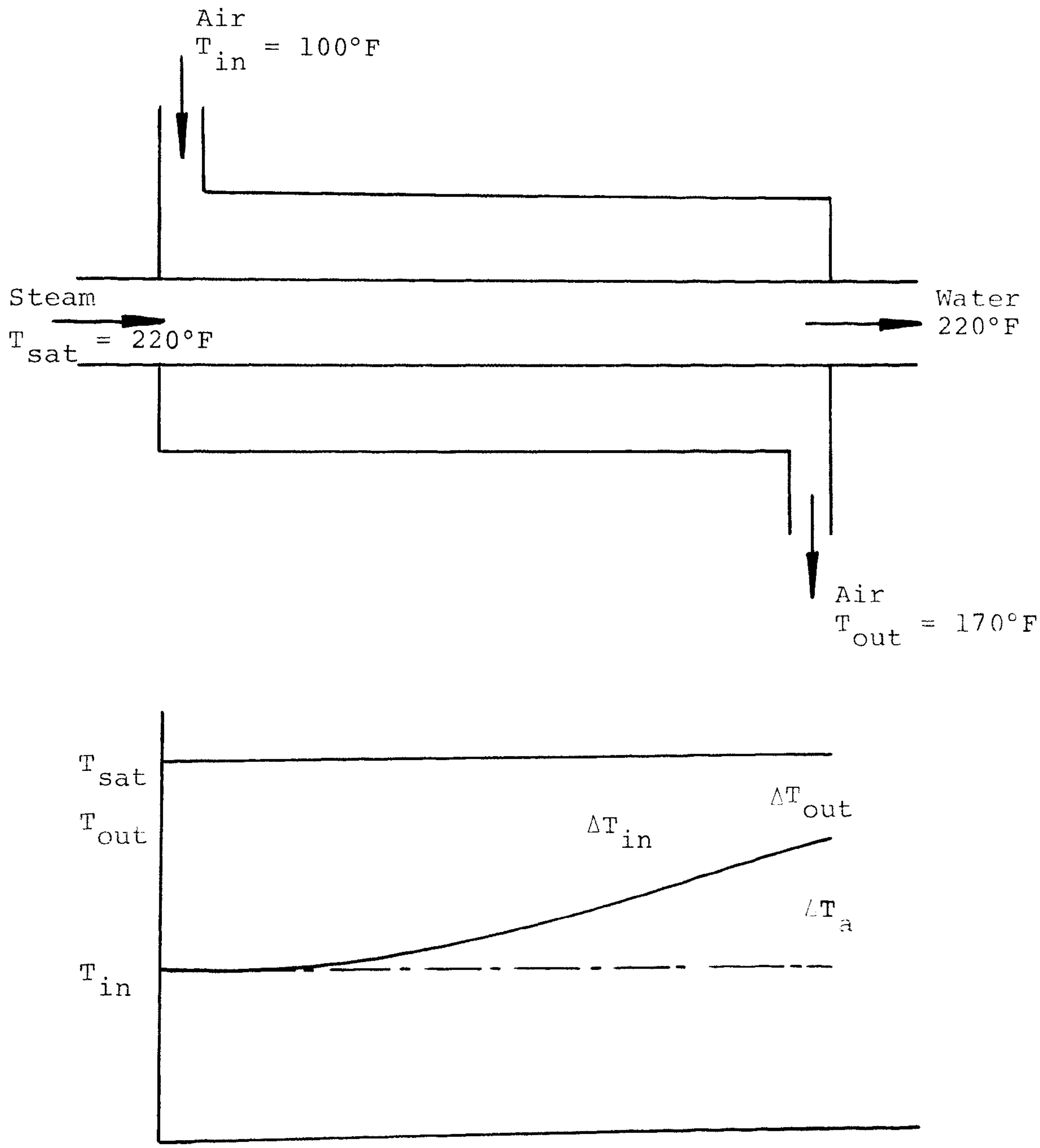

Figure 46. Schematic Condenser With Temperature Profile.

T_{sat} = Condensation temperature of steam = 220°F

T_{in} = Air entering temperature = 100°F

T_{out} = Air leaving temperature = 170°F

$\Delta T_{in} = T_{sat} - T_{in}$

$\Delta T_a = T_{out} - T_{in}$

$\Delta T_{out} = T_{sat} - T_{out}$

$$\Delta T_{lm} = \frac{\Delta T_a}{\ln\left(\frac{\Delta T_{in}}{\Delta T_{out}}\right)} ,$$

$$= 80°F.$$

Thus the log mean temperature on the air side will be

$$T_{lm} = T_{sat} - \Delta T_{lm} .$$

$$= 140°F.$$

The air properties should correspond to this temperature.

(4) Pressure drop on air side: The air side pressure drop is assumed to be 10%, and this assumption will be verified later when the exact rise in air temperature has been determined.

(5) Mass flow rate of air: Assuming the entering air is dry and there are no radiation heat losses, the heat lost by the condensing steam is gained by the flowing air. This can be expressed as

$$\dot{M}_a \times C_{pa} \times (T_{out} - T_{in})_{air} = \dot{M}_w \times \Delta H \qquad (6.1)$$

where

$\dot{M}_a$ = Mass flow rate of air,

C_{pa} = Specific heat of air at log mean temperature,

$(T_{out}-T_{in})_{air}$ = Rise in air temperature,

$\dot{M}_w$ = Mass flow rate of steam,

ΔH = Latent heat of condensation.

After substituting the following values in equation 6.1, the air flow can be evaluated.

C_{pa} = 0.2403 BTU/lb°F [14],

$(T_{out}-T_{in})_{air}$ = 70°F,

$\dot{M}_w$ = 225 lbs/hr,

ΔH = 970 BTU/lb [6].

The required air flow is

$\dot{M}_a$ = 12911 lbs/hr.

The air flow rate per unit free flow area is given by

$$G_a = \frac{\dot{M}_a}{A_{fr,a} \times \sigma_a}, \qquad (6.2)$$

where

G_a = Mass flow rate of air per unit free flow area,

$A_{fr,a}$ = Frontal area,

σ_a = Ratio of free flow area to the frontal area.

After substituting the following values in equation 6.2:

$$\dot{M}_a = 129.11 \text{ lbs/hr},$$

$$A_{fr,a} = 2.22 \text{ sq ft},$$

$$\sigma_a = 0.78 \text{ (Figure 45)},$$

the resulting mass flow rate of air per unit free flow area is:

$$G_a = 7448.0 \text{ lbs/hr-ft}^2.$$

(6) Air side heat transfer coefficient: The air side heat transfer coefficient is a function of the Reynolds' number, Prandtl number and Nusselt number.

The Reynolds' number is calculated from

$$N_{R,a} = \frac{4\gamma_h G_a}{\mu_a}, \tag{6.3}$$

where

$N_{R,a}$ = Air side Reynolds' number,

γ_h = Hydraulic radius,

G_a = Mass flow rate of air per unit free flow area,

μ_a = Viscosity of the air at the log mean temperature.

After substituting the following values in equation 6.3:

γ_h = 0.00288 ft (Figure 45),

G_a = 7448 lbs/hr-ft ,

μ_a = 0.0486 lbs/hr-ft [14],

the Reynolds' number is found to be

$$N_{R,a} = 1766.$$

From the data published in graphical form in reference 14, where $N_{ST}(N_{PR})^{\frac{2}{3}}$ and f are expressed as a function of Reynolds' number:

$$N_{ST}(N_{PR})^{\frac{2}{3}} = 0.0077,$$

$$f = 0.03,$$

where:

N_{ST} = Nusselt number,

N_{PR} = Prandtl number,

f = Friction factor.

From the definition of Nusselt number, i.e.

$$N_{ST} = \frac{ha}{C_{pa} \times G_a}.$$

The air side heat transfer coefficient is

$$ha = \frac{N_{ST}(N_{PR})^{\frac{2}{3}}}{(N_{PR})^{\frac{2}{3}}} \times C_{pa} \times G_a \qquad (6.4)$$

where:

C_{pa} = Specific heat of air at the log mean temperature.

After substituting:

$$N_{ST}(N_{PR})^{\frac{2}{3}} = 0.0077 \text{ [14]}$$

$$N_{PR} = 0.695 \text{ [14]}$$

$$C_{pa} = 0.2403 \text{ BTU/lb},$$
$$G_a = 7448.0 \text{ lbs/hr-ft}^2,$$

in equation 6.7, the value of the air side heat transfer coefficient is found to be

$$ha = 17.7 \text{ BTU/hr-ft}^2 \text{ °F}.$$

(7) Water side heat transfer coefficient: The water side mass flow rate is $\dot{M}_w = 225$ lbs/hr, and the water side mass flow rate per unit area is [14].

$$G_w = \frac{\dot{M}_w}{A_{fr,w} \times \sigma_w} \tag{6.5}$$

where

G_w = Water side mass flow rate per unit area,

σ_w = Ratio of water side free flow area to total area,

$A_{fr,w}$ = Water side frontal area.

After substituting

$\dot{M}_w$ = 225.0 lbs/hr,

$A_{fr,w}$ = 0.33 sq ft [14],

σ_w = 0.129 [14],

the mass flow rate per unit area is found to be

G_w = 5233 lbs/hr-sq ft.

The water side heat transfer coefficient is a function of the Reynolds' number, viscosity, thermal conductivity and fluid density.

The Reynolds' number is given by

$$N_{R,W} = \frac{4\gamma_h G_w}{\mu_w} \qquad (6.6)$$

where

γ_h = Hydraulic radius,

G_w = Mass flow rate of water,

μ_w = Viscosity of water.

After substituting the following values in equation 6.6:

γ_h = 0.0036 ft (Figure 45),

G = 5233.0 lbs/hr-sq ft,

μ = 0.654 lbs/hr-ft [14],

the Reynolds' number is found to be

$N_{R,W}$ = 115.0.

The film coefficient on the water side is given by

$$hw = 1.47(N_{R,W})^{\frac{1}{3}} \left(\frac{\mu_w^2}{K_w^3 \rho_w^2 g}\right)^{\frac{1}{3}} \qquad (6.7)\,[15]$$

where

hw = Water side heat transfer coefficient,

$N_{R,W}$ = Reynolds' number,

μ_w = Viscosity of water,

K_w = Thermal conductivity of water,

ρ_w = Density of water,

g = Gravitational constant.

After substituting the following values in equation 6.7:

$N_{R,W}$ = 115.0,

μ_w = 0.654 lb/hr-ft (Corresponding to 220°F),

K_w = 0.395 BTU/hr-ft °F (Corresponding to 220°F),

ρ_w = 59.6 lbs/ft^3 (Corresponding to 220°F),

$g = 4.17 \times 10^8$ ft/hr-hr,

the value of water side heat transfer coefficient is found to be

hw = 1820.0 BTU/hr-ft^2 °F.

(8) Overall heat transfer coefficient: The overall heat transfer coefficient is defined as

$$\frac{1}{W_c} = \frac{1}{\eta_o h} + \frac{1}{(\frac{\alpha_w}{\alpha_a})\, hm} \tag{6.8}$$

where

W_c = Overall heat transfer coefficient of the condenser,

η_o = Overall effectiveness,

h_a = Air side heat transfer coefficient,

α_w = Ratio of water side heat transfer area to total volume,

σ_a = Ratio of air side heat transfer and to total volume,

hw = Water side heat transfer coefficient.

In equation 6.8 the thermal resistance of the metal is neglected because of its small thickness and very high conductivity (200 BTU/ lb). Overall effectiveness is given by:

$$\eta_o = 1 - (\frac{A_f}{A})\ (1 - \eta_f) \qquad (6.9)$$

where

$\frac{A_f}{A}$ = Ratio of fin area to total area,

η_f = Fin effectiveness and is defined as the ratio of heat transfer rate from a fin to the heat transfer rate that would be obtained if the entire fin surface area were to be were to be maintained at the same temperature as the primary surface.

Fin effectiveness is calculated from:

$$\eta_f = \frac{\tanh \sqrt{\frac{2ha}{Kt_t}}\ l}{\sqrt{\frac{2ha}{Kt_t}}\ l} \qquad (6.10)$$

where

ha = Air side heat transfer coefficient,

K = Conductivity of metal,

t_t = Thickness of the fin,

l = Length of the fin.

After substituting

$ha = 17.7$ BTU/hr-ft^2 °F,

$K = 225$ BTU/hr-ft °F,

$t_t = 0.004$ inch,

$l = 0.225$ inch,

in equation 6.10, the fin effectiveness is found to be

$\eta_f = 0.949.$

Thus the overall effectiveness (From equation 6.9) is found to be:

$$\eta_o = 0.95 \text{ For } \frac{A_f}{A} = 0.845 \quad [14].$$

After substituting the following values in equation 6.8:

$\eta_o = 0.95,$

$ha = 17.73$ BTU/hr-ft^2 °F,

$\alpha_w = 42.1$ ft^2/ft^3 [Figure 45],

$\alpha_a = 270.0$ ft^2/ft^3 [Figure 45],

$hw = 1820.0$ BTU/hr-ft^2 °F,

the value of the overall heat transfer coefficient is found to be:

$$W_c = 15.85 \text{ BTU/hr-ft}^2 \text{ °F.}$$

It should be noted that the water side heat transfer coefficient is large as compared to the air side heat transfer coefficient; therefore, the overall heat transfer coefficient is largely governed by the air side heat transfer coefficient.

(9) Exit air temperature: The air exit temperature will now be calculated and compared to the assumed value. If all heat losses are neglected and it is assumed that all of the heat rejected by condensing steam is supplied to the air, the heat balance equation will be:

$$q = W_c A \Delta \underline{T}_m = \dot{M}_a C_{pa} \Delta T_a \qquad (6.11)\,[14]$$

where

q = Total heat transfer,

W_c = Overall heat transfer coefficient,

A = Heat transfer area,

$\Delta \underline{T}_m$ = Log mean temperature difference,

$\dot{M}_a$ = Mass rate of air flow,

C_{pa} = Specific heat of air at log mean temperature,

ΔT_a = Temperature rise of air.

Since

$$T_{out} = T_{sat} - \Delta T_{out} \quad \text{(Figure 46)},$$

and

$$\Delta T_{lm} = \frac{\Delta T_a}{\ln\left(\frac{\Delta T_{in}}{\Delta T_{out}}\right)}$$

$$T_{out} = T_{in}\, e^{-(W_c A/\dot{M}_a C_{pa})} \,. \tag{6.12}$$

After substituting the following values in equation 6.12:

T_{in} = 120°F (Figure 46),

W_c = 15.85 BTU/hr-ft -°F,

$\dot{M}_a$ = 12911.0 lbs/hr,

C_{pa} = 0.2403 [14],

A = 150.0 sq ft*.

The air side temperature increase is found to be

T_{out} = 56.0°F.

Therefore, the outlet temperature will be:

---

*$A = \alpha_a V_c$

where:

α_a = Ratio of heat transfer area to total ,

Volume = 270 ft^2/ft^3 [14],

and

V_c = 0.555 ft^3.

$$T_{out} = T_{sat} - T_{out}$$
$$= 164.0°F.$$

The assumed value of T_{out} was 170°F. The entire process should now be repeated with an assumed value of 164°F outlet temperature. However, the air properties will not change appreciably, and an air outlet temperature of 170°F will be satisfactory, for a first approximation, to calculate fan power.

(10) Actual air side pressure drop: The pressure drop across the condenser is given by:

$$\frac{P}{P_1} = \frac{G^2}{2g}\frac{V_1}{P_1}\left\{(1 + \sigma^2)\left(\frac{V_2}{V_1} - 1\right) + f\,\frac{L}{\gamma_h}\,\frac{V_m}{V_1}\right. \qquad (6.13)\ [14]$$

where

$\frac{\Delta P}{P_1}$ = Percentage pressure drop,

G = Mass flow rate of air per unit area,

g = Gravitational constant,

V_1 = Specific volume of air at pressure P_1,

σ = Ratio of free flow area to frontal area,

V_2 = Specific volume of exit air,

f = Friction factor,

L = Length of body parallel to air flow,

γ_h = Flow passage hydraulic radius,

V_m = Mean specific volume of air.

After substituting the following values in equation 6.13, the pressure drop can be evaluated:

P_1 = 14.7 psia at STP,

G = 7448.0 lbs/hr-ft^2,

g = 4.17 X 10^8 ft/hr^2,

V_1 = 14.1 ft^3/lb at 14.7 psia and 100°F,

σ = 0.78 [14],

V_2 = 16.05 ft^3/lb at 14.7 psia and 170°F,

f = 0.0306 [14],

L = 0.25 ft,

γ_h = 0.00288 ft,

V_m = 15.07 ft^3/lb.

Hence, the normalized pressure drop is found to be:

$\frac{\Delta P}{P}$ = 0.00138, from which

ΔP = 0.019 psi.

The pressure drop across the condenser is therefore very small. In equation 6.13, the value for V_2 was based on atmospheric inlet pressure and an assumed pressure drop across the condenser of 10%. Now a new value of V_2 should be assumed (corresponding to $\frac{\Delta P}{P}$ = 0.00138) and the entire calculation should be repeated until the assumed and actual pressure drops agree closely. However, the actual pressure drop will never exceed 10% because the value of V_2 will decrease as the percentage pressure drop is reduced. Hence for a conservative estimate and to provide some allowance for entry and exit losses, it is reasonable to assume a 10% pressure drop.

(11) Fan power: The fan power can be estimated by:

$$HP = \frac{Q\Delta P}{33000}$$

where

Q = Volume of air moved in cfm,

ΔP = Pressure drop in psi.

After substituting:

$$Q = V \ \dot{M}_a,$$

$$= 3460.0 \text{ cfm},$$

and $\Delta P = 0.147$ psi,

the theoretical air hp is found to be 2.2 hp. A typical Schwitzer induced draft fan design with the following characteristics, will supply the needed air flow:

Diameter = 15.5 inches,

No. of blades = 5,

PPM = 3000,

Pressure rise = 1.05 in of water,

Air moved = 3400 cfm,

Power consumed = 2.5 hp.

VII. LAYOUT AND TRANSMISSION DESIGN

A. Schematic Layout.

Figure 47 shows a schematic layout of the power plant. It can be described briefly as follows.

High pressure steam generated in the boiler (1) is supplied to the engine (6) after lubricating oil is added in a hydrostatic lubricator (3). Here a small amount of steam is condensed and this condensate displaces lubricating oil which floats in the steam in the form of small droplets. A steam safety valve (2) blows off steam in case the boiler pressure exceeds the design pressure of 500 psia. The steam throttling valve (4) on the supply line is controlled by manually and overspeed governor on the engine shaft.

Steam admission to the engine (6) is controlled by an inlet valve mechanism (5), which is positioned by a three dimensional cam on the engine shaft. Exhaust steam from the engine passes to the air cooled condenser (7) after passing through the oil separator (24), where lubricating oil is separated and returned to the hydrostatic lubricator (3). The condensate accumulates in hot well and or water tank (8) and is supplied to the boiler under pressure by a positive displacement water pump (9). This pump is driven by an electric motor (10) which also drives a combustion air blower (11), fuel pump (12), and a lubricating pump (13). The blower (11) supplies air to the preheating chamber (25) located under the boiler, where it is preheated by the exhaust gases. The fuel pump (12) supplies fuel from fuel tank (14) to the combustion chamber (25), also located under the boiler. The lubricating pump (13) supplies lubricating oil to the output shaft journal bearings.

The power developed by the engine is supplied to the rear wheels for locomotion by a V-belt and pulley system (16) and (17). Also the power for mower blades (20) and (21), an alternator (22), and condenser fan (23) is supplied by the engine through V-belt and pulley systems as shown in Figure 47.

B. Transmission Design.

The transmission system was designed following the standard procedure in reference 24. It was possible to avoid gear drives [except at the differential] by using less expensive V-belts throughout the system.

Power is supplied at both ends of the engine; one end drives the rear wheels through a V-belt clutch and differential; the other end powers various system components and the accessory shaft.

Specifications of the various drive systems are listed in Table 6.1.

C. Arrangement of Components.

The component layout selected must meet the following requirements:

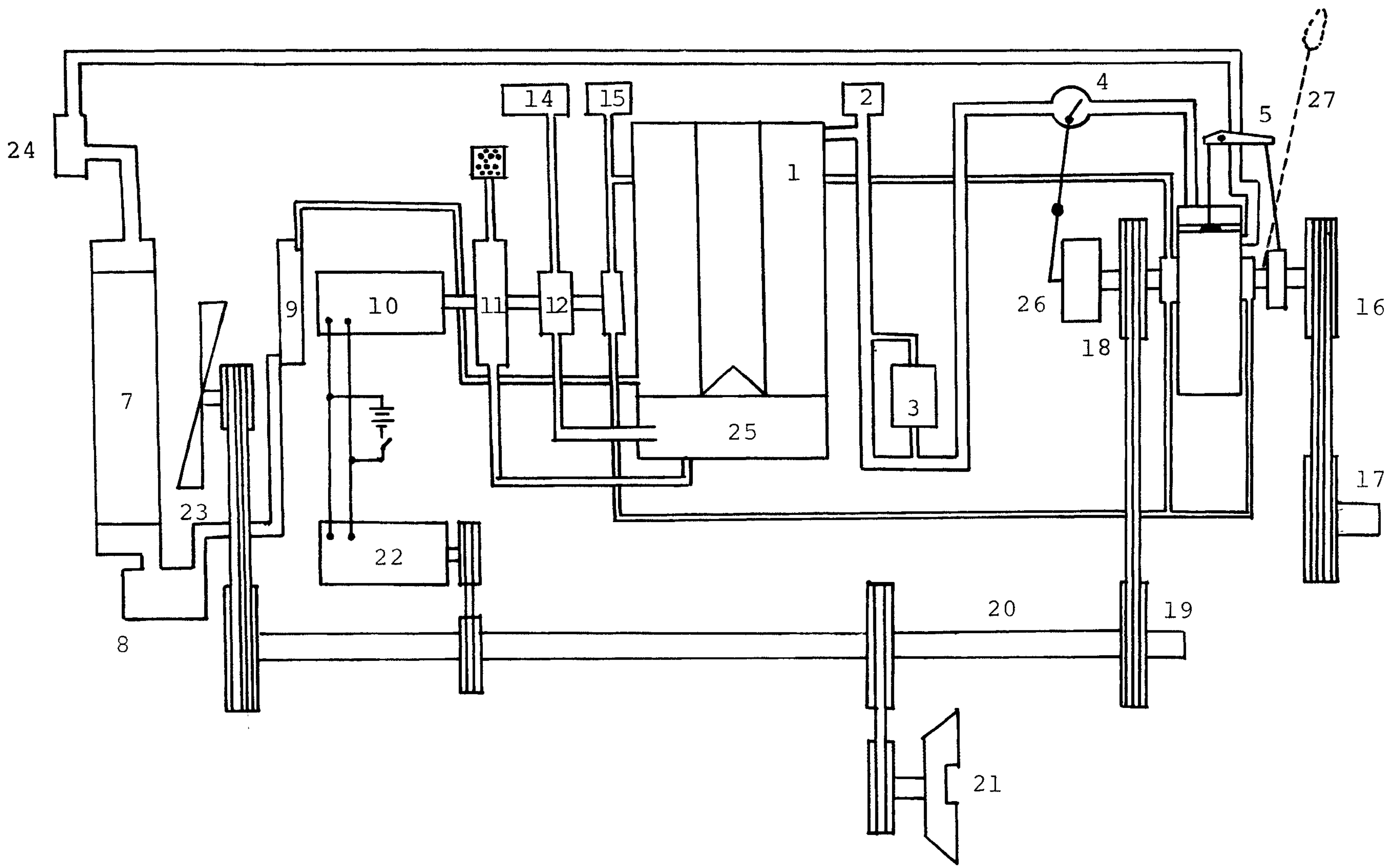

Figure 47. Schematic Layout.

Figure 47. Schematic Layout.

1. Boiler
2. Steam Safety Valve
3. Hydrostatic Lubricator
4. Throttle Valve
5. Steam Admission Valve Mechanism
6. Engine
7. Condenser
8. Water Tank
9. Water Pump
10. Electric Motor
11. Blower
12. Fuel Pump
13. Lubricating Pump
14. Fuel Oil Tank
15. Lubricating Oil Tank
16. Drive Pulley for Rear Wheel Locomotion
17. Driven Pulley for Rear Wheel Locomotion
18. Drive Pulley for Accessory
19. Driven Pulley for Accessory on Jackshaft
20. Jackshaft
21. Mower Blades
22. Alternator
23. Condenser Fan
24. Oil Separator
25. Oil Separator

26. Overspeed Governor
27. Cut-off Control (Manual)
28. Fuel Control
29. Water Flow Control
30. Blow off Valve

TABLE 6.1 TRANSMISSION DESIGN

Pulley	Position Number in Figure	Pitch Circle Diameter in Inches	Number of Belts[1]	HP Rating Continuous	RPM
Rear Wheel Drive Pulley	13	7.4	4	20.*	1000.
Rear Wheel Driven Pulley	14	7.4	4	20.*	1000.
Accessory Drive Pulley	8	6.0	2	9.	1000.
Accessory Driven Pulley	9	6.0	3	11.	1000.
Driven Pulley to Generator	10	3.0	1	2.	2000.
Drive Pulley to Mower	7	4.0	2	6.	1000.
Driven Pulley on Mower	11	6.0	2	6.	660.
Drive Pulley to Fan	4	6.0	1	2.5	1000.
Driven Pulley on Fan	3	2.0	1	2.5	3000.

[1]Standard B Section V-belts [24].

*The rating is not continuous.

(1) The condenser should be mounted foremost so that it is exposed to ambient air and as much ram effect as possible.

(2) The space behind the condenser should be relatively free from obstruction, to achieve maximum air flow.

(3) The water tank should be located as low as possible to take advantage of gravity for draining.

(4) The center of gravity of all components should lie as close as possible to the longitudinal axis of the tractor.

One possible layout is shown in Figure 48. This arrangement appears feasible, and results in a tractor of approximately the same size as the John Deere Model 112, 10 HP lawn and garden tractor.

It is not desirable to locate the boiler immediately behind the condenser because the boiler size may obstruct the air flow. But, if the engine is located next to the condenser, transmission of power and engine control appear to be more complicated. The simplest and most compact arrangment results when the engine is located behind the boiler and both are offset from the longitudinal axis of the tractor. This arrangement is necessary to

(1) Reduce the length of the tractor

(2) Accommodate the feed pump, fuel pump and

blower conveniently,

(3) Allow placement of the steering column along the longitudinal axis.

The power supply for a mowing attachment and an auxiliary take-off is as shown in Figure 47. The mower drive belt is twisted through a 90 degree angle which may reduce the belt life; however the arrangement is commonly used on small tractors.

D. Flywheel Design.

The function of a flywheel is to store excess energy supplied by the engine and to release stored energy when engine output is less than that required by the external load. The engine is represented by the area of torque displacement diagram shown in Figure 35. The area is calculated by subdividing the diagram into smaller regular geometric shapes; the energy is found to be 21,110 ft-lb. The average torque, 118 ft-lb, is obtained by calculating height of a rectangle with same area and same base. Thus, the energy represented by the area abc is the is the excess energy, (when torques due to rotor and bearing friction and seal torque are neglected) which increases the kinetic energy of the flywheel. The area abc represents 8746 ft-lb-degrees or 152 ft-lb-radians.

The increase in kinetic energy of the flywheel is expressed by

$$U = \frac{W}{g} K^2 \eta W_o{}^2$$

where

U = Increase in kinetic energy,

W = Weight of the flywheel,

g = Gravitational constant,

K = Radius of gyration,

η = Coefficient of fluctuation,

W_o = Mean speed.

The flywheel will be designed at coefficient of speed fluctuation of ± 5% at 1000 r.p.m. After substituting the following values into the above equation

U = 152.0 ft-lb,

g = 32.2 ft/sec^2,

η = 0.1,

W_o = 104 rad/sec.

WK^2 is found to be 4.5 lb-ft^2. For a disc flywheel of mean diameter 9.0 inches the corresponding value of K^2 is 0.07 ft^2, and the flywheel weight is 64.0 lbs. The usual practice of combining the flywheel and engine pulleys into single units is followed here. Figure 48

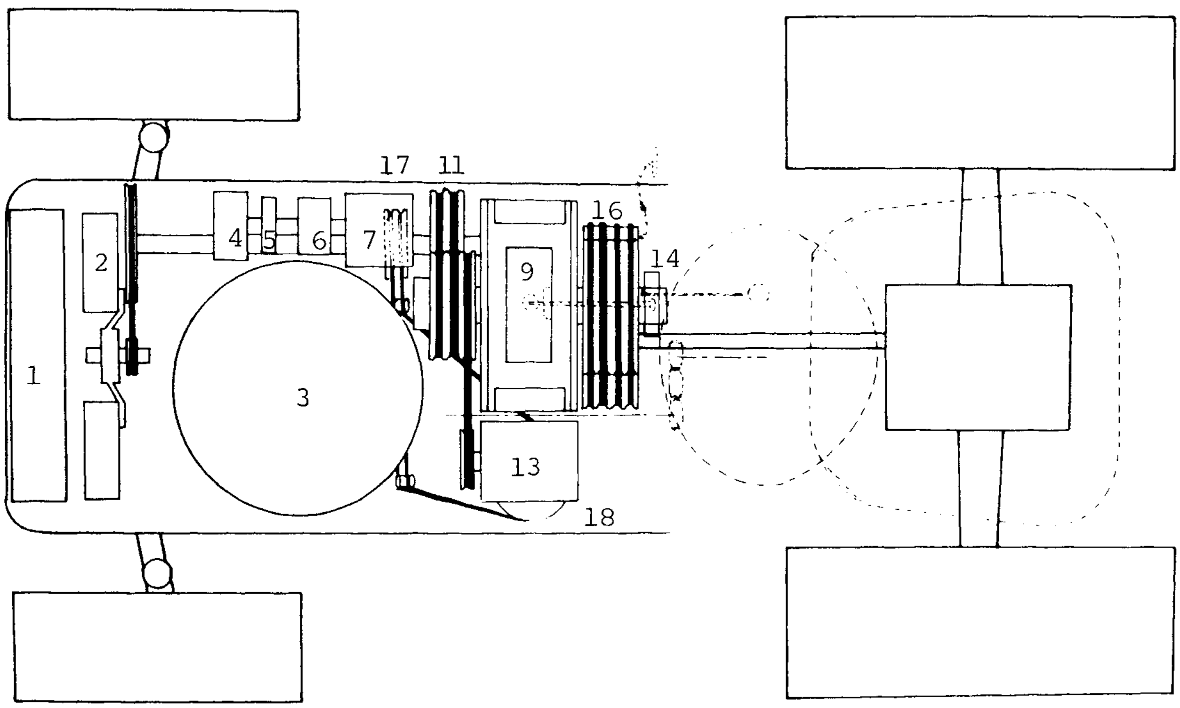

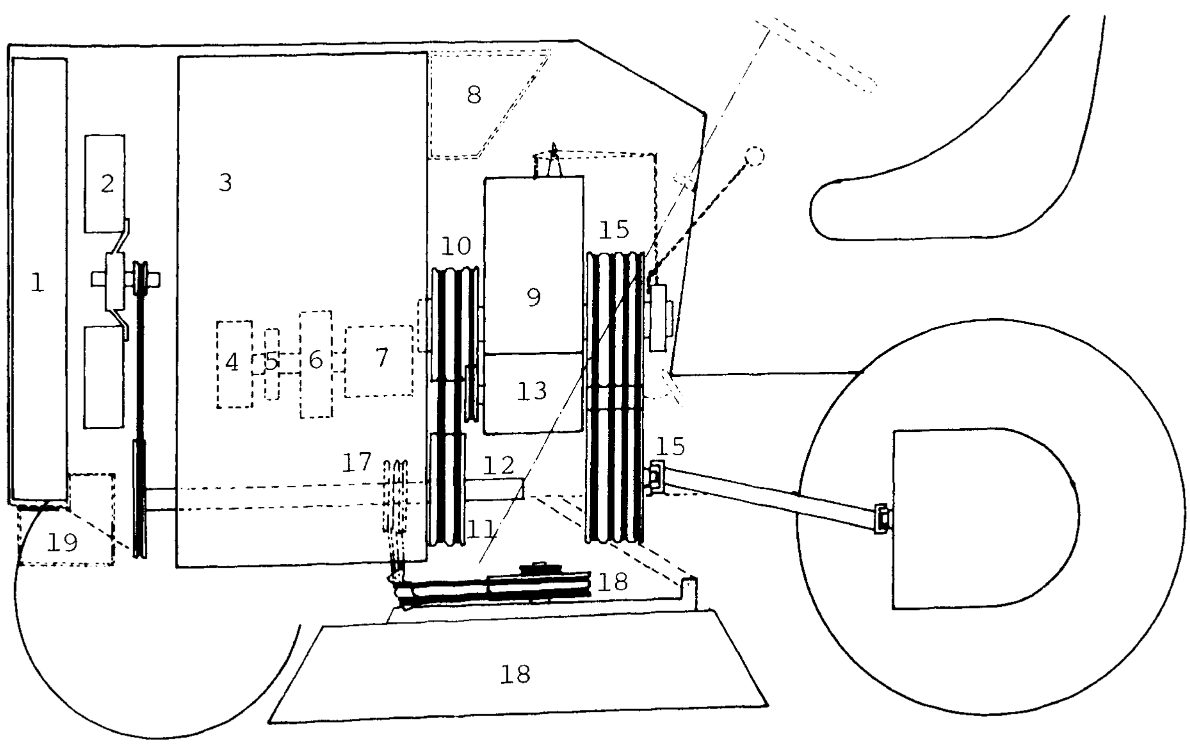

Figure 48. Arrangement of Components.

Figure 48. Arrangement of Components.

1. Condenser
2. Condenser Fan
3. Boiler
4. Blower
5. Fuel Pump
6. Water Pump
7. Electric Motor
8. Fuel Tank
9. Engine
10. Accessory Drive Pulley
11. Accessory Driven Pulley
12. Jack Shaft Extension for Power Take-off
13. Generator
14. Rear Wheel Drive Pulley
15. Rear Wheel Driven Pulley
16. V-belt Clutch Pulley
17. Mower Driven Pulley
18. Mower Driven Pulley
19. Water Tank

VIII. SUMMARY AND CONCLUSION

In 1967 a group of engineers, scientists and academic people was established by the U. S. Department of Commerce to investigate the feasibility of an electrically powered vehicle. This group, known as the Morse Committee, found the electrically powered vehicle unsuitable in its present state of development and mentioned in the report that

> "A study of existing literature and inspection of modern working engines shows that the reciprocating steam engine power plant may be a reasonable alternative to the internal combustion engines, in terms of meeting both performance and emission requirements."

Following this study, numerous persons and firms investigated preliminary designs [2,3,]. Some of the investigators tested steam-powered Doble and Stanely passenger cars to establish emission levels [10,25]. General Motors even built two passenger cars suitable for modern transportation needs. After thoroughly testing these cars, engineers at General Motors found the vapor cycle engine an unattractive alternative to a properly controlled spark ignition engine [25]. They concluded that:

(1) Even though steam cars produced low emissions, the oxides of nitrogen exceeded the 1975 proposed standards and hydrocarbons exceeded

1980 standards.

(2) Overall fuel economy was poor.

(3) Vehicle performance was poor. This was due to the low net power which could be packaged into the available space, because of the relatively large size and weight of the overall power plant.

(4) The construction, maintenance and control of the vehicle were expensive and complicated.

Some other investigators working in this field have also concluded that reliability is a completely unknown factor and servicing of a vapor-cycle vehicle will pose some problems. The power plant volume is relatively large. Reduction in boiler is possible, but may result in failure to meet short-term high output demands. Higher steam temperature (1000°F) and pressure 2000 psi) can reduce the boiler size and improve system efficiency, but this results in lubrication problems which are as yet unsolved. Water is the most practical working fluid, but it freezes in winter climates and requires special arrangements for draining and storage in an insulated tank [3]. And last but not least, relatively complex controls are required for safe and efficient operation. However many of these disadvantages do not apply to the use of a small steam engine for nonautomotive uses such as garden tractors.

It has been demonstrated that steam engine fuel economy is superior to that of an internal combustion engine in low speed ranges up to 30.0 mph [Figure 5]. Therefore, a steam cycle should prove economical for vehicles like tractors and tanks which are not built for speed. Furthermore, a cheaper grade of fuel can be used, provided a suitable burner is designed.

The steam engine has a large stall torque and a relatively constant low speed torque characteristic, compared to the internal combustion engine. This can be very advantageous for vehicles engaged in low speed activities requiring a large tractive effort. Besides, a relatively simple clutch transmission assembly can replace the conventional multi-speed or automatic transmission required with internal combustion engines. For small power plants, an inexpensive V-belt clutch transmission can be used.

The size of components is not a significant problem for tractor applications because no passenger room is required. Also the space for the power plant is not limited to "space under the hood."

Although the start-up time for a steam-powered vehicle is relatively long, this is not a serious disadvantage for the application considered in this study. Furthermore, the steam engine is better able to meet temporary overloads for short periods than is the internal combustion engine, because of its favorable low-speed torque characteristic.

Although these are a number of problems associated with vapor cycle engine, it should not be forgotten that the steam engine has benefitted from only a small fraction of the research and development that have been applied to the internal combustion engine. One major problem is the size of components required in the vapor cycle system. As demonstrated by this study, the boiler is the bulkiest and heaviest component. Boiler size and weight (almost 1/5 of the tractor weight) can be reduced by increasing steam temperature, pressure and achieving more efficient combustion. As mentioned earlier this leads to lubrication problems, one of which is that the oil deposits on boiler tubes and causes cracking. The boiler size can be reduced to some extent by incorporating water and air preheaters. However, this will again lead to complications in component arrangement, reliability and maintainance. The monotube, once through, forced circulation boiler appears to be the most suitable because of its smaller size, and minimal water capacity. However, the boiler has to be oversized to respond rapidly to changes in steam demand. Extensive research is still needed for development of an efficient combustion chamber and burner.

A rotary engine, either of the type discussed here or of the Wankel type, appears to be an attractive substitute for a reciprocating engine, because each occupies less volume for the same power output. This will partly compensate for other relatively large components such as the boiler and condenser. The rotary engine discussed in this study should give improved efficiency because the clearance volume is substantially reduced and design and construction are simplified. However the face and apex seals require further development, although some firms have claimed that the sealing problem in the Wankel engine has been solved for internal combustion designs. If the lubrication and sealing problems are solved satisfactorily, higher steam pressures will result in still smaller sizes of the engine and boiler. One possibility is the use of self-lubricating materials that can be used as well for sealing.

The condenser is a major factor limiting the power and output of the system. The condenser fan consumes up to 2.5 hp and may be relatively more noisy than a conventional radiator fan because of its larger size. Some investigators working in the field of heat transfer are trying to develop a rotating condenser and they expect to reduce the condenser size considerably. For tractors the condenser size will be limited because its location is fixed. In contrast, a Japanese firm is developing a vapor cycle plant for automobiles using a flourocarbon working fluid, in which the condenser is within the roof panel.

Since the condenser capacity is limited, water will be the only working fluid that will be suitable. As mentioned previously, during heavy load operation, the condenser will not be able to condense all of the fluid, and if blow-off is not provided the engine back pressure will rise and engine power will decrease. Such blow-off would be dangerous and costly if a toxic working fluid were used. However the use of water poses a potential freezing problem; to avoid this problem some kind of draining system must be used to blow all the water into a single tank after shut down. If this tank is well insulated the freezing problem is less serious [3].

The arrangement of components will be a design challenge and will require considerable experimentation.

A. Steam Powered Application for Underdeveloped Countries.

Particularly for underdeveloped countries of Asia and Latin America, the development of a steam powered tractor should prove very advantageous, partly because the automotive industry itself is in an early stage of development. The relatively simple design of a low-speed steam engine will make these countries less dependent on importing expensive parts from foreign countries. Furthermore, most underdeveloped countries are in tropical climates, where freezing temperatures are seldom encountered. Finally, the cheaper grade of fuel required will be more economical, especially where oil refining is in an early stage of development.

B. Conclusion.

As a result of this study, it can be concluded that for vehicles like tractors, where the volume of power-plant per unit volume of vehicle is not a major design factor, a steam power cycle appears feasible and worthy of further development. Component sizes can be reduced if lubrication problems are solved, so that higher operating pressures are possible. Of course, one could produce a frightening list of design problems to be faced, but most of these could no doubt be solved by a determined attack in the spirit of "Don't stand looking at your hill - climb it."

IX. BIBLIOGRAPHY

1. Steam Engines Again? Yes - but with a New Approach. Automotive Engineering, October 1970, Vol. 78, No. 10.

2. Vickers, P. T., Amann, C. A., Mitchell, H. R., and Cornelius, W., "The Design Features of the GM SE-101- A Vapor Cycle Powerplant," SAE Paper No. 700163.

3. Palmer, R. M., "An Exercise in Steam Car Design," The Institute of Mechanical Engineers, Automobile Division, London, Proceedings 1969-70, Vol. 184, Part 2A, No. 10.

4. Strack, W. C., "Condersers and Boilers for Steam-powered Cars: A Parametric Analysis of Their Size, Weight and Required Fan Power," NASA TN D 5813, Washington D.C., May 1970.

5. Neil, E. B., "Thermodynamics of Vapor Power Plants for Motor Vehicles", SAE Quarterly Transaction, 1968 (April) 2, No. 2.

6. Lewit, E. H., Thermodynamics Applied to Heat Engines, Third Edition, Sir Isaac Pitman & Sons, Ltd., London.

7. Johnson, R. P., The Steam Locomotives, Simmons-Boardman Publishing Corporation.

8. Low, D. B., Theory of Machines, Fourth Edition, Longmans, Green and Company.

9. Doolittle, J. S., and Zerban, A. H., Engineering Thermodynamics, Theory and Application, Third Edition, International Textbook Company, Scranton, Pennsylvania.

10. Dooley, J. L., and Bell, A. F., "Description of Modern Automotive Steam Power Plant," SAE Paper No. S338, 1962 (January).

11. Fraas, A. P., "Application of Modern Heat Transfer and Fluid Flow Experience to the Design of Boilers for Automotive Steam Power-plants," SAE Paper No. 690047, 1969 (January).

12. Boiler Code, A.S.M.E.

13. Keenan, J. H., and Kays, J., Gas Tables, John Wiley and Sons, Inc.

14. Kays, W. M., and London, A. L., Compact Heat Exchanger, The National Press, Palo Alto, California.

15. McAdams, Heat Transmission, Third Edition, McGraw Hill.

16. Perry, J. H., Chemical Engineers Handbook, Fourth Edition, McGraw Hill.

17. Eckert and Drake, Heat and Mass Transfer, Second Edition, McGraw Hill.

18. Thom, J. R. S., "Prediction of Pressure Drop During Forced Circulation Boiling of Water," Int. J. of Heat Mass Transfer, Vol. 7, No. 7, July 1969.

19. Klein, J. F., Design of High Speed Steam Engines, Third Edition, Bethlehem, Pennsylvania, Times Publishing Company, 1911.

20. Baumeister and Marks, Standard Handbook for Mechanical Engineers, Seventh Edition, McGraw Hill.

21. Ansdale, R. F., The Wankel R. C. Engine, Design and Performance, A. S. Barnes and Company, Inc., Cranbury, New Jersey, 08512.

22. Spots, F. M., Elements of Machine Design.

23. Stuart, D. D., Dusatko, and Zoucha, C. F., "How to Minimize Size of Condenser for Steam Car," Automotive Engineering, Vol. 79, No. 10, October 1971.

24. Mechanical Power Transmission Equipment, Engineering Catalog, Dodge, D-66.

25. Vickers, P. T., Mondt, J. R., Haverdinb, W. H., and Wade, W. R., "General Motor's Steam Powered Passenger Cars - Emissions, Fuel Economy and Performance," SAE Paper No. 700670.

X. VITA

The author was born in 1947, in Bhavnagar, India.

He graduated from Home School, Highschool, Bhavnagar in 1963. He entered B.V.M. Engineering College, S.P. University, India in 1964 and received the Bachelor of Engineering degree in Mechanical Engineering in May 1969. He came to the United States for further studies on Hindu and Jain Education funds and since September 1969 has been working towards Master of Science degree in Mechanical Engineering at the University of Missouri Rolla.